4. SITE 401

The Shipboard Scientific Party[1]
With Special Contributions by
Maurice Bourbon, Ecole Nationale Supérieure des Mines de Paris, Paris, France
David N. Lumsden, Department of Geology, Memphis State University, Memphis, Tennessee
and
D. Mann, Department of Energy, Thames House South, London, United Kingdom

SITE DATA

Position: 47°25.65′N, 08°48.62′W

Water Depth (sea level): 2495 corrected meters, echo-sounding

Bottom Felt at: 2555.5 meters, drill pipe

Penetration: 341.0 meters

Number of Cores: 28

Total Core Recovery: 103.22 meters

Percentage Core Recovery: 38.7%

Oldest Sediment Cored:
Depth sub-bottom: 341.0 meters
Nature: Coralline calcarenites
Age: Late Jurassic (Kimmeridgian-Portlandian)
Basement: Not reached

Principal Results: Site 401 was situated on the planated edge of a tilted fault block underlying the southern edge of the Meriadzek Terrace on the north Biscay margin (Figure 1). The site was continuously cored below 84.5 meters and terminated in Kimmeridgian-Portlandian shallow-water carbonates at 341.0 meters.

Four lithologic units were distinguished. Unit 1 (0-20 m) of Quaternary age consists of olive-gray calcareous mud and yellowish brown calcareous ooze. Unit 2 (20-171.5 m) of middle Oligocene (or younger) to middle Eocene age consists of greenish gray nannofossil chalk and marly nannofossil chalk. An 18-m.y. hiatus separates the middle Eocene from the uppermost Eocene-lower Oligocene. Unit 3 (171.5-247.0 m) is of early Eocene to Late Cretaceous age. The Eocene and uppermost Paleocene beds consist of yellowish brown to orange brown nannofossil and marly calcareous chalks. Hiatuses are present between the lower and upper Paleocene and between the lower Paleocene and the Maestrichtian. The Maestrichtian to Campanian beds consist of laminated nannofossil and foraminiferal calcareous chalk. Unit 4 (247-341 m) is upper Aptian to Kimmeridgian/Portlandian and is separated by a 34-m.y. hiatus from Unit 3. Thin upper Aptian oozes comprise the upper part of the sequence and are separated by a large gap from the underlying bioclastic limestones which indicate ages at the top from possible Neocomian to late Tithonian to Berriasian. This gap corresponds to erosion during the Early Cretaceous of the crest of the tilting block. Intraclast grainstones comprising the lowest part of the unit are of Kimmeridgian to Portlandian age.

The presence of shallow water Aptian carbonates at Site 401 compared to the temporally equivalent sediments of Hole 400A shows that a substantial submarine relief (~ 2000 m) existed at the end of the rifting phase. Following subaerial erosion in the Early Cretaceous at Site 401, the deposition of upper Aptian chalks in an outer shelf environment is evidence of the onset of subsidence. The Campanian/Maestrichtian chalks were deposited in 1500 meters depth and the Tertiary beds close to the present depth. The presence of coral debris in the Kimmeridgian/Portlandian, the Tithonian/Berriasian, and the Neocomian sections suggests the existence of an extensive carbonate platform that became dissected by rifting. Less probably, the deposition of these shallow water carbonates could have been restricted to bathymetric highs forming the top of tilted blocks previously created during Late Jurassic. Abundant biogenic silica in the middle Eocene is associated with a decrease in surface and bottom water temperatures and with a prominent erosional unconformity.

BACKGROUND AND OBJECTIVES

Site 401 was originally proposed as a mid-slope hole to establish variations in the facies of margin sediments above and below unconformities to provide, for comparative purposes, the subsidence history of a shallower site on the margin. Loss, however, of the major part of the drill string at Hole 400A necessitated a review of the drilling program because the remaining drill string length of 15,587 feet precluded drilling at the original site.

Detailed results of Hole 400A are discussed in the preceding site chapter but, in brief recapitulation, the hole penetrated a series of oozes and nannofossil chalks exhibiting dissolution cycles and ranging in age from early Tertiary to Recent. Extensive dissolution of both nannoplankton and foraminifers in lower Miocene, Oligocene, Eocene, and Paleocene beds rendered those parts of the section less valuable for biostratigraphic purposes. Prominent hiatuses occur between the lower Oligocene and middle Eocene and between the upper Paleocene and Maestrichtian. Only 15 meters of deep water Upper Cretaceous chalks are present and they rest uncon-

[1]Lucien Montadert (Co-Chief Scientist), Institut Français du Pétrole, Rueil-Malmaison, France; David G. Roberts (Co-Chief Scientist), Institute of Oceanographic Sciences, Surrey, England; Gerard A. Auffret, Centre Océanologique de Bretagne, Brest, France; Wayne D. Bock, Rosenstiel School of Marine and Atmospheric Science, Miami, Florida; Pierre A. Dupeuble, Université de Rouen, Mont-Saint-Aignan, France; Ernest A. Hailwood, University of Southampton, Southampton, United Kingdom; William E. Harrison, University of Oklahoma, Norman, Oklahoma; Hideo Kagami, University of Tokyo, Tokyo, Japan; David N. Lumsden, Memphis State University, Memphis, Tennessee; Carla M. Müller, Geologisch-Paläontologisches Institut der Universität, Frankfurt am Main, Federal Republic of Germany (now at: Institut Français du Pétrole, Rueil-Malmaison, France); Detmar Schnitker, University of Maine, Walpole, Maine; Robert W. Thompson, Humboldt State University, Arcata, California; Thomas L. Thompson, University of Oklahoma, Norman, Oklahoma; and Peter P. Timofeev, USSR Academy of Sciences, Moscow, USSR.

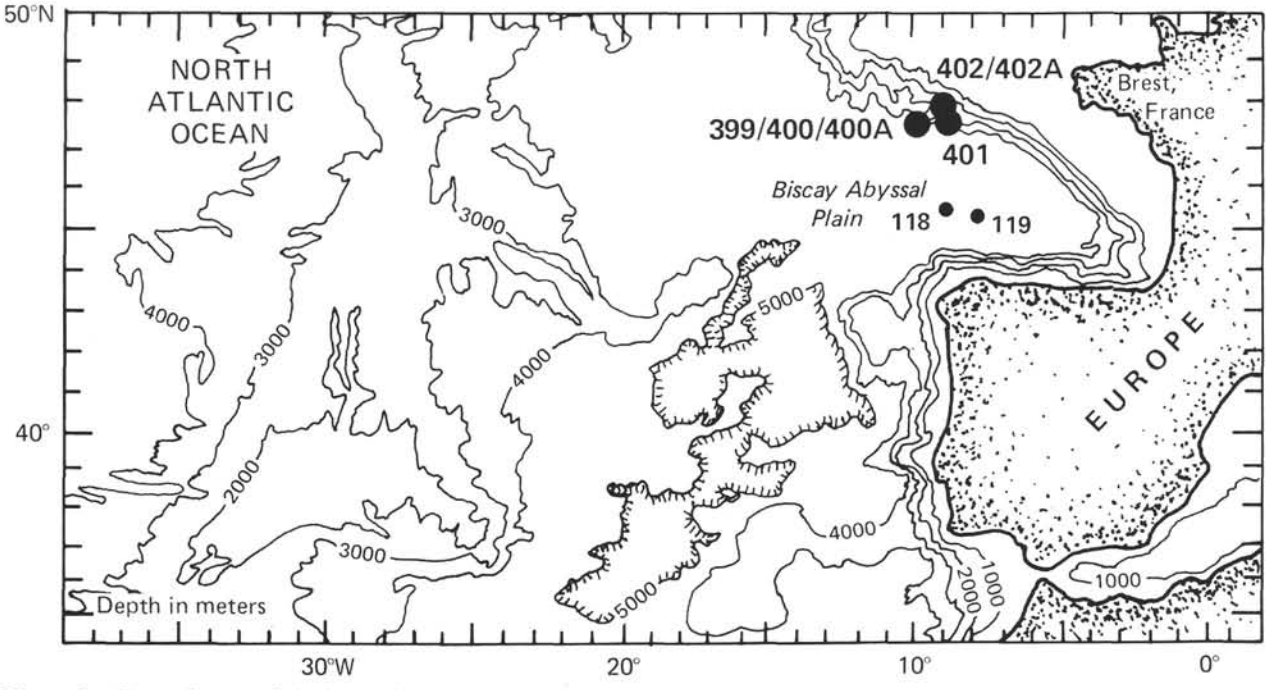

Figure 1. *General map of the Bay of Biscay showing locations of Holes 400A, 402A, and Sites 401, 118, and 119.*

formably on carbonaceous limestones of Albian/Aptian age. The unconformity, contemporaneous with that recorded on the adjacent shelf and lands, marks a hiatus of about 30 m.y. Contemporaneous Albian/Aptian shallow water carbonates previously dredged from the Meriadzek Terrace suggest that the carbonaceous limestones were deposited in a water depth of about 2000 meters. The drill string loss prevented penetration through seismic formation III (Montadert et al., this volume) to "pre-rift" sediments.

One obvious and important problem posed by the results from Hole 400A was the fluctuating CCD during the Tertiary and Cretaceous. Within the section, variations in carbonate content can be related to changes in carbonate production, or to real variations in depth of the CCD, or to increased production of biogenic silica by upwelling. A more complete section from a shallower environment, less subject to dissolution, would help resolve the subtle balance among these factors, as well as be valuable for biostratigraphic purposes. A more complete Cretaceous sequence was important to examine the striking change in environment indicated by the change from carbonaceous limestones to pure chalks. The paleoenvironment of carbonaceous limestone deposition, both in terms of early margin history and their almost ubiquitous distribution in the world ocean, represented a major problem of oceanographic gradients that might be resolved by penetrating sediments deposited, at a shallower site, between the photic zone and 2000 meters depth in Albian/Aptian time. Other questions included the tectonic and oceanographic significance of the "Cenomanian" unconformity separating deep water sediments. In the case of younger hiatuses, a relationship to tectonic events or to oceanographic changes could be postulated on regional geological and geophysical evidence. Finally, it was important to penetrate pre-rift sediments to establish the environment before and during rifting.

In summary, the principal objectives of the hole were:

1) comparison of pre-, syn-, and post-rift sediments by penetration into pre-rift sediments;

2) comparison of Lower Cretaceous facies with Hole 400A, with special reference to the paleoenvironment of carbonaceous limestone deposition;

3) for biostratigraphic purposes, sampling of a more complete lower Tertiary section not subject to dissolution;

4) examination of the facies changes associated with unconformities in comparison with those observed at Hole 400A, to assess their tectonic and oceanographic implications;

5) history of variations in the CCD or of variations in biogenic/silica carbonate production as a function of changing ocean circulation.

On the bases of the results from Hole 400A and the regional picture of the margin provided by the multichannel seismic profiles, Site 401 was selected on the southern edge of the Meriadzek Terrace (Figures 1, 2 and 3) at SP660 on profile S21 close to intersecting profile S27 and within two miles of profile OC209. The proposed site was located on the outer edge of a fault block within one mile of a site where Lower Cretaceous and Upper Jurassic sediments previously had been dredged. These data and the absence of thick sedimentary cover on the outer edge of the block indicated that the potential reservoir provided by the reefal Lower Cretaceous was open towards the southwest and northwest. Further, pyrolysis studies indicated that the carbonaceous limestones were immature and were unlikely to be a source of hydrocarbons at these burial depths. Finally, the seismic velocity data on the site showed that pre-rift sediments could be penetrated at about 350 meters below the sea bed. The decision was made to drill using the bit release sub in the bottom hole assembly in order to permit logging upon completion of the hole.

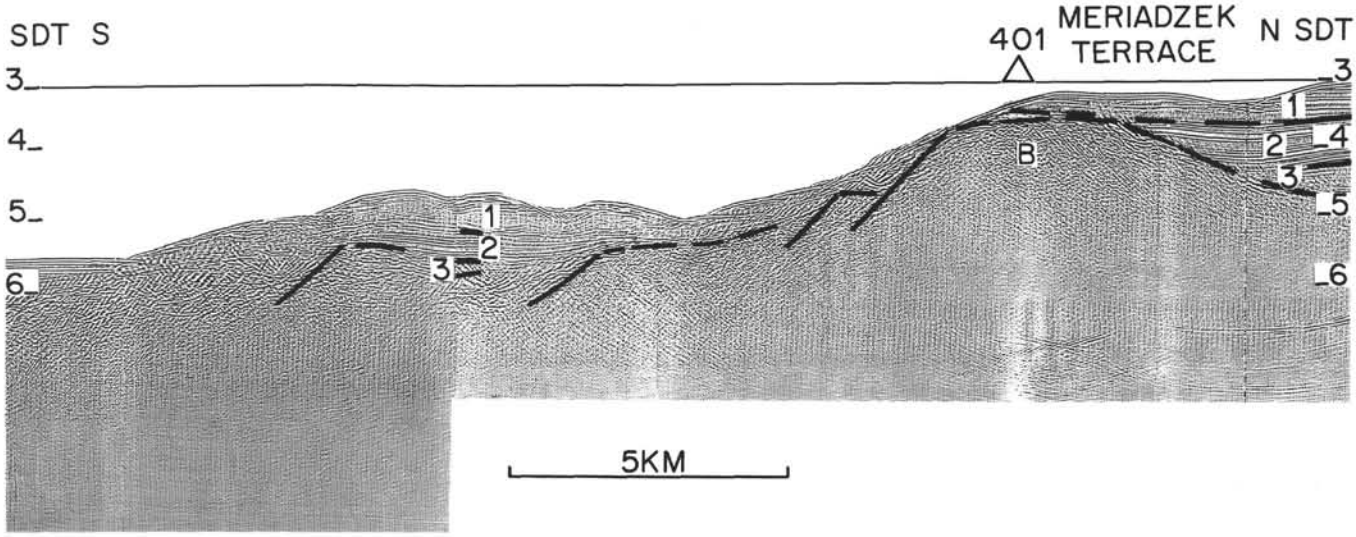

Figure 2. *Multichannel seismic profile IFP-CNEXO S21 through Site 401.*

SITE APPROACH AND DRILLING OPERATIONS

The proposed Site 401 was located in an easily identifiable position at a break in slope marking the edge of the Meriadzek Terrace about 2.2 miles south of a U-shaped channel on the escarpment crest. The planned approach to Site 401 involved steaming eastward from Hole 400A to a point well south of Site 401 before turning northward along 352 degrees (Figure 4) to run at reduced speed along the control seismic line IFP-CNEXO S21, in order to facilitate recognition of the site.

Before reaching the turning point at 0052 hours, considerable time had elapsed since the last satellite fix at 2342 hours on 5 June. The dead-reckoned position was thus uncertain, made more so because the lightening of the ship from loss of the drill pipe made previous speed estimates invalid. At 0052 hours on 6 June, the vessel reduced speed to an apparent five knots (150 rpm) turning northward along 352 degrees. Discrepancies between the PDR depths and the control seismic line, and a comparison with a 1:250,000 chart prepared by Berthois (personal communication), suggested the ship's track lay some 2.5 miles east of the control seismic profile. This suggestion was later verified by a satellite fix and by our failure to cross the channel just north of the site. At 0156 hours on 6 June, the vessel altered to 270 degrees prior to obtaining another satellite fix and continued on this heading for 3 miles before turning onto 175 degrees at 0233 hours to directly cross the site. On this heading, the channel to the north was crossed at 0310 hours and, shortly afterward, at 0320 hours, a 13.4-kHz beacon was dropped on the edge of the escarpment. The vessel continued on this heading while retrieving the geophysical gear before turning northward on 357 degrees to occupy the site. The depth of the beacon was shallower than that at the proposed shot point and an offset of 1000 feet to the south was introduced at 0455 hours.

Drilling Operations

At 0800 hours on 6 June, the rig crew began making up the bottom hole assembly having previously magnafluxed the stand of drill collars in the derrick and made up the bit release mechanism. Although the bottom hole assembly was made up at 0800 hours, various incidents, such as blockage of the mousehole and lack of power to the Bowen sub, delayed spudding in. At 2130 hours on 6 June, the first core barrel was dropped but retrieved only water. Successive drops of the core barrel also yielded water cores indicating a substantial difference between PDR depth (correlated to the rig floor) and rig floor depth. At 0345 hours on 6 June a core was finally cut at the mud line at 2555.5 meters below the rig floor. The rig floor depth was subsequently confirmed by the mud line depth detected by the logging equipment. The cause of the discrepancy is not clear.

The hole was then washed to a depth of 2631.5 meters before beginning to drill and core continuously (Table 1). The second core cut at 85.5 meters sub-bottom yielded lower Oligocene sediments. Owing to poor recovery in the first four cores, the heave compensator was locked out in Cores 6, 7, 8, and 11, and recovery down to 208 meters sub-bottom averaged in excess of 75 per cent. Between 0230 and 0315 hours on 8 June, the brushes in the gyro failed, necessitating pulling of four DBL's before the fault was rectified and the drill pipe could be run back to bottom. Core recovery declined from 74 per cent in Core 15 to core catcher only in Cores 20, 21, and 22. The poor recovery may be due in part to the hard Jurassic limestones penetrated below 250 meters. Cores 25 to 28 yielded only cuttings despite 15 barrels of mud being spotted at 2230 hours to clear the hole. The accumulation of cuttings was due to drilling hard limestones and may be similar to cuttings accumulated when drilling basalts. At 0250 hours on 9 June, drilling was terminated and the hole prepared for the logging program by spotting 20 barrels of 87 weight 45 viscosity mud. At 0800 hours on 9 June, the release sub was lowered to drop the bit. At 0840 hours, the first attempt made to release the bit failed and the center bit was run to attempt to jar the bit loose. At 1045 hours, the center bit was pulled and a further 20 barrels of mud were spotted before pulling pipe prior to the logging operation. Running in of the gamma, sonic, caliper, and variable density tools at 1400 hours on 9 June showed the bit release had worked successfully. After various test runs, logging with these

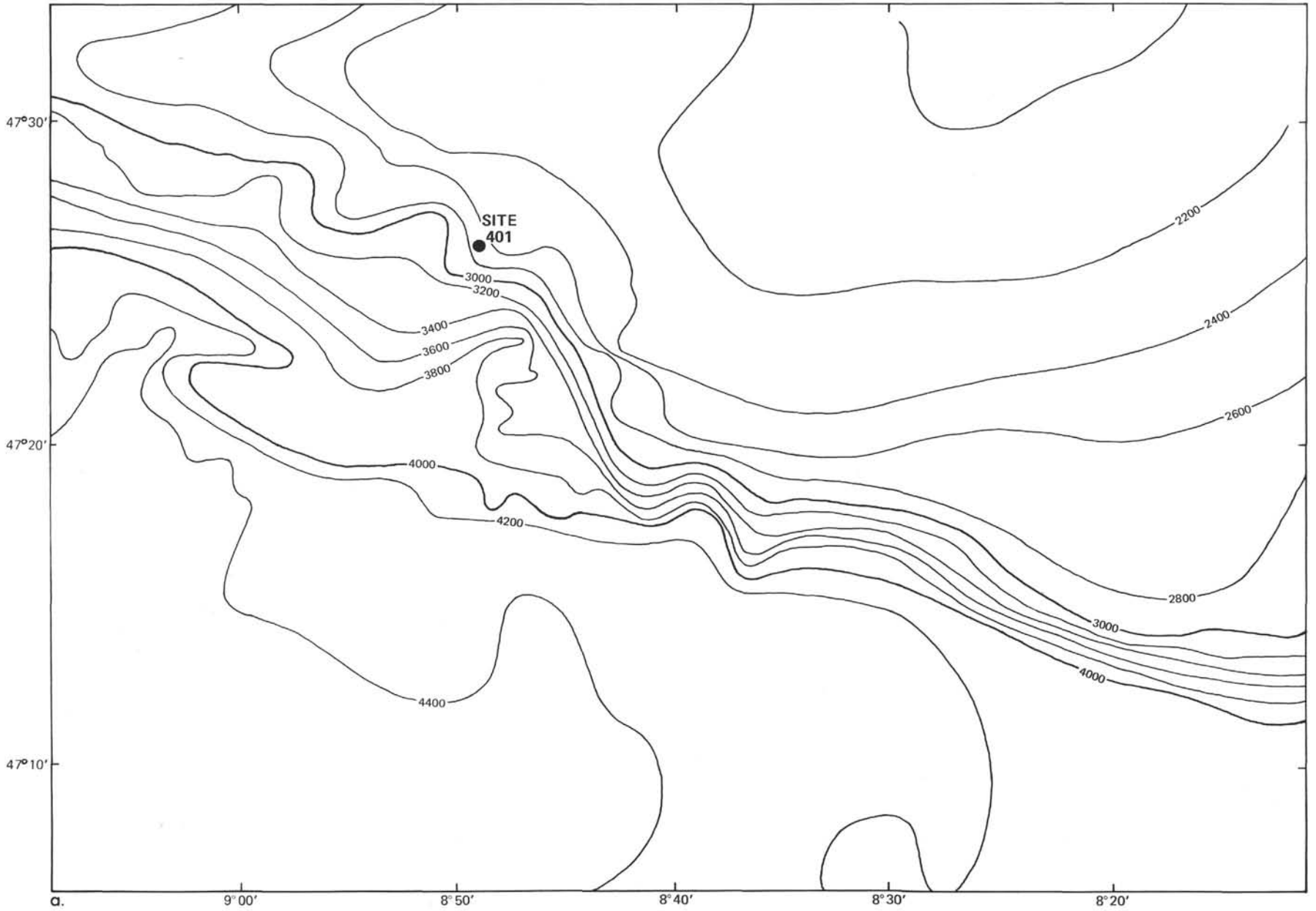

Figure 3a. *Bathymetry in the vicinity of Site 401.*

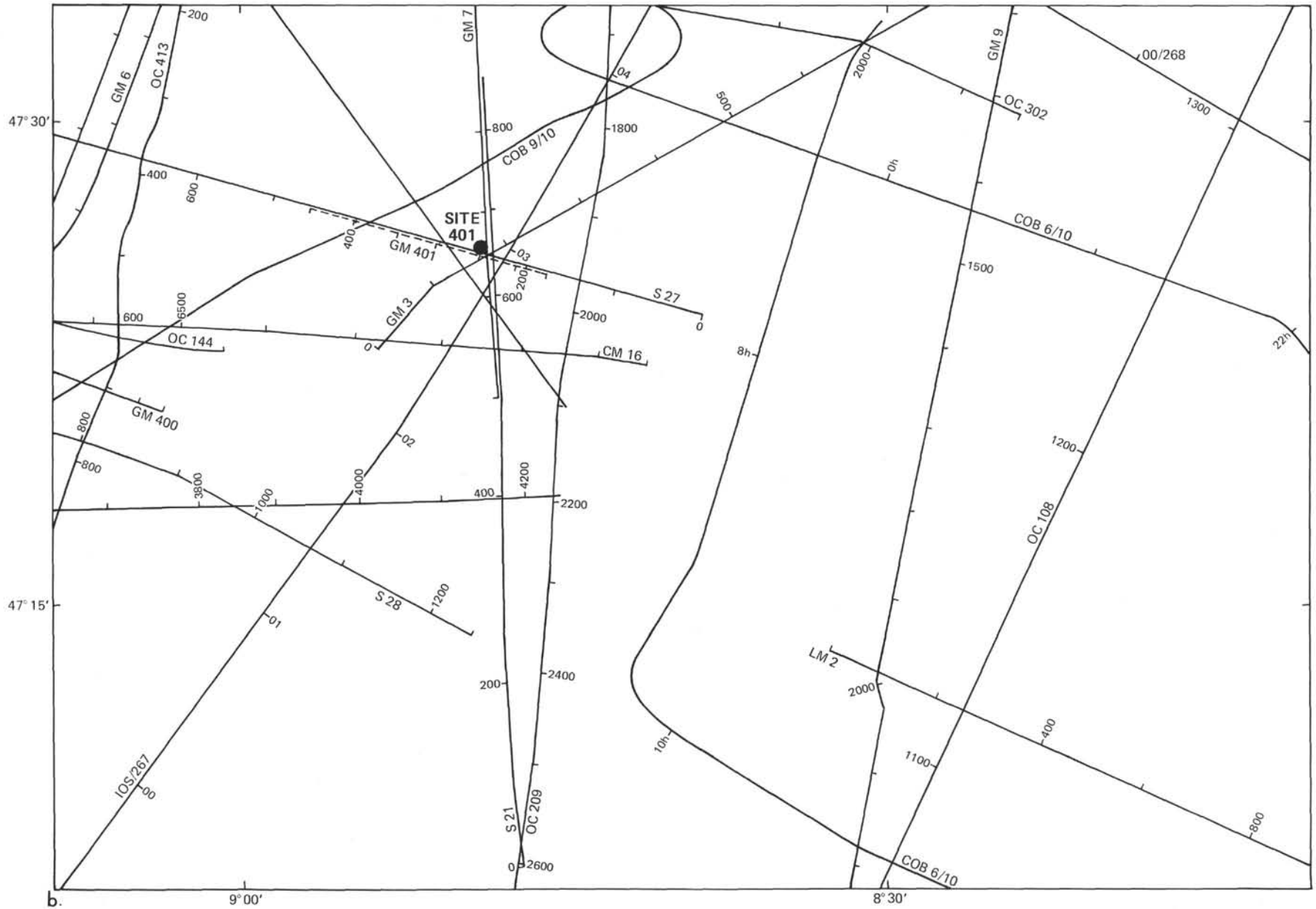

Figure 3b. *Location of seismic profiles in the area of Site 401.*

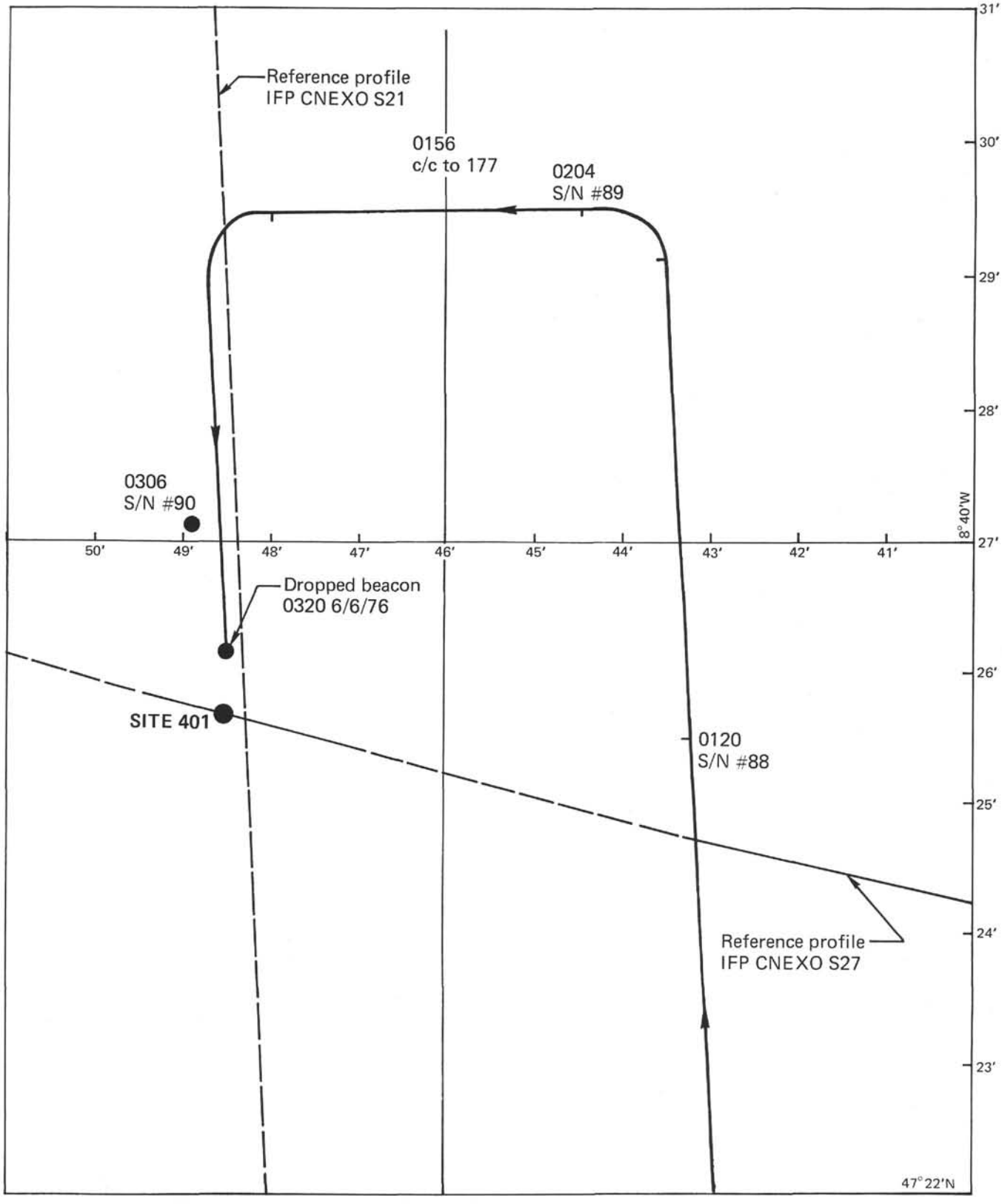

Figure 4. *Approach of* Glomar Challenger *to Site 401.*

tools was completed by 1955 hours on 9 June. No problems were experienced in pulling the tool out of the hole. Two successive logging runs were made using gamma/induction and gamma/density/neutron, respectively. Logging operations were completed at 0300 hours on 10 June and the pipe was pulled out of the hole between 0415 and 0845 hours on 10 June. The rig floor was secured and the vessel departed for Site 402 at 0915 hours on 10 June.

TABLE 1
Coring Summary, Site 401

Core	Date (June 1976)	Time	Depth From Drill Floor (m)		Depth Below Sea Floor (m)		Length Cored (m)	Length Recovered (m)	Recovery (%)
1	7	0120	2547.0	2555.5	0	8.5	8.5	8.5	100
2	7	0905	2631.5	2641.0	84.5	94.0	9.5	0.71	7.7
3	7	1015	2641.0	2650.5	94.0	103.5	9.5	0.46	4.0
4	7	1242	2650.5	2660.0	103.5	113.0	9.5	0.33	3.0
5	7	1300	2660.0	2669.5	113.0	122.5	9.5	5.6	58
6	7	1410	2669.5	2679.0	122.5	132.0	9.5	5.78	61
7	7	1525	2679.0	2688.5	132.0	141.5	9.5	8.58	90
8	7	1642	2688.5	2698.0	141.5	151.0	9.5	9.91	100
9	7	1805	2698.0	2707.5	151.0	160.5	9.5	8.90	94
10	7	1957	2707.5	2717.0	160.5	170.0	9.5	9.69	100
11	7	2130	2717.0	2726.5	170.0	179.5	9.5	7.1	74
12	7	2310	2726.5	2736.0	179.5	189.0	9.5	7.24	75
13	8	0047	2736.0	2745.5	189.0	198.5	9.5	7.3	77
14	8	0231	2745.5	2755.0	198.5	208.0	9.5	7.07	74
15	8	0630	2755.0	2764.5	208.0	217.5	9.5	2.04	21
16	8	0810	2764.5	2774.0	217.5	227.0	9.5	3.66	39
17	8	0910	2774.0	2783.5	227.0	236.5	9.5	3.56	37
18	8	1010	2783.5	2793.0	236.5	246.0	9.5	2.49	27
19	8	1156	2793.0	2802.5	246.0	255.5	9.5	1.64	17
20	8	1345	2802.5	2812.0	255.5	265.0	9.5	0.12	1
21	8	1538	2812.0	2821.5	265.0	274.5	9.5	0.19	2
22	8	1705	2821.5	2831.0	274.5	284.0	9.5	0.20	2
23	8	1910	2831.0	2840.5	284.0	293.5	9.5	1.83	19
24	8	2130	2840.5	2850.0	293.5	303.0	9.5	0.32	3
25	8	2220	2850.0	2859.5	303.0	312.5	9.5	0	0
26	8	0000	2859.5	2869.0	312.5	322.0	9.5	0	0
27	9	0125	2869.0	2878.5	322.0	331.5	9.5	0	0
28	9	0250	2878.5	2888.0	331.5	341.0	9.5	0	0
Total							265.0	103.22	39%

LITHOLOGY

At Site 401, drilling penetrated 341.0 meters sub-bottom to terminate in shallow water limestones of Late Jurassic age (Figure 5). The hole was washed to 84.5 meters after an 8.5 meters core was cut at the mudline; a 9-meter core was recovered at an unknown point in the washed interval.

The section penetrated at Site 401 has been subdivided into four main lithologic units (Table 2, Figure 5) on the basis of lithology, downhole logs, and X-ray mineralogical studies.

Unit 1

A single 8.5-meter core, cut at the mudline, is the only sample of this unit the base of which, at 20 meters, has been defined by a sharp decrease in the gamma log. The core consists of olive-gray calcareous mud at the base and olive-gray to yellow-brown marly calcareous ooze at the top. Two upward-fining cycles are present in the uppermost 2.5 meters. Carbonate content averages 38 per cent, changing from 64 per cent at the top (mostly foraminifers) to 24 per cent at the base (mostly nannofossils). Interglacial and glacial microfaunas are present.

Unit 2

Unit 2 was cored only between 84.5 and 171.5 meters. Lower to middle Oligocene nannofossil oozes found in a washed core cut somewhere between 20 and 84.5 meters have been included in Sub-unit 2A.

Sub-Unit 2A

The sub-unit is composed of uniform light greenish gray to greenish gray nannofossil chalk, with a uniform nannofossil content throughout (60-70%) and a persistent sponge spicule content averaging 5 per cent. Total carbonate averages 70 per cent and quartz 5 per cent; smectite comprises the major clay mineral component with minor amounts of illite, chlorite, and zeolite. Sedimentary structures are rare. The base of the sub-unit corresponds to the hiatus of 1.8 m.y. between the upper and the middle Eocene.

Sub-Unit 2B

Sub-unit 2B is defined by its lower carbonate content of 50 per cent and higher quartz content of 10 per cent. The major lithologies present are nannofossil chalks, siliceous nannofossil chalks, and marly nannofossil chalks. Carbonate content averages 50 per cent, quartz 10 per cent, and smectite is the dominant clay mineral; illite is rare. A fibrous clay, probably sepiolite, is present in small amounts. Siliceous components vary between 12 and 49 per cent. Disseminated dark flecks, patches, streaks, and laminae of fine pyrite are common throughout. Some larger aggregates appear to be manganese nodules. Burrows range from being absent to moderately abundant with scattered occurrences of *Zoophycos*. Laminae occur in Cores 7 and 8. Benthic foraminifers point to bathyal deposition above the CCD. A sedimentation rate of 10 to 16 m/m.y. is indicated.

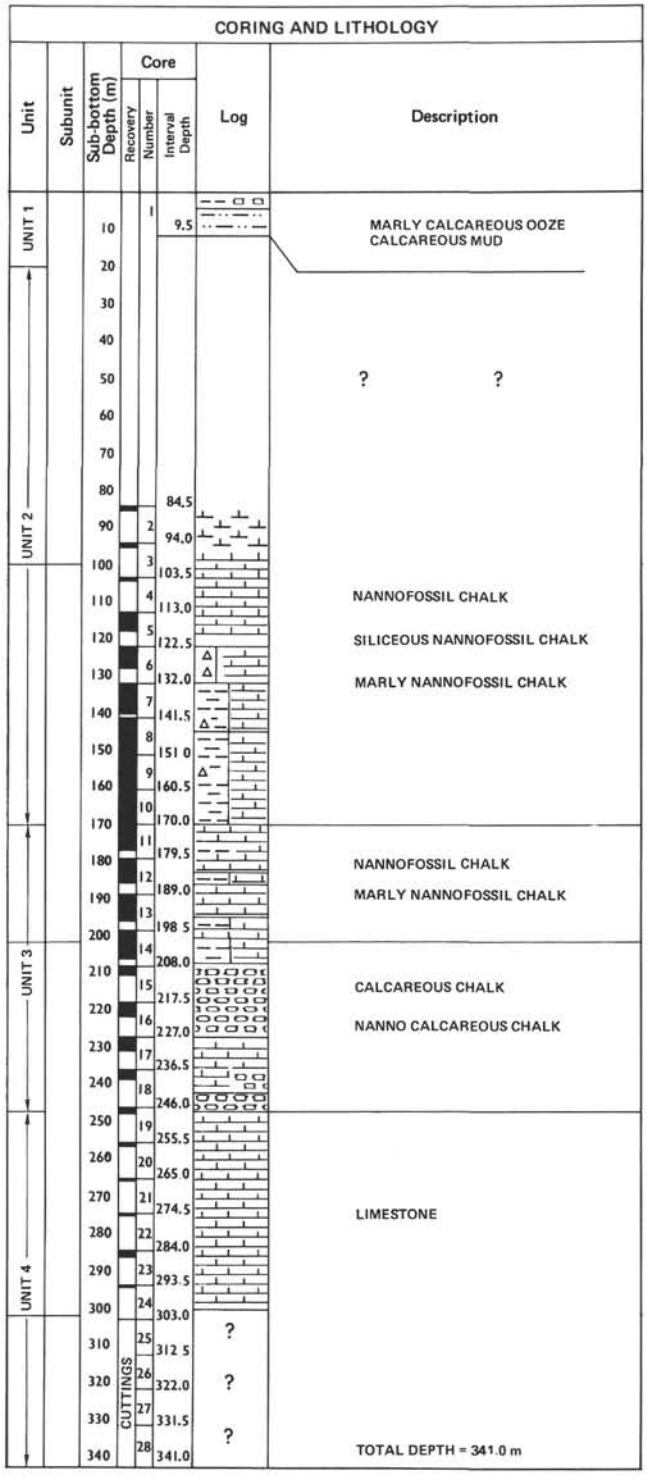

Figure 5. *Lithologic summary of Site 401.*

Unit 3

The division between Units 2 and 3 has been drawn at the middle Eocene/lower Eocene boundary where decrease in quartz, illite, smectite, and carbonate contents occurs. The contact is also marked by color changes and a sharp rise in magnetic intensity values from near zero values in Unit 2 to values of 11 microgauss near the top of Unit 3.

Unit 3 is subdivided into three sub-units distinguished principally by variations in color and carbonate content.

Sub-Unit 3A

The sub-unit consists of yellowish brown to orange-brown nannofossil chalks and marly chalks. Compared to the sub-units above and below, it is characterized by low quartz, high kaolinite, and a decrease in smectite. Carbonate content reaches a maximum value of 76.6 per cent compared to 28 per cent in the underlying Sub-unit 3B. A dark yellowish brown layer of collophane occurs towards the base of the unit. Burrows are slight to moderate. Slickensided fractures of varied orientation that dip as steeply as 45 degrees occur in Core 13. Deposition in bathyal conditions at a rate of 5 m/m.y. is indicated.

Sub-Unit 3B

The sub-unit consists of yellowish brown to grayish orange marly chalk with a carbonate content as low as 28 per cent and a concomitant increase in the detrital components (quartz 12%, smectite 80%). Chlorite and kaolinite become absent towards the base of the unit.

Sub-Unit 3C

Grayish orange nannofossil chalk constitutes the dominant lithology. The sub-unit is distinguished from Sub-unit 3B by a sharp increase in carbonate content to between 80 and 90 per cent; kaolinite and chlorite are also absent. Within the unit, a hiatus of 2.6 m.y. between the middle and lower Paleocene is present at 219.5 meters and a second hiatus of 2 m.y. between the lower Paleocene and Maestrichtian is present at 236.5 meters. No major change in lithology occurs across either hiatus although there is evidence from the sparse X-ray data for increases in clay content below each hiatus. Towards the top of the unit, disseminated manganese grains are present and a manganese nodule occurs at 246.2 meters. A granite pebble (probably cavings) occurs in the Maestrichtian nannofossil chalks. Attapulgite, sepiolite, and clinoptilolite are locally abundant. Between 217.5 and 227 meters, burrows are offset by microfaults. The rare benthic foraminifers indicate bathyal deposition.

Contact Between Units 3 and 4

The contact between the deep water chalks of Unit 3 and the shallow water upper Aptian limestones of Unit 4 below is sharp and marks an abrupt change in the environment of the site (Lumsden, this chapter).

Above the contact is a grayish orange foraminiferal chalk of Campanian age, with darker brown streaks and laminae that become more common down towards the contact. Seven centimeters above the contact, a 5-cm-thick bed of very pale orange chalk (75% unspecified carbonate) is present. Below this bed, a 1 to 2-cm-thick bed of soft, light brown, marly chalk rests on a lithified very pale orange limestone. The top of the underlying upper Aptian section, at 122 cm below the top of Core 19, is a phosphatic crust (hard ground?) consisting of cauliflower-like structures that are closely comparable to structures observed in phosphatic crusts of the same age observed in the Briançonnais platform of the Western Alps (see Bourbon, this chapter).

TABLE 2
Lithologic Units, Site 401

Unit	Sub-unit	Core	Sub-Bottom Depth (m)	Lithology	Age
1		1 and upper washed zone	0-20	Calcareous mud, marly calcareous ooze	Quaternary
2	2A	2-4	20-113	Nannofossil chalk	Early/middle Oligocene to late Eocene
			HIATUS		
	2B	5-11	113-171.5	Nannofossil chalk, siliceous nannofossil chalk, marly nannofossil chalk	Middle Eocene
3	3A	11-13	171.5-194	Nannofossil chalk, marly chalk	Early Eocene to late Paleocene
	3B	13-14	194-200.5	Marly chalk	Eocene to late Paleocene
	3C[a]	14-19	200.5-247.2	Nannofossil chalk	Late Paleocene to Campanian
4	4A	19-20	247.2-265	Limestone	Late Aptian to late Tithonian/Berriasian
	4B	21	265-274.5	Limestone	Late Tithonian/Berriasian
	4C	22	274.5-284	Limestone	Kimmeridgian/Portlandian
	4D	23-24	284-303	Limestone	Kimmeridgian/Portlandian

[a]Sub-unit 3C contains two hiatuses, one at 219.5 meters between middle and lower Paleocene and one at 236.5 meters between lower Paleocene and Maestrichtian.

Unit 4

Core recovery in the hard lithified limestones of this unit was poor. Identification of the lithological sub-units has been made principally from the downhole logs calibrated with the limited core data. Detailed description by Lumsden, of the various lithologies, is given following this summary.

Sub-Unit 4A

Electric log data suggest that this unit has low porosity, not exceeding 20 per cent. Changes in cementation with depth may be indicated by cycle skipping on the sonic and VDL logs. Thin-section and hand-specimen descriptions have revealed the following lithologies: orange-pink pellet intraclast grainstone micrites, pellet intraclast grainstones, and packstones that contain fragments of coral, algae, pelecypods, foraminifers, crinoids, and ostracodes. Planktonic foraminifers and nannoconids indicate external shelf, near-shore depositional environments.

Sub-Unit 4B

Downhole log data suggest a tight section with porosities in the range of 5 to 10 per cent. Limestones recovered in this interval are pellet grainstones.

Sub-Unit 4C

Pellet grainstones with crinoids, foraminifers, pelecypods, and algae fragments were recovered in this interval. The electric logs show an increase in neutron porosity and a reduction in sonic velocity suggesting that pellet grainstones persist throughout the interval.

Sub-Unit 4D

The logs show increasing density and velocity with a slightly more porous section towards 300 meters. Principal lithologies recovered in this interval include pale orange pellet intraclast grainstones containing crinoids, fragments of corals, brachiopods, foraminifers, and pelecypods. Some of the intraclasts appear to be algal oncolites. In a thin section from Core 24 (31-33 cm), a 5-mm coral head and algal mat are present. Porosity values range from 30 per cent to as low as 5 per cent and comprise solution as well as intragranular porosity.

CONDENSATIONS AND HIATUSES IN THE CRETACEOUS/EOCENE SERIES OF SITES 401 AND 402 AND COMPARISON WITH SOME SECTIONS OF THE NORTHERN CONTINENTAL MARGIN OF TETHYS (BRIANÇONNAIS-FRENCH ALPS)

Maurice Bourbon

Introduction

This contribution does not result from a study of samples; rather, it deals only with hiatuses and condensations in sedimentary sequences on two continental margins (1) the Bay of Biscay and (2) the Briançonnais (northern continental margin of the ancient Tethyan Ocean) that are comparable to those reported at Sites 401 and 402 of DSDP Leg 48. The choice of the Briançonnais for comparison is because the author is most familiar with their geology. Obviously, many other localities of the western Tethys, or even of the Atlantic, could have been chosen.

Bay of Biscay

Site 401 is located on top of a tilted block at the edge of the Meriadzek Terrace; it shows hiatuses and condensations at several levels in the Cretaceous/Eocene sequence (Figures 6 and 7):

In Sample 19-1, 121-125 cm, there is a probable hiatus or a level of intense condensation below the upper Aptian, marked by streaks and mottles, and comprising P-Mn-Fe cauliform structures (Plate 1, Figures 1, 2) similar to oceanic stromatolites such as those of Blake Plateau (Monty, 1973) or of the Briançonnais zone (Bourbon, 1971, Plate 1, Figures 3, 4, 5).

Sample 19-1, 90 cm, shows a hiatus between the Aptian and the Campanian without P or Mn crusts at the contact.

Sample 14-3, 125 cm, shows possible condensation of sedimentation by the presence of an Mn nodule.

Sample 13-4, 123-128 cm shows a possible hiatus in the lower Eocene, indicated by the presence of collophanite.

Site 402 is located on a spur, north of the Meriadzek escarpment; it shows also a hiatus between the Albian and Eocene.

Briançonnais

Comparable hiatuses and condensations occur also in the Briançonnais zone, at the boundary between the Middle and Upper Jurassic, in the Lower Cretaceous, in places in the Upper Cretaceous, and in the Paleocene.

Some of these hiatuses are clearly associated with the early stages of evolution of the margin, which commonly shows deposition of platform carbonates, unconformities associated with phosphatic crust or Fe-Mn nodules, and deposition of deep pelagic sediments. Such is the case in Sample 401-19-1, 121-126 cm, and at the boundary of the Middle and Upper Jurassic in the Briançonnais zone.

In other instances, the origin of the hiatuses is less certain. It may be due to subsequent evolution of the continental margin wherein active tectonism, such as intense and sudden subsidence, occurred during certain periods, as for example during Cenomanian/Turonian times (Figures 6 and 7), accompanied by roughly synchronous erosion by bottom currents. The origin of the hiatus in the Paleocene is particularly difficult to determine, but this hiatus is widespread and known in several oceans (Lemoine, 1953; van Andel et al., in press). Bottom current erosion during this period also exists in the Briançonnais zone (Bourbon, in press).

Acknowledgments

I would like to thank the Deep Sea Drilling Project and especially David Roberts and Lucien Montadert for giving

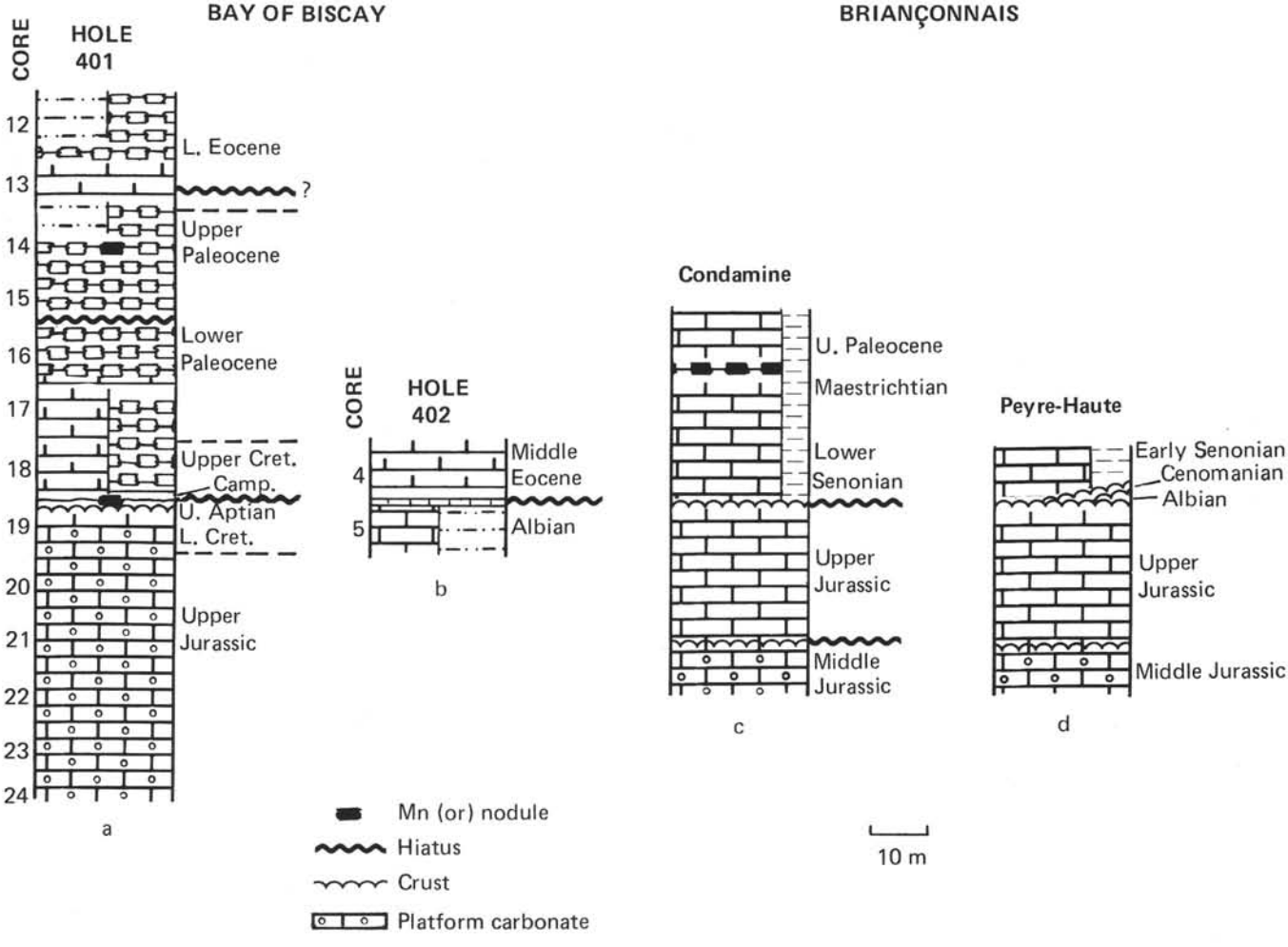

Figure 6. *Marine hiatuses and condensations in two sections in the Bay of Biscay.*

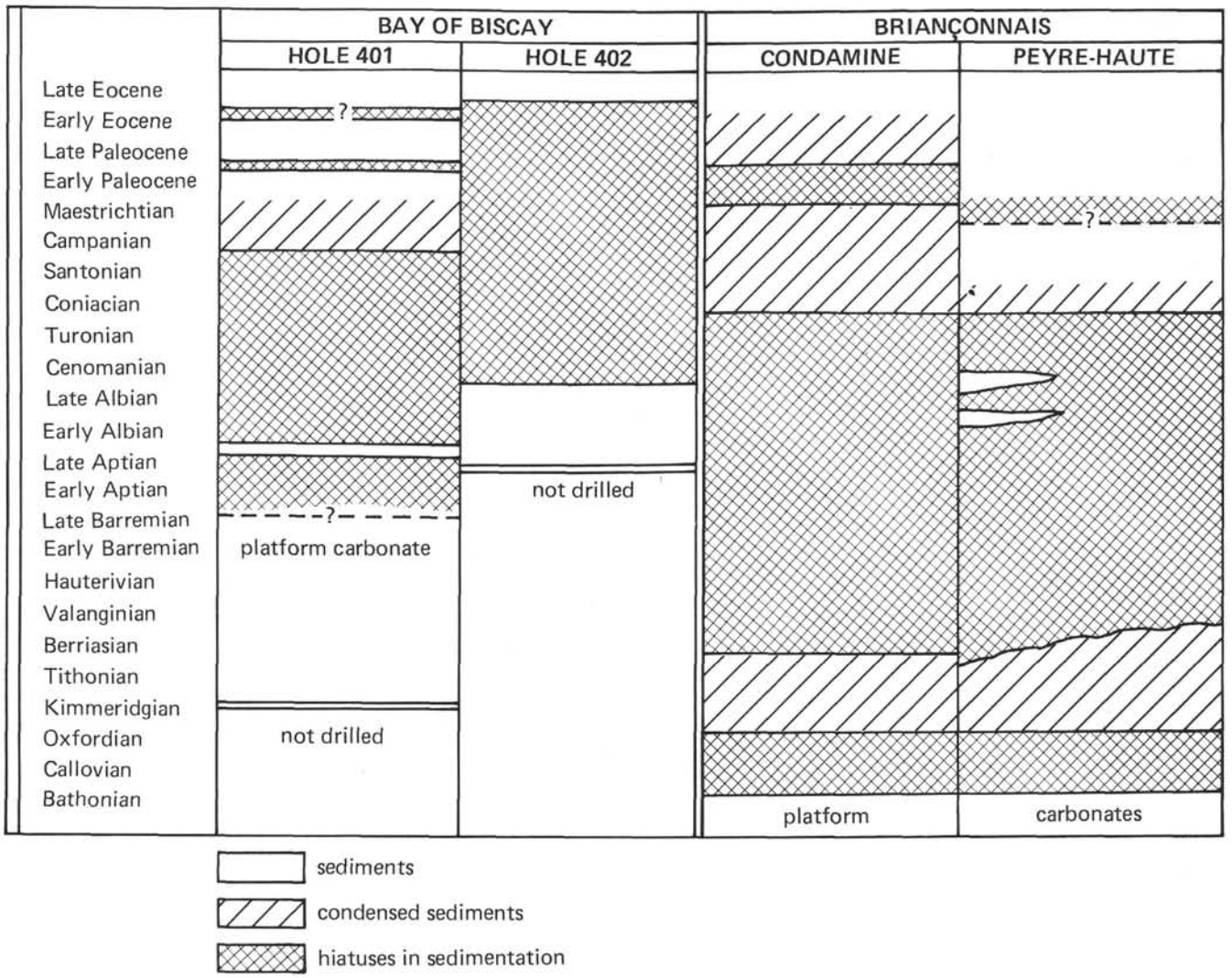

Figure 7. *Hiatuses and condensations in the sedimentary sequences of the Bay of Biscay and the Briançonnais; attempt at comparison.*

me the opportunity to write a paper on Leg 48 results. I am also grateful to Edward L. Winterer who has reviewed this text.

PETROLOGY OF JURASSIC/CRETACEOUS SHALLOW MARINE CARBONATES: DSDP SITE 401, THE BAY OF BISCAY

David N. Lumsden

Introduction

Site 401 penetrated 94 meters of hard, Jurassic to Cretaceous limestones of shallow water origin in the sub-bottom interval from 247.3 to 341.0 meters. Shallow water carbonates have been drilled at other DSDP sites, but the previous locations have been on isolated seamounts obviously not related to large scale reservoir-source rock complexes (James and Hopkins, 1972; Hesse, 1973; Matter and Gardner, 1975). The location of Site 401 on the margin of the Meriadzek Terrace is of considerable economic interest because the limestones are porous and are a potential petroleum reservoir. Of more general interest is the fact that Site 401 was involved in both shallow and deep water phases of the opening of the Bay of Biscay. Thorough study of these limestones is of potential value in determining both the age and nature of the opening of the Bay and the age and nature of carbonate cementation.

Sample recovery was poor, with only 4.3 meters of core recovered from the 94.0 meters penetrated. A maximum of 1.83 meters was recovered in Core 19 and there was no recovery in Cores 25 to 28. The samples were partially rounded and abraded chunks severely disrupted by drilling; one cannot assume, therefore, that the recovered samples are from the depths plotted in Figure 8. Weakly cemented friable zones almost certainly were disaggregated and lost during drilling, the samples obtained thus represent only the more solid, well-cemented portions.

Well-preserved fossils are rare, which makes dating difficult and speculative. From numerous thin sections, Dupeuble (this volume) has determined that the chalks immediately overlying the limestone are Campanian (Sample 19-1, 90 cm); that the top of the shallow water

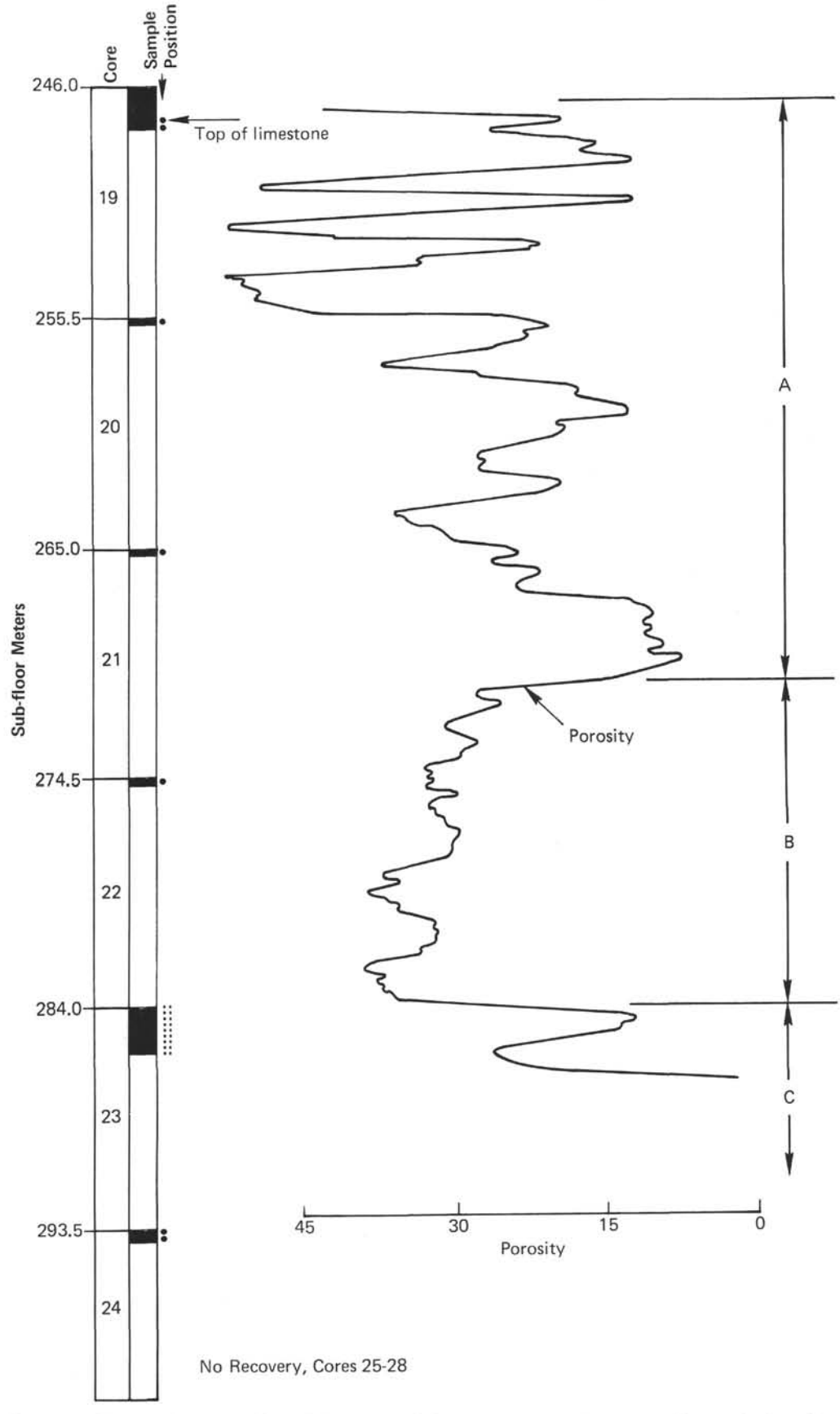

Figure 8. *Relation between Site 401 cores and the neutron porosity curves. Intervals A to C are for text discussion purposes.*

limestone in Core 19 is probably Upper Aptian, indicating a substantial (Santonian to Albian) unconformity between the chalks and the limestones; that Cores 20 to 21 are of late Tithonian to Berriasian age; and that Cores 22 to 24 are possibly Kimmeridgian to Portlandian.

The contact between the shallow water limestone and the overlying deep water chalks (depth of deposition possibly 1500-2000 m) is sharp (Figure 9). Although no evidence for solution is visible, paleontologic dating indicates a hiatus between them. It is possible that the sharp contact may be the result of drilling effects that forced a chunk of the solid limestone into the relatively undisturbed overlying chalks. The lower contact of the limestone was not penetrated.

Sample color is dominantly white, grading upward into very pale orange at the top. Most specimens have visible porosity and some are quite friable. Corals, crinoid columnals, rounded intraclasts, and peloids are visible megascopically. Grain size is commonly coarse with, in some samples, clasts up to 6 cm in diameter.

Mineralogy

From thin-section, X-ray diffraction, and scanning electron microscope analyses, it is determined that the only mineral present is low-magnesium, non-ferroan calcite. Two samples (23-1, 106 cm and 23-2, 17 cm) have a single low unexplained peak at 44.8 degrees two theta. This peak does not fit any of the common sedimentary minerals (Cook et al., 1972) nor does it fit expected contaminants such as aluminum oxide.

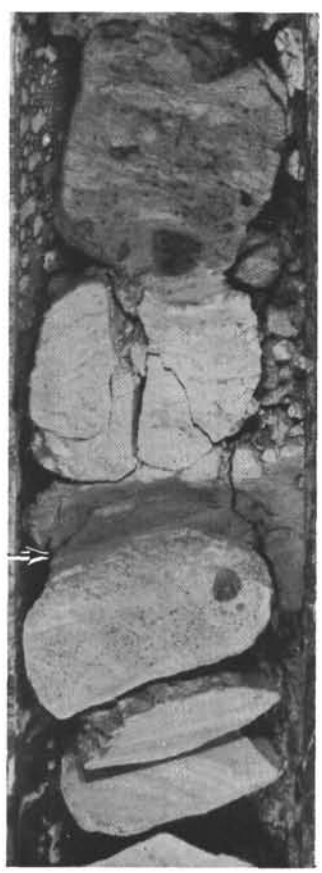

Figure 9. *Contact between deep marine (bathyal) chalks above and shallow-water hard limestones below is very sharp (at arrow). There is no evidence for solution either above or below the contact. Scale lines drawn at 5-cm intervals. Sample 401-19-1, 115-135 cm.*

Petrography

The samples (Table 3) are classified using Dunham's (1962) terms (Introductory chapter, this volume). Of the 14 examined specimens, the bulk are peloidal, well-rounded and well-sorted grainstones with a maximum grain size generally in the granule or pebble range. Boundstone accounts for four (possibly six) of the samples. Although boundstone is difficult to identify in thin section, the presence of large, apparently unabraded, coral fragments, large particles (up to 3 cm), and poor sorting (smaller grains in patches between larger coral fragments) suggest boundstone. The remaining samples are wackestone and welded peloid packstones.

Framework

Three groups of framework grains, peloids, clumps, and fossils, occur in these samples.

Peloids: This term is used to describe members of a polygenetic group that form 2 to 65 per cent of the framework grains present (Table 3).

Micritized grains have a variably thick envelope of micrite coating a core of fossil or, less commonly, sparry calcite. The coating has a sharp external boundary, but its internal margin grades into the core material (Plate 2, Figure 1). The coating is the result of the boring of endolithic algae rather than simple mechanical coating (Bathurst, 1966). In thin section, micritized grains are well rounded with smooth lobate shapes partially corresponding to the original morphology of the core grain. In most cases the nature of the core material is evident, but in many grains either the plane of the thin section has not exposed the core or else the grain is entirely micritized. Where such grains are small they are impossible to distinguish from peloids of fecal origin. Swinchatt (1969) concluded that abundant micritized grains indicate shallow water, certainly less than 40 meters and probably less than 18 meters.

Fecal pellets are also present but not common, and are distinguished by their small size (commonly 0.03 mm or less), good sorting, elliptical shape, and somewhat darker color. They often occur in patches and, when disseminated, they are indistinguishable from small micritized grains.

Because of their small size, many of the grains included as peloids in point count analysis may actually form as the algal lumps discussed below.

Clumps: This term is adapted here to cover a polygenetic group of intraclasts, algal lumps, and large micritized grains, so similar and gradational in character that separate recognition is difficult.

Intraclasts (Folk, 1962) are present but are quantitatively insignificant. They occur in boundstones or partially disrupted lime mudstones (Samples 19-1, 141 cm; 21-1, 15 cm; 23-1, 19 cm).

The vast majority of the grains called clumps are probably algal lumps, grains that appear to be aggregates of diverse primary grains bound together by algae. A typical example can be seen in Plate 2, Figure 2. These grains

TABLE 3
Summary of Petrographic Data, Shallow-Water Limestone, Site 401

Sample (Interval in cm)	Depth Sub-Bottom (m)	Class: Lime Mudstone	Wackestone	Packstone	Grainstone	Boundstone	Point Count (per cent) Grains: Peloids	Clumps	Fossils	Matrix: Micrite	Spar: Neospar	Cement	Void	Maximum Detrital Grain Size: >2.0	1.0 - 2.0	0.5 - 1.0	0.25 - 0.5	<0.25	Maximum Cement XL Size: 1.0 - 4.0	0.25 - 1.0	0.062 - 0.25	0.016 - 0.062	0.004 - 0.016	Fossils Present: Echin	Cural	Algal	Furam	Pelec	Other	Cement Types: Isopach	Meniscus	Bimudal	2 Generation	Rim	Pore Types: Inter	Intra	Solution	Framework	Remarks
19-1, 141	247.41				x		6	33	3	24		31	3	x					✓					✓	✓	✓	✓	✓	✓	✓		✓	✓	✓	✓				Boundstone (?)
19-1, 66	247.57				x		10	34	17	0		38	1	x							✓			✓	✓	✓	✓	✓	✓	✓				✓					Boundstone (?)
20-1, 10	255.60			x			5	5	4	75		0	10	1			x					✓			✓	✓			✓				✓	✓				Welded texture
21-1, 15	265.15		x												x				✓					✓		✓				✓				✓			✓	Disrupted, fecal pellets
23-1, 30	284.30				x		36	8	19	8		15	14			x						✓		✓	✓	✓	✓	✓	✓				✓	✓				Uniform
23-1, 0	284.00		x																														✓					Poor TS, no analysis
23-1, 19	284.19					x																		✓	✓	✓			✓		✓			✓	✓				Patchy, large corals
23-1, 30	284.30			x			2	5	16	54		19	3			x								✓	✓		✓	✓		✓			✓	✓				Disrupted, welded
23-1, 40	284.40					x	14	2	13	17		25	28					x					✓	✓	✓		✓	✓	✓	✓			✓	✓				
23-1, 50	284.50			x			32	2	5	45		12	4	x								✓		✓						✓			✓	✓				Uniform
23-1, 64	284.64			x			20	3	13	39		12	13	x								✓		✓	✓	✓	✓		✓		✓			✓				Uniform
23-1, 85	284.85				x		13	52	4	2		22	9	x								✓	✓			✓			✓				✓	✓				Uniform
23-1, 101	285.01					x								x							✓				✓				✓				✓	✓				Large coral
23-1, 106	285.06				x		7	49	5	6		23	10	x								✓	✓	✓					✓	✓			✓					Similar to interstitial above
23-1, 119	285.19				x		4	47	3	1		43	2	x								✓	✓	✓						✓			✓					Uniform, as above
23-1, 134	285.34				x		59	0	2	1	24	12	2			x																	✓	✓		✓		Uniform
23-2, 8	285.58				x		56	11	4	2		4	20	3	x						✓			✓		✓	✓	✓	✓					✓	✓				A. A.
23-2, 16	285.66				x		65	3	9	2		0	20	1	x						✓			✓		✓	✓	✓	✓					✓	✓				Uniform
23-2, 17	285.67				x		47	13	0	4	10	23	3	x							✓			✓		✓	✓	✓	✓		✓			✓	✓		✓		Uniform
23-2, 25	285.75				x		59	13	5	1		4	14	4	x						✓			✓	✓		✓	✓	✓	✓	✓			✓	✓	✓	✓		Uniform, bimodal (?)
23-2, 32	285.82				x		59	8	3	1		22	6			x					✓		✓	✓	✓								✓					Uniform
24-1, 0	293.50			x			38	30	3	19		8	2	x							✓			✓										✓					Welded
24-1, 10	293.60				x		15	15	5	42		4	19		x						✓			✓										✓					Patch
24-1, 27	293.77					x																			✓								✓					Coral
24-1, 31	293.81					x																			✓								✓					Coral

Note: In some samples neospar and cement spar are not distinguished.

presumably form in a manner similar to oncolites or the SS stromatolites of Logan et al. (1964), but in Site 401 samples, they usually are not laminated (one grain shows a suggestion of lamination but it may be a micritized oolite). Many of the grains assumed to be algal in origin may actually be intraclasts. It is also difficult to distinguish between small algal lumps and large micritized grains (Plate 2, Figure 3).

Fossils: When present in the interior of micritized or algal lump grains, fossils were not counted individually, but their nature is tallied in Table 3. Of the uncoated fossils, the most common are echinoderm spines and crinoid columnals. Coral is common as finely comminuted particles and in large fragments. Algae, although abundant, are difficult to identify generically. Some samples (e.g., 23-1, 1 cm) contain fragments resembling the red coralline alga *Archaeolithothamnium* (Johnson, 1969). Forms similar to the codiacean genus *Lithocodium* are also present (Plate 2, Figure 3). Other samples (e.g., 19-1, 141 cm) contain a variety of red and green algae (Plate 2, Figures 3, 4). Ostracodes, pelecypods, gastropods, and foraminifers are ubiquitous but quantitatively insignificant. Rudistids may be present, but fragments are not large enough for unequivocal identification.

Cement

Spar cement binds the grains into a solid, if porous, limestone. It is typically fine to medium crystalline (0.04 to 0.22 mm), clear spar with blocky, equant, anhedral crystals. Crystal size is commonly finer adjacent to grains and coarser toward the center of interstices. Some primary voids are unfilled with uniform coating around the margins. In a few cases meniscus cement (Dunham, 1971) appears to be present and thick rim cement is common.

Two generations of cement are evidenced by (a) lines of inclusions (Sample 19-1, 141 cm, Plate 2, Figure 5), (b) cloudy spar juxtaposed to clear spar (Sample 19, CC, Plate 3, Figures 1, 2) and (c) bimodal crystal size with fine marginal and large centripetal spar (Plate 2, Figure 6). The latter is similar to that occurring in shallow water carbonates; beachrock (Bathurst, 1975); and reefs (Ginsburg et al., 1971).

Meniscus cement (Plate 3, Figure 3) may possibly be the result of a postdepositional meteoric phase of cementation.

Although the common rim cement *appears* to replace surrounding micrite or microspan (Plate 3, Figure 4), it fails to encroach on adjacent grains and is interpreted to be first generation followed by the second generation, centripetal microspar.

Matrix

Micrite (< 4 microns) is present in all samples (trace to 75%) but generally matrix is subordinate to cement. Much of the material classed as spar in Table 3 is neomorphic spar (Folk, 1965). *Structure grumeleuse,* dispersed clots of micrite in fine spar (Cayeux, 1935), is common.

Porosity

Visible porosity is present in all samples and ranges from 1 to 28 per cent of volume. Most pores are interparticle but intraparticle, solution, and shelter pores also are present.

Structures

In hand specimen, samples appear massive and structureless; one sample showed a small patch of

lamination. Most grain contacts were point, a few were planar. Post-depositional fracturing of grains is rare (Plate 2, Figure 3; Plate 3, Figure 4). On the whole, the fabric is open and uncompacted.

Geophysical Logging

The neutron log, partially reproduced in Figure 8, shows that the overall porosity of the limestone is variable but relatively high.

The log suggests a threefold subdivision of the limestone. Sub-unit A, from 247.3 to 271 meters, consists of 1- to 3-meter-thick alterations of very porous (50%) to moderately porous (15%) intervals. Sub-unit B, from 271 to 284.5 meters, is a uniform, high porosity zone (approximately 35%). Sub-unit C is a generally dense zone with porosity in the 10 to 15 per cent range, that extends from 284.5 to 341.0 meters (total depth). This subdivision cannot be supported unequivocally by the sparse sample data.

Summary and Conclusions

Site 401 bottomed in a hard, Jurassic to Cretaceous limestone of shallow water origin. The limestone is dominantly coarse sand peloidal grainstone and very coarse sand to pebble coral boundstone. The dominant grain components are micritized fossils and algal lumps. Fossils are abundant and include algae, coral, crinoid, mollusk, and foraminifer fragments. The rock is bound into a hard limestone by low magnesium, blocky, spar cement. Porosity is excellent, possibly reaching 50 per cent, being largely interparticle with intraparticle, shelter and solution porosity also present.

Cementation appears to have occurred in two successive stages, the first of which most likely was syndepositional. It is conceivable that the first generation cement was aragonite and/or high magnesium calcite as is suggested by the bimodal crystal size distribution. If such was the case, it was replaced by the low magnesium calcite of the second generation cement. The locus of the second generation most likely occurred in the marine environment, prior to deposition of the overlying marine oozes, but there is some slight evidence that it may have been produced by meteoric processes.

The dominance of high-energy facies, the presence of shallow water fossils, and the abundance of micritized grains all point to deposition of the limestone in shallow agitated water in depths of 0 to 10 meters. The few wackestone and packstone samples may have originated in small sheltered ponds or within growth framework cavities.

Speculative Considerations

It is tempting to regard these limestones as reef-related. The abundance of algae and coral material, the boundstone nature of some specimens, and the shallow, high-energy environment witnessed by the texture are characteristic of reefs. If the limestones were deposited in proximity to a reef, its position on the seaward edge of the fault block underlying the Meriadzek Terrace is of interest and may imply reefal growth on other blocks.

Another interesting aspect is the preservation of excellent primary porosity within parts of the interval. The subsidence of fault blocks from very shallow agitated marine to deep bathyal marine conditions may have preserved the excellent primary porosity by sealing with impermeable chalks.

Acknowledgments

I am sincerely grateful for the comments and criticism of Edward D. Pittman and Laurel Babcock, Amoco Petroleum, and Lawrence G. Walker, Union Oil Co.

BIOSTRATIGRAPHY

A discontinuous sequence of sediments ranging in age from Late Jurassic to the late Eocene/early Oligocene and Quaternary was encountered at Site 401 (Figure 10).

Upper Cretaceous to Quaternary sediments are unconsolidated nannofossil or foraminiferal oozes and chalks, containing well-preserved microfossils. Carbonate dissolution is not apparent at Site 401, suggesting that the CCD lay below the deposition level throughout the time recorded by the sediments. Sponge spicules are abundant in Eocene sediments, confirming a generally high spicule productivity at that time, rather than a uniquely high rate of carbonate dissolution as might have been concluded from the evidence of Hole 400A.

Core 1 contained late Quaternary sediments showing a strong glacial-interglacial contrast in the microfauna.

Only middle and early Oligocene microfossils were recovered from the washdown core. The sedimentation rate plot suggests that the stratigraphic sequence is discontinuous in the non-cored interval.

Continuous coring commenced at 84.5 meters subbottom in lowermost Oligocene or upper Eocene sediments. Sedimentation was apparently continuous from the early Paleocene to the late Eocene. The oldest Tertiary sediments are recorded from Sample 17, CC; they are early Paleocene in age, NP 3, on the basis of nannofossils, or P.1 on the basis of planktonic foraminifers. Throughout this interval Site 401 was at bathyal depth as indicated by typical deep water benthic foraminifers. Very few "midway" type benthic foraminifers, which are thought to be of neritic origin (Berggren and Aubert, 1975) were present in samples from this interval. Upper Cretaceous (Maestrichtian and Campanian) sediments are separated from the Paleocene sediments by a hiatus of little more than one million years. The benthic foraminifers of the Upper Cretaceous sediments are essentially the same as those in the overlying Paleocene sediments, suggesting their deep water (bathyal) deposition.

The remainder of the sequence consists of a thin intercalation of upper Aptian sediments underlain by indurated limestones of Early Cretaceous and Late Jurassic age, all possibly deposited in shallow water. The principal subsidence of Site 401 thus must have occurred after the Late Jurassic/Early Cretaceous and before the Late Cretaceous, a time interval of about 25 million years.

Foraminifers

Quaternary foraminifers were recovered from Core 1. Interglacial, possibly Holocene faunas were of the "transitional" type, glacial faunas of the subarctic type of Bé and Tolderlund (1971).

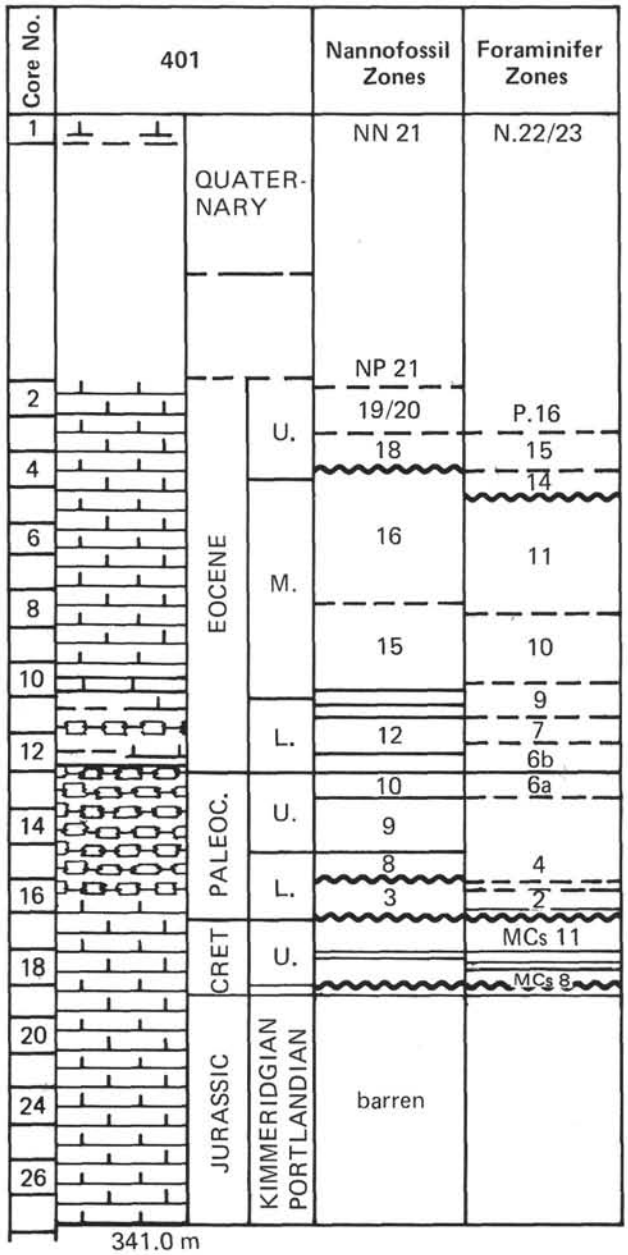

Figure 10. *Biostratigraphic summary, Site 401.*

The core that resulted from the washdown procedure between 9.5 and 84.5 meters sub-bottom contained middle Oligocene planktonic foraminifers. Below that depth Sample 2, CC yielded, among other species, *Hantkenina alabamensis, Globigerinatheca index,* and *Globorotalia cocoaensis* which, although commonly reported from the upper Eocene only, are reported by Blow (1969) to occur as well in the oldest Oligocene.

The boundary between the lower and middle Eocene occurs between Samples 4, CC and 5-3, 119-121 cm. A hiatus of over 2 m.y. possibly exists between Samples 5-3, 119-121 cm and 6-2, 53-55 cm. Between these two samples the foraminiferal Zones P.13 and P.12 were not encountered. Noteworthy is the extended interval over which sediments of Zone P.11 and P.10 age were found; Cores 6, 7, and 8 are dated P.11, Cores 9 and 10 are dated P.10, thus about 45 meters of sediments in this interval were deposited in 2.2 m.y.

The mid-to-lower Eocene boundary lies either between Cores 10 and 11 or within the top of Core 11. Sample 11-4, 95-97 cm contained well-preserved *Globorotalia caucasica, G. quetra, Globigerina prolata,* among others, assigning it to Zone P.9. Zones P.8, P.7, and P.6b are each represented. Division between Zones P.6b and P.6a, the Eocene-Paleocene boundary, occurs between Sample 12, CC which contains *Globorotalia acuta, G. quetra,* and *G. broedermanni,* and Sample 13, CC which contains *G. velascoensis* and *Pseudohastigerina wilcoxensis,* among others. Zone P.5 was not encountered, probably due to insufficient sampling density; the upper and middle Paleocene Zones P.4, P.3, and P.2 are well defined by many species. The oldest Paleocene sediments were encountered in Sample 17, CC which contained *Globigerina daubjergensis, G. triloculinoides, Globorotalia pseudobulloides,* and *G. trinidadensis,* in abundance.

A hiatus of not much more than one million years separates the Tertiary from the youngest Mesozoic deposits. Diverse and abundant foraminifers of the *Globotruncana mayaroensis* Zone (MCs 11) are recovered from Sample 18-1, 12-13 cm. From Samples 18-1, 18-20 cm to 18-1, 86-88 cm the *Globotruncana gansseri* Zone (MCs 10) of the upper to middle Maestrichtian is present as defined by the presence of *Globotruncana contusa, G. stuarti,* and *Racemiguembelina fructicosa.* The lower Maestrichtian *G. stuarti/G. falsostuarti* Zone (MCs 9) occurs from Sample 18-1, 124-128 cm to 18-2, 8-10 cm. The planktonic foraminiferal fauna of this zone is less diversified.

Uppermost Campanian sediments of the *Globotruncana calcarata* Zone (MCs 8) are present from Samples 18-2, 58-60 cm to 18, CC. From Sample 19-1, 34-36 cm to 19-1, 89-92 cm *Globotruncana elevata, G. stuartiformis, G. arca,* and *G. fornicata* are common to abundant, indicating a Campanian age, the *G. elevata/G. stuartiformis* Zone (MCs 7). In the Upper Cretaceous sediments, benthic foraminifers are rare and indicative of a bathyal environment.

Upper Aptian (Gargasian-MCi 19) occurs in samples from Samples 19-1, 123-125 cm and 19-1, 127-128 cm, which yield *Hedbergella* sp cf. *H. infracretacea, Schakoina cabri, Globigerinelloides duboisi,* and *G. gottisi.* Hard, reddish bioclastic limestone was recovered from Samples 19-1, 128 cm to 19, CC. It contains fragments of corals, echinoids, algae, stromatoporids (?), gastropods, pelecypods and, occasionally, sponge spicules with some rare *Neotrocholina.* This microfacies has a general resemblance to that of Early Cretaceous age of southwest France, but in the absence of good stratigraphic markers no precise age assignment is possible.

The few pieces of white, porous limestone recovered in the following cores are composed of pellets and fragments of echinoderms, corals, and pelecypods. Rare calpionellids (*Calpionella* gr. *C. alpina, Tintinopsella* gr. *T. carpathica*) in Samples 20-1, 1 cm and 21-1, 11 cm date these as latest Tithonian to Berriasian.

Sample 22-1, 10 cm is particularly rich in large coral fragments. Some foraminifers such as *Nautiloculina, Trocholina,* and one specimen of *Conicospirillina* suggest a

Late Jurassic age. Thin sections from Core 23 show the limestone to be composed of pellets and bioclasts. Among echinoids, pelecypod, and coral debris, such foraminifers as *Conicospirillina basiliensis, Pseudocyclammina, Trocholina, Nautiloculina,* and possibly *Kurnubina* occur. In addition to algal oncolites and *Thaumatoporella parvovesiculifera,* fragments of *Cladocoropsis mirabilis* are present. Such an assemblage is mainly known from Kimmeridgian and Portlandian deposits. The limestone recovered in Core 24 is porous and, in addition to the fossils mentioned above, the algae *Lithocodium aggregatum* and *Baccinella irregularis* could be identified, which confirm the Late Jurassic age assignment (Kimmeridgian to Portlandian).

The thin deposit of upper Aptian sediment could possibly have originated in an upper continental slope environment, and the entire sequence of indurated limestones indicates a shallow water deposit, reefal to peri-reefal. The presence of calpionellids in such shallow water deposit suggest proximity to the open sea.

Nannofossils

Pleistocene sediments of the *Emiliania huxleyi* Zone (NN 21) were recovered in Core 1 (0-8.5 m). Nannofossils are scarce, being mainly reworked Cretaceous species.

The washdown core contained middle Oligocene nannofossil ooze of the *Sphenolithus distentus* Zone (NP 24); the sediments are rich in slightly etched nannofossils; *Sphenolithus distentus, S. predistentus*, and *Helicosphaera recta* are frequent in some samples. Lower Oligocene sediments of the *Ericsonia subdisticha* Zone (NP 21) occur in Core 2. Nannofossils are abundant, but are slightly etched and broken. *Chiasmolithus oamaruensis*, which indicates low surface water temperatures, is common in some layers.

The *Isthmolithus recurvus/Sphenolithus pseudoradians* Zone (NP 19/NP 20) of the upper Eocene occurs in Core 3 (94.0-103.0 m). The sediments are rich in slightly broken nannofossils; discoasters are abundant. Sample 4, CC contains the *Chiasmolithus oamaruensis* Zone (NP 18). Nannofossils are abundant, but strongly broken.

A hiatus, which represents an interval of about one million years, involving the *Discoaster saipanensis* Zone (NP 17), lies between Samples 4, CC and 5-1, 35-36 cm.

The *Discoaster tani nodifer* Zone (NP 16) and the *Chiphragmelithus alatus* Zone (NP 15) of the middle Eocene are present from Samples 5-1, 35-36 cm to 11-1, 32-35 cm (113.0-170.5 m). The sediments have abundant siliceous microfossils and calcareous nannofossils. Coccoliths are slightly etched to well preserved, whereas the discoasters are slightly overgrown. The boundary between nannoplankton Zones NP 16 and NP 15 lies between Sample 6, CC and 7-1, 51-52 cm, defined by the last occurrence of *Rhabdosphaera gladius*. This index species occurs only sporadically, whereas *Chiasmolithus gigas,* which is typical for the lower part of nannoplankton Zone NP 15, is present in almost all samples. Few specimens of *Discoaster lodoensis* and *C. alatus* were observed. Further investigations must show if the latter species has a longer range or if these few specimens are reworked.

The *Discoaster sublodoensis* Zone (NP 14) is represented only in Samples 11-2, 22-23 cm and 11-3, 25-26 cm. The occurrence of *Rhabdosphaera inflata* seems to be restricted to this zone. Samples 11-3, 80-82 cm to 11-5, 39-40 cm include the *Discoaster lodoensis* Zone (NP 13). Nannofossils are abundant, the coccoliths are etched and broken, and the discoasters are overgrown.

Samples 11, CC to 12, CC encompass the *Marthasterites tribrachiatus* Zone (NP 12) with *Discoaster lodoensis* and *Marthasterites tribrachiatus*. Nannofossils are abundant, but poorly preserved. The *Discoaster binodosus* Zone (NP 11) is recognized from Samples 13-1, 48-49 cm to 13-3, 46-47 cm, and the *Marthasterites contortus* Zone (NP 10) from Samples 13-3, 107-108 cm to 13, CC. Determination of the nannoplankton Zone NP 10 is based on the presence of *Discoaster multiradiatus, D. diatypus,* and *Marthasterites tribrachiatus,* whereas *M. contortus* is missing.

On the basis of nannofossils, the Paleocene/Eocene boundary lies between Core 13 and Core 14. The upper Paleocene *Heliolithus riedeli* Zone, NP 8, and *Discoaster multiradiatus* Zone, NP 9, are present from Samples 14-1, 26-27 cm to 16-3, 21-22 cm (-198.5 to -220.0 m). The sediments contain abundant well preserved to slightly overgrown nannofossils.

A hiatus, which represents an interval of less than 4 m.y. lies between Samples 16-3, 21-22 cm and 16, CC.

Samples 16, CC to 17, CC encompass to the *Chiasmolithus danicus* Zone (NP 3). Nannofossils, badly preserved, are common. The abundance of *Braarudosphaera bigelowi* may indicate the influence of near-shore waters. Small specimens of *Ellipsolithus* sp. cf. *E. macellus* are scarce.

Another hiatus, representing an interval of about 2 m.y. exists between the Upper Cretaceous of Core 18 and the lower Paleocene sediments of Core 17, according to the nannofossil age determinations.

The uppermost zone of the Maestrichtian (*Tetralithus murus* Zone) is present from Samples 18-1, 11-12 cm to 18-1, 27-28 cm. Sample 18-1, 85-86 cm involves the *Lithraphidites quadratus* Zone of the Maestrichtian; nannofossils therein are extensive but strongly etched and broken.

The uppermost Campanian/lowermost Maestrichtian (*Broinsonia parca/Tetralithus trifidus* Zone) is determined from Samples 18-1, 120-121 cm to 19-1, 98-99 cm. Unequivocal determination of the *Tetralithus trifidus* Zone is not possible because *T. trifidus* is missing, but *Lucianorhabdus cayeuxii* becomes abundant in Samples 18-1, 120-121 cm; 18-1, 130-131 cm; and 18, CC. The uppermost part of Samples 19-1, 27-28 cm to 19-1, 98-99 cm involves the *Broinsonia parca* Zone.

Sample 19-1, 127-128 cm from marls just above the reddish limestone contains a nannoplankton assemblage which consists mainly of nannoconids such as *Nannoconus bucheri, N. elongatus, N. kamptneri, N. minutus, N. truitti,* and *N. wassali*. Other species of this assemblage are: *Watznaueria barnesae, W. communis, W. britannica, Manivitella pemmatoides, Lithraphidites carniolensis, Corollithion achylosum, Parhabdolithus asper, P. embergeri, P. infinitus, P. splendens, Cretharhabdus*

crenulatus, Chiastozygus litterarius, and *Stephanolithion laffittei*. This assemblage is of late Aptian age. Abundance of nannoconids is typical of neritic water deposits. The hiatus between the upper Aptian and the Campanian represents an interval of about 38 million years.

The limestones recovered at Site 401 from 247.5 to 341.0 meters sub-bottom are barren of nannofossils.

Dinoflagellates

Most Tertiary samples processed from Site 401 are barren of dinoflagellate cysts apart from one or two exceptions notably including Sample 401-2-1, 34-36 cm which yielded *Chiropteridium lobospinum* (Gocht) Gocht, a species with a known European stratigraphic range of lower to upper Oligocene (Harker and Sarjeant, 1975), together with many reworked Eocene species. This sample has been assigned an early Oligocene age based on calcareous micropaleontological evidence.

PHYSICAL PROPERTIES

Although determinations of physical properties (in addition to downhole logs for spontaneous potential, gamma ray, formation density, neutron porosity, sound speed, and resistivity) involved 46 samples from 341 meters of hole for an average of one sample per 7.4 meters; 36 samples came from the interval between 84 to 247 meters for an average of one sample per 4.5 meters. The introduction to this volume includes discussion of purpose and procedures for these measurements and related calculations.

The ranges of determinations include: coring time (0.5-5 min/m), sound speed (1.3-6.4 km/s), wet bulk density (1.68-2.71 g/cm^3), sound impedance (2.7-17.4 g/cm^2 s $\times$ 10^5), porosity (35-67%), and water content (11-39% by weight). The data presentation consists of numerical tables (Table 4) and depth plots on the superlogs in the pocket of this volume.

Various combinations of compaction, cementation, fracturing, and unloading (cores brought to the surface versus *in situ*) as well as composition may explain physical property trends and the agreement or disagreement between measurements on cores versus downhole. Subsequent paragraphs discuss each of the following three sub-bottom

TABLE 4
Physical Property Summary, Site 401

Sample (Interval in cm)	Depth Sub-Bottom (m)	Strength: Vane Shear (g/cm^2) Original	Strength: Vane Shear (g/cm^2) Remold	Sound Velocity (km/s) (Hamilton Frame) ∥ to Beds	Sound Velocity (km/s) (Hamilton Frame) ⊥ to Beds	Anisotropy ∥-⊥	Anisotropy ∥-⊥ / ⊥	C°	Wet Bulk Density (g/cm^3) GRAPE (2 Minute) ∥ Beds	Wet Bulk Density (g/cm^3) GRAPE (2 Minute) ⊥ Beds	Wet Bulk Density (g/cm^3) Syringe (wt./vol.)	Wet Bulk Density (g/cm^3) Chunk (wt./vol.)	Sound Impedance [g/cm^2/sec] 10^5 GRAPE Density	Sound Impedance [g/cm^2/sec] 10^5 Chunk Density	Porosity (%) GRAPE Wt. H_2O Volume	H_2O (wt. %)	CO_3 (%)	Lithology
1-2, 100	2.50																	Nannofossil ooze
1-3, 84-86	3.85	28	1															Brown mud
1-3, 127-130	4.285			1.32				19										Brown mud
1-4, 78-80	5.29	39	18	1.61				20	1.68		1.69		2.70		66.6	39.38		Brown mud
1-4, 144-150	5.97							20			1.67				61.26	36.71		Brown mud
1-6, 66-70	8.18	33	35	1.35							1.74			2.35	54.58	31.41		Brown mud
2-1, 0-3	84.53			1.82				23	1.92			1.89	3.49	3.44	48.75	25.85	78.6	Nannofossil chalk
3-1, 25-29	94.27			1.67	1.64	+0.03	0.02	20	1.89			1.87	3.16	3.12	49.10	26.32	63.3	Nannofossil chalk
3-2, 134-135	96.85										1.70				60.57	35.62		Nannofossil chalk
4-1, 12-14	103.62			1.67				22	1.90			1.92	3.17	3.21	44.29	23.12	69.4	Nannofossil chalk
4-1, CC	103.62							21	1.79			1.90			47.50	24.87		Nannofossil chalk
5-2, 13-19	114.65			1.75	1.70	+0.05	0.09	21	1.92			1.87	3.36	3.27	48.03	25.65	64.3	Nannofossil chalk
5-4, 80-90	118.35											1.83			51.54	28.69	39.8	Nannofossil chalk
5-4, 80-90	118.35										1.79				52.66	29.42		Nannofossil chalk
6-2, 25-32	124.29			1.75	1.60	+0.15	0.09	22	1.86			1.88	3.26	3.29	47.60	25.33	55.1	Nannofossil chalk
6-4, 52-60	127.56			1.69	1.65	+0.04	0.02	22	1.86				3.14					Nannofossil chalk
7-2, 90-96	134.43			1.71	1.70	+0.01	0.01	22	1.87	1.90		1.83	3.22	3.13	50.31	27.44	52.0	Nannofossil chalk
7-4, 106-113	137.60			1.80				22	1.95	1.95		1.95	3.51	3.51	44.07	22.57	50.0	Nannofossil chalk
7-6, 95-98	140.47			1.72	1.69	+0.03	0.02	22	1.86	1.89		1.85	3.23	3.18	48.71	26.28	49.0	Nannofossil chalk
8-2, 101-105	144.03			1.86	1.78	+0.08	0.04	22	1.98	1.95		1.92	3.66	3.57	45.27	23.55	43.9	Nannofossil chalk
8-5, 72-78	148.25			1.81	1.76	+0.05	0.03	22	1.86	1.86		1.89	3.37	3.42	46.81	24.78	48.0	Nannofossil chalk
9-2, 109-114	153.62			1.72	1.69	+0.03	0.02	22	1.89	1.91		1.86	3.27	3.20	49.34	26.58	49.0	Nannofossil chalk
9-5, 31-36	157.34			1.76	1.69	+0.07	0.04	23	1.90	1.76		1.85	3.22	3.26	50.06	27.12	50.0	Nannofossil chalk
10-2, 81-86	162.84			1.83	1.78	+0.05	0.03	22	1.90	1.96		1.95	3.53	3.57	44.28	22.74	53.0	Nannofossil chalk
10-5, 24-29	166.77			1.86	1.79	+0.07	0.04	22	2.27	1.98		1.94	3.96	3.61	45.28	23.34	50.0	Nannofossil chalk
11-2, 5-10	172.25			2.02	2.02	0.0	0.00	21	2.14	2.15			4.33					Nannofossil chalk
11-2, 113-119	172.65			2.16	2.09	+0.07	0.03	21				2.10		4.54	34.57	16.44	70.0	Nannofossil chalk
11-3, 19-23	173.21			2.02	2.03	-0.01		21	2.04	2.03		2.01	4.11	4.06	40.89	20.38	67.0	Nannofossil chalk
11-5, 55-59	176.57			1.74	1.72	+0.02	0.01	21	1.98	1.93		1.94	3.42	3.38	45.68	23.58	52.0	Marly chalk
12-1, 35-40	179.88			1.76	1.73	+0.03	0.02	21	2.01	1.98		1.94	3.51	3.41	45.92	23.67	46.0	Marly, limy ooze
12-4, 67-72	184.70			1.95	1.96	-0.01		21	1.96	1.97		1.93	3.83	3.76	45.03	23.35	69.0	Marly, limy ooze
13-2, 27-32	190.80			1.91	1.86	+0.05	0.03	21	2.00	2.03		2.00	3.85	3.82	41.48	20.79	75.0	Marly, limy ooze
13-4, 2-8	193.55			1.91	1.89	+0.02	0.01	21	2.05	2.06		2.05	3.93	3.92	39.33	19.21	63.0	Marly, limy ooze
14-2, 30-34	200.32			1.78	1.77	+0.01	0.01	22	1.98	1.94		1.92	3.49	3.42	48.38	25.14	61.0	Marly, limy ooze
14-3, 134-139	202.87			1.94	1.91	+0.03	0.02	22	2.00	2.04			3.92					Marly chalk
14-4, 72-78	203.75			2.16	2.03	+0.13	0.06	22	2.14	2.10		2.05	4.58	4.43	38.37	18.75	74.0	Marly chalk
14-5, CC 84-89	204.59			1.83	1.81	+0.02	0.01	22	2.01	1.97		1.95	3.64	3.57	43.79	22.44	64.0	Marly chalk
16-2, 23-27	219.25			1.84	1.83	+0.01	0.01	22	1.84	1.82		1.81	3.37	3.33	49.73	27.50	68.0	Nannofossil chalk
16-2, 135-150	220.43											1.93			43.69	22.59	76.0	Nannofossil chalk
17-2, 129-132	229.81			1.88	1.75	+0.13	0.07	22	1.96	1.80		1.94	3.53	3.65	44.17	22.72	87.0	Foraminiferal chalk
18-2, 14-18	238.16			2.06	2.07	-0.01		22	1.94	1.99		1.96	4.05	4.04	43.45	22.16	91.0	Foraminiferal chalk
19-1, 140-141	247.41				6.42			22		2.71			17.40					Limestone "reef"
20																		
21																		
22																		
23-1, 21-26	284.24				4.99			22	2.52				12.57					Limestone

intervals: 0 to 115 meters, 115 to 170 meters, and 170 to 341 meters.

The top interval, from the ocean bottom to depth 115 meters, consists of progressively more compact carbonate material (70-90% $CaCO_3$) with three influxes of radioactive material at 0 to 20 meters, 35 to 50 meters, and 73 to 80 meters (note the gamma-ray curve) which reduce the content of $CaCO_3$ to the range of 40 to 70 per cent. The few measurements on mudline cores (3-8 m) and at 85 meters probably represent the total range of physical properties in this interval. Sound speed and wet bulk density maxima would coincide with $CaCO_3$ maxima where the porosities and water contents would be least. These fluctuations in $CaCO_3$ may cause seismic reflections at depths of about 20, 50, and 80 meters. The increase in coring time at the bottom of the interval (85-115 m) reasonably reflects the high $CaCO_3$ content and perhaps initial cementation as suggested by the sound speed anisotropy.

The physical properties for the 115 to 170 meter sub-bottom interval of siliceous, marly, nannofossil chalk generally suggest progressively increasing cementation with depth but with puzzling anomalies at depths 115 to 120 and 145 to 155 meters. Although the $CaCO_3$ content (40-60%) continues rather uniformly through the interval, the sound speeds and wet bulk densities increase with depth. The sound speeds measured on the cores show close accord with the downhole logs as well as persistent anisotropy. Slight decreases in porosity and water content suggest some compaction.

Wet bulk densities measured on cores fall within 5 per cent less than the downhole measurements except for the 5-meter interval between depths of 115 and 120 meters where the downhole log shows an abrupt decrease to 10 per cent below the core measurements. Perhaps the indicated low in $CaCO_3$ (40%) has produced undercompaction which reasonably would appear on the downhole log, but might be missed on the core measurements by selection of more compact samples only. Some support for this conclusion comes from the higher values of porosity (53%) and water content (28%) derived from syringe samples at sub-bottom depth 118 meters compared to chunk samples at depths 115 and 124 meters, which show consistent porosity of 48 per cent and water content of 25 per cent.

Perhaps undercompaction due to high fluid pressure also explains the 145 to 155 meter interval. Sound speed and wet bulk density decrease where the $CaCO_3$ content increases, but the porosity and water content also increase.

Physical properties from cores of the bottom interval of chalks and limestones (170-341 m) generally parallel the percentage of $CaCO_3$, showing close accord with the downhole measurements, except at 185 to 195 and 205 to 238 meters where microfracturing perhaps attenuated the sound speed measurements on cores relative to downhole. Generally the coring times, sound speeds, and wet bulk densities increase or decrease with per cent $CaCO_3$, whereas the porosities and water contents vary inversely with $CaCO_3$ content.

Probable seismic reflectors indicated by sound impedance highs at sub-bottom depths in meters of 170, 204, and 247 apparently mark well-cemented limestones. The $CaCO_3$ in each case exceeds 70 per cent, the sound speeds and wet bulk densities increase abruptly where the porosities and water contents decrease abruptly. The top two markers exhibit sound speed anisotropy. Core measurements agree closely with downhole measurements for sound speed and wet bulk density, thereby providing close depth coordination between the core data and the downhole logs.

DOWNHOLE LOGGING

D. Mann

At Site 401, the following logs were run:

1) Borehole Compensated Sonic/Gamma-Ray/Caliper/Variable Density (BHCS/CR/CAL/VDL).

2) Induction 6FF40/Spherically Focused Log/Spontaneous Potential (ISF/SP).

3) Compensated Neutron/Formation Density/Gamma-Ray (CNL/FDC/GR).

The ISF failed on the main logging run but the preliminary check run which was recorded down to 2820 meters (270 m) has been incorporated into the composite log (Figure 11).

The sonic log shows some stair stepping due to ship motion (the heave compensator was not used). Because the caliper jammed soon after coming off bottom, the caliper data are unreliable.

All depths quoted in this report refer either to depths marked on the logging runs, using the density/neutron as the base log or, in parentheses, their equivalent sub-sea bottom depths.

In the discussion of the lithological units and sub-units the information and depths have been used from the site summaries. Figure 12 demonstrates the good correlation between lithology and the logging results. Where depth discrepancies appear artificial, a double arrow marking has been used. Other logging markers which may have lithological/sedimentological significance have been additionally marked in the depth column.

Log Interpretation

Unit 1 — 2550.0 to 2634.5 meters (0-84.5 m)

The only log recorded through this interval was the gamma-ray curve. Recording was made through drill pipe and this has resulted in a corresponding loss of definition. The log shows entry to the drill pipe at 2663.0 meters (118.0 m) and the sea bed at 2550.0 meters. A much higher gamma-ray reading straddles the whole of the Quaternary interval indicating a much higher relative percentage of clay minerals in this stratigraphic unit in agreement with the high detrital clay content of Core 1, 2550.0 to 2559.5 meters (0-9.5 m). Two other minor gamma-ray peaks were observed from 2582.5 to 2593.0 meters (32.5-43.0 m) and 2614.0 to 2619.0 meters (64.0-69.0 m) and relate to relative increases in clay mineral content.

Unit 2 — 2634.5 to 2724.0 meters (84.5-174.0 m)

There is a discrepancy in logged versus drilled depths and the logs would place the lower boundary at 2722.8 meters (172.8 m). Much of the unit consists of nannofossil chalk which appears reasonably homogeneous on the logs with a fairly constant gamma-ray value of 25 to 30 API units. Both the sonic and density logs show gradients from top to bottom of the section. In view of the uniform lithology, the

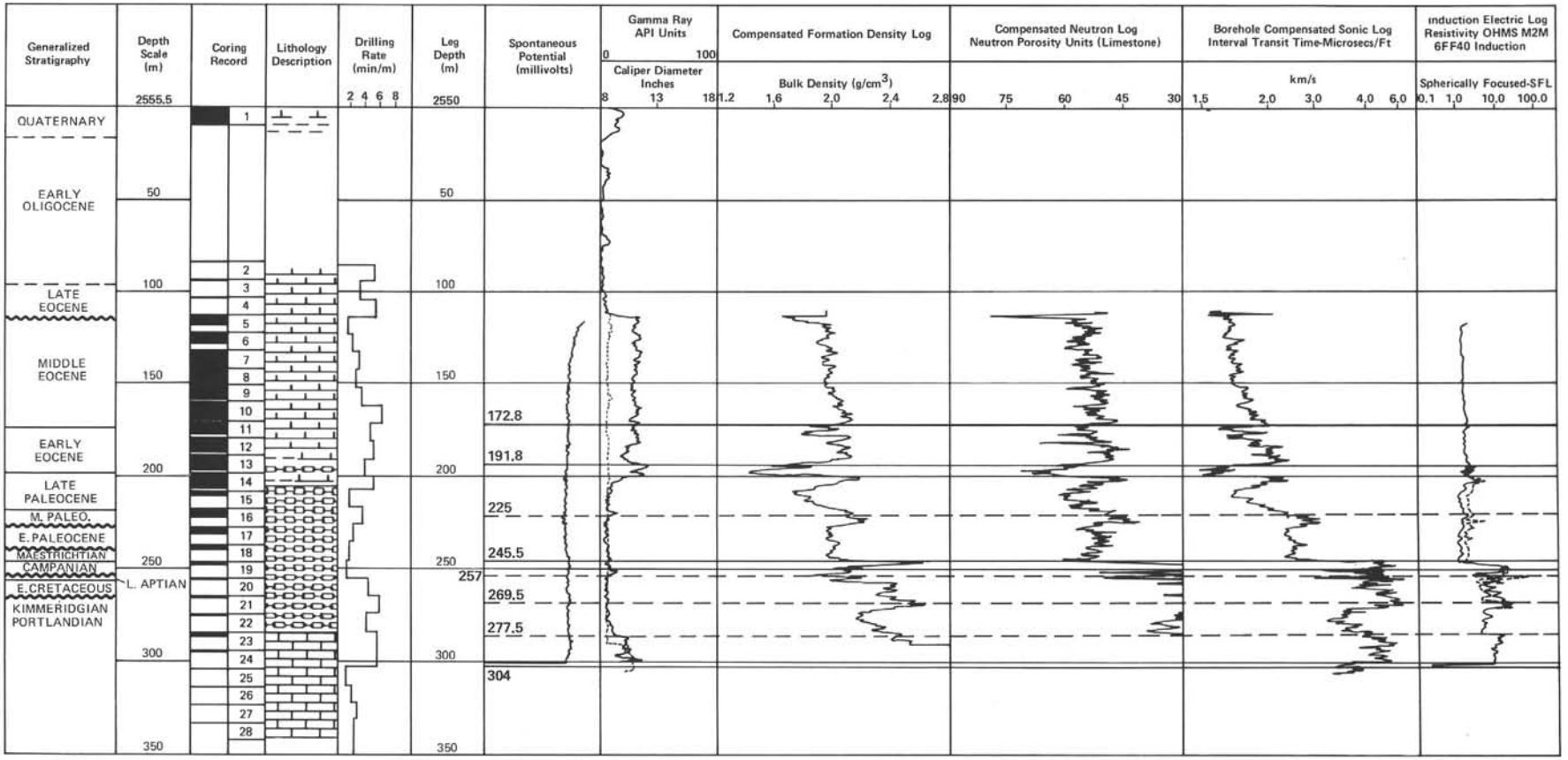

Figure 11. *Generalized stratigraphy of Site 401, well logs, and principal logging breaks, Site 401.*

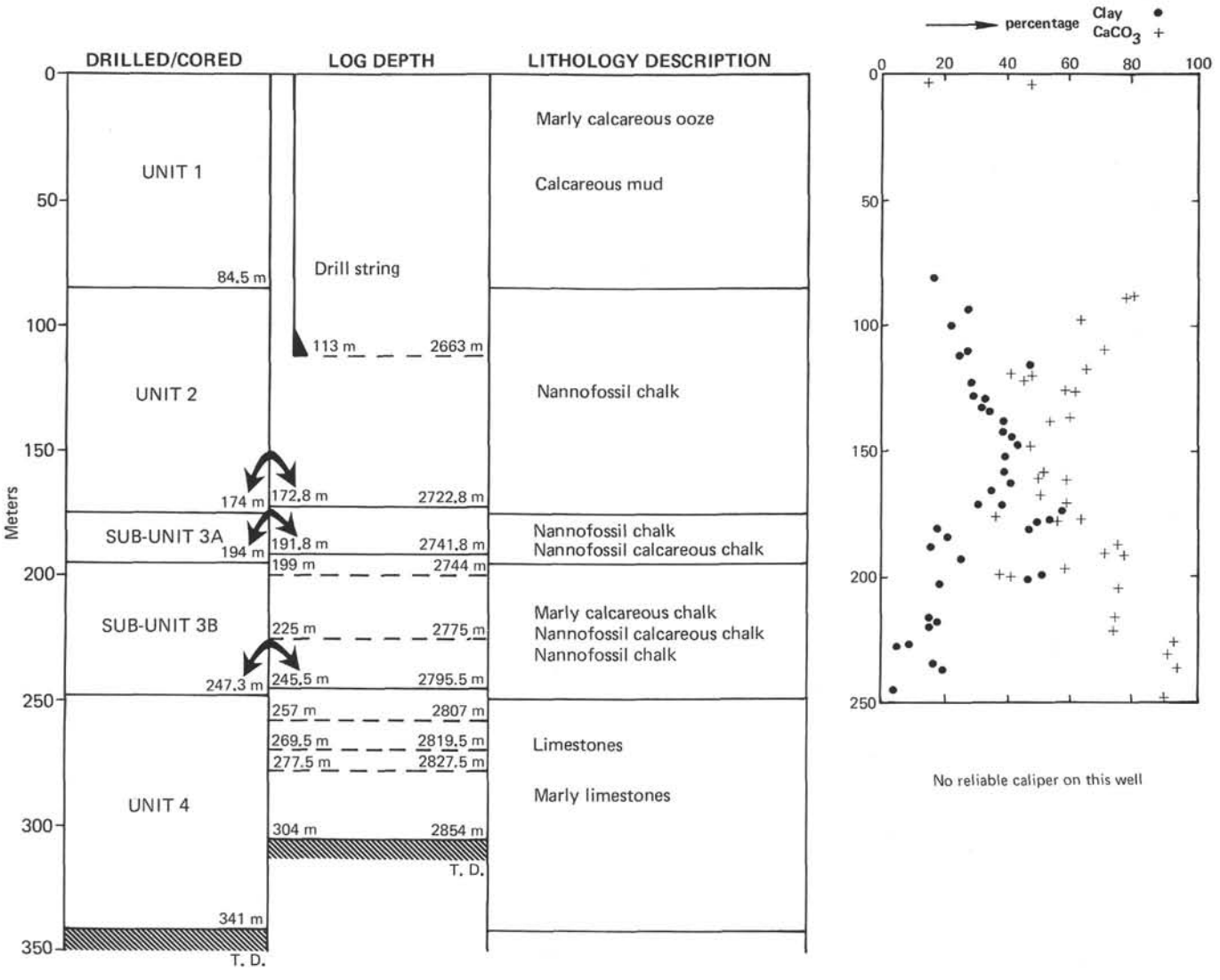

Figure 12. *Correlation of lithologic units and logging breaks, Site 401.*

gradients may be due to compaction effects with depth. At the base of the unit, density and sonic logs show a marked break between 2722.0 and 2722.8 meters (172.0-172.8 m) that corresponds to the thin bed of yellow marly chalk seen in Core 11. This break has been marked on Figure 13.

The crossplots taken in Unit 2 all show fairly tight groupings confirming its uniform lithology. The small amount of scatter is probably due to hole size effects.

The physical properties log shows a fairly constant carbonate content in the range 40 to 65 per cent over the interval actually recorded by the logs, 2664.0 to 2722.8 meters (114.0-172.8 m), with the exception of the marly chalk noted above where the carbonate content drops markedly (see Table 4 and Figure 12).

Sub-Unit 3A — 2724.0 to 2744.0 meters (174.0-194.0 m)

Three peaks on the density/neutron curves 2725.0 to 2727.5 meters (175.0-177.5 m) have similar characteristics to the marly chalk at the base of Unit 2. This bed is followed by a thicker sequence of nannofossil calcareous chalk from 177.5 to 191.8 meters. The Core 12 description indicates the upper part is marly (clay up to 60%), while immediately below this section carbonate (42-55%) increases at the expense of clay mineral content which drops to 20 per cent. The gradual reduction in the gamma ray reading also reflects the increasing carbonate content (Figure 13).

Sub-Unit 3B — 2744.0 to 2797.3 meters (194.0-247.3 m)

The equipment log depth for the top of this unit is at 2741.8 meters (191.8 m). At the top of the unit there is a return to the marly chalks 2741.8 to 2743.7 meters (191.8-193.8 m) seen at the base of Unit 2. The gamma ray log shows two sharp peaks at 2744.0 to 2745.5 meters (194.0-195.5 m) indicating a marked increase in clay mineral content (clay up to 60% recorded in smear slides). A thin but more calcareous section occurs between the two GR peaks with an accompanying trough on the gamma-ray curve. A further section of marly chalks occurs from 2745.8 to 2749.0 meters (195.8-199.0 m). The section from 191.5 to 199.0 meters appears "washed out" so the absolute readings are unreliable. Nevertheless the *relative* readings on the gamma-ray, sonic, neutron, and density curves support the observations made above.

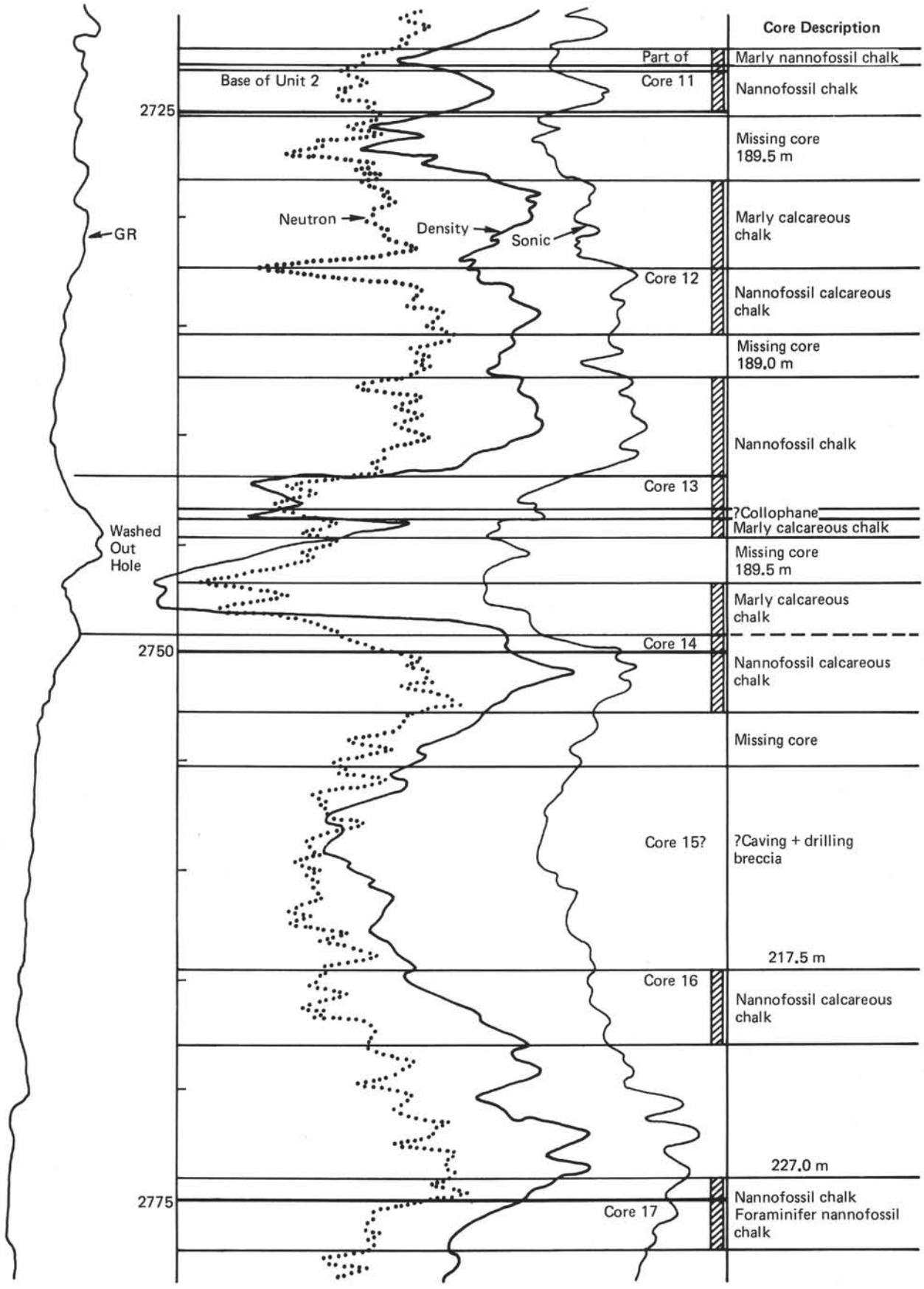

Figure 13. *Core log correlation, Site 401, Cores 11 to 17, 2725.0 to 2775.0 meters.*

The physical properties log, after proper depth alignment, shows a sharp drop in carbonate content over the interval of higher gamma-ray readings excepting the thin calcareous section mentioned above. The increase in detrital material marked by increasing clay content may also help to explain the suspected caving in this zone (191.5-199.0 m).

At 2749.0 meters (199.0 m) nannofossil calcareous chalks become important and continue to 2775.0 meters (225 m). The peak and trough appearance of the logging curves in this section is partly due to hole effects because carbonate is predominant (average 50-60%). There is also a marked decrease in porosity with depth seen on the density and sonic readings.

From 2775.0 to 2795.5 meters (225.0-245.5 m) the lithology appears uniform reflected by carbonate contents of between 80 and 90 per cent. The gamma ray is extremely flat and low over the whole of this section. Figure 14 is a section from the 1:200 scale neutron/density/GR curve with the sonic log superimposed. Due to poor core recovery an approximate lithology has been inferred from the logs.

Unit 4 — 2797.3 to 2891.0 meters (247.3-341.0 m)

The total depth registered by the logs is 304 meters and the tools were unable to reach the total drilled depth of 341.0 meters. The contact between Sub-unit 3B and Unit 4 is clear and abrupt, indicating sudden change in lithology. Density values and sonic velocities increase dramatically and the density value at the contact approaches that of pure limestone (2.71 g/cm^3). This is the top of the reefal facies.

The unit can be subdivided conveniently into the following zones based on log response. Zone 1 (2795.5-2807.0 m [245.5-257.0 m]) shows wide fluctuations in the sonic, density, neutron, and resistivity curves indicating an alternation of harder and softer material in what is predominantly a limestone matrix. However, the poor core recovery and absence of a good caliper log, render any explanations tentative. In general, the zone is not very porous (probably not exceeding 20%) with the sonic log giving the better indications in the poor hole conditions. The major excursions (to higher neutron and lower density values) are a function of hole conditions. The sonic and VDL logs also indicate cycle skipping. The alternating lithologies may reflect changes in cementation with depth, leaving sections of the rock less well supported and friable. However, some change in the texture of the rock from packstone to grainstone is in evidence.

Zone 2 (2807.0-2819.5 m [257.0-269.5 m]) indicates a tight section with porosities mainly in the range 5 to 10 per cent with few excursions to higher values. The density has a more settled range of values in excess of 2.30 g/cm^3 with a trend towards denser limestone at the base of the zone. The pellet grainstone recovered in Core 21 suggests that the sonic values are the more reliable.

Zone 3 (2819.5-2827.5 m [269.5-277.5 m]) at the top, is marked by sharp changes in the readings on all curves. The reduction in sonic velocity and density readings, and the increase in neutron porosity indicate a more porous section of limestone. In confirmation a moderately porous (25-30%) pellet grainstone was recovered in Core 22.

Zone 4 (2827.5-2854.0 m [277.5-304.0 m]) returns to a denser limestone lithology, shown by increasing density and velocity readings but with a slightly more porous section covering the lower 4 meters. Cores 23 and 24 recovered intraclast grainstones and incraclast pellet grainstones.

In Figure 14, the approximate sonic values of porosity have been annotated. The neutron values of porosity are considered unreliable.

Crossplots

Crossplotting techniques of various physical parameters are widely used in the mineral and hydrocarbon industries to help determine lithology and, where appropriate, fluid characteristics. In most cases these plots involve only two parameters of interest but the so-called "Z" plot allows superimposition of a third parameter which in many cases improves the quality of information determined from the plots. Various combinations of parameters were tried in an attempt to confirm predictions from cores and information inferred from the straight comparison of log recorded values. In several cases, the results were more confusing than helpful (mainly due to hole conditions) and in the case of Site 401 only three types of plot were retained — the lithoporosity crossplot, neutron versus density crossplot, and the density versus sonic crossplot. Of these plots, the density/sonic gave the best discrimination of lithologies mainly because (1) of the general compaction effects seen on the sonic with depth, (2) the marked difference in sonic response when the clay mineral content was high, and (3) in bad hole conditions the sonic values tend to be more reliable than the density/neutron readings. These plots were subdivided into convenient depth zones based on logging characteristics and then a final composite made over all the zones to show the general pattern within the hole.

Lithoporosity "Z" Plot[2]: Gamma Ray (GR) Relative Intensity Superimposed

This plot is porosity independent and the main corridor of meaningful readings has been drawn in by east-west-trending lines.

Figure 15 (2663.0-2797.0 m [113.0-247.0 m]) shows the relative gamma-ray intensity plotted as a number between 1 and 10. Sub-unit 3A with GR intensities of 7, 8, and 9

---

[2]The values of M and N in these crossplots were derived as follows:

$$M = \frac{\Delta^{tf} - \Delta^{t}\log}{\rho\log - \rho f} \times .01$$

where

Δ_{tf} = Transit time in μs/ft in fluid
$\Delta^{t}\log$ = Value of sonic reading in μs/ft
ρf = Density of fluid in g/cm^3

$$N = \frac{(\phi_N)_f - (\phi_N)\log}{\rho\log - \rho f}$$

$\rho\log$ = Density log reading in g/cm^3
$(\phi_N)_f$ = Value in porosity units of fluid read by neutron as a decimal
$(\phi_N)_{\log}$ = Value in porosity units of neutron log reading as a decimal

0.01 is a scaling factor to make the units of M and N compatible.

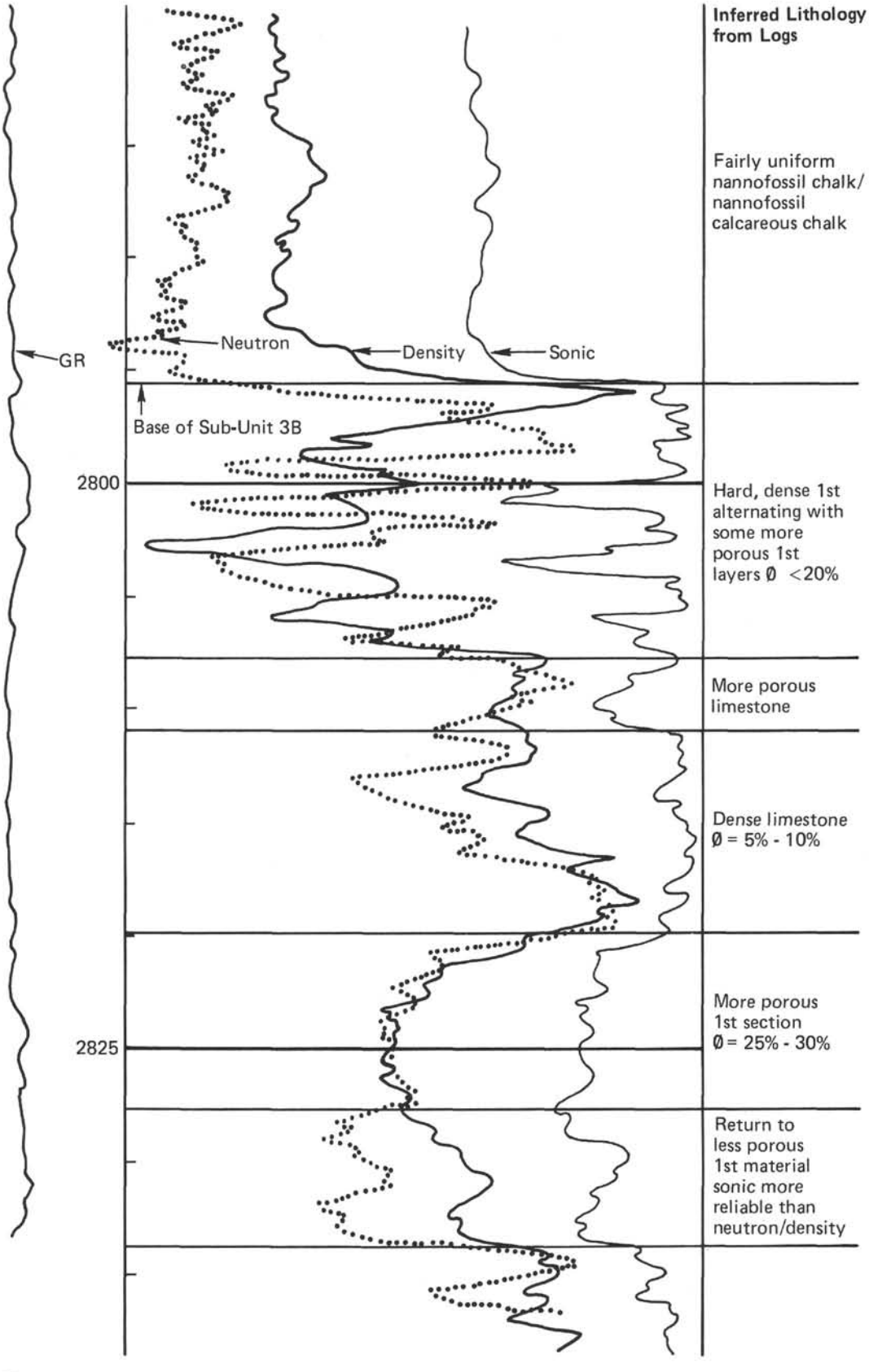

Figure 14. *Logs and inferred lithology, Site 401, 2780 to 2835 meters.*

shows clearly in the box marked. Sub-unit 3B (ignoring the washed-out section at the top) shows a trend in the direction of the northeasterly arrow with the higher velocity formations towards the base of the interval indicated by the top of the arrow head. Sub-unit 3B is the section of most indurated rock types and porosities, in general, are low.

Figure 16 (2797.0-2820.0 m [247.0-270.0 m]) is affected by bad hole conditions and cycle skipping on the sonic.

Figure 17 (2820.0-2834.0 m [270.0-284.0 m]) shows a well-defined lithology with practically no scatter. The GR is on a slightly rising trend and shows values in the range 3 to 4 in a predominantly limestone lithology.

Figure 18 is a composite of all zones between 2663.0 and 2834.0 meters (113.0-284.0 m).

No lithoporosity values are available below 284.0 meters because readings from all three porosity devices (sonic, density, and neutron) are required to deduce M and N values.

Neutron vs. Density "Z" Plot: Gamma Ray/Relative Intensity Superimposed

Figure 19 (2663.0-2797.0 m [113.0-247.0 m]) shows a pattern similar to the lithoporosity plot with a well-defined upper section from 2663.0 to 2735.0 meters (113.0-185.0 m) with a large scatter of points from 2743.0 to 2750.0 meters (193.0-200.0 m) where hole size effects predominate. There is a gradient in the direction of the arrow covering the interval 202.0 meters to the base of Sub-unit 3B at 247.0 meters. The plot appears to define an important lithology unit from 2773.0 to 2780.0 meters (223.0-230.0 m) where the gamma ray is at its lowest reading.

Figure 20 (2797.0-2820.0 m [247.0-270.0 m]) shows the characteristics from the upper part of Unit 4. There is a wide scatter in the interval 247.0 to 260.0 meters where hole conditions were poor. The intervals opposite the higher gamma-ray intensity readings are most degraded, suggesting that the higher clay content is leading to washed-out hole. From 2810.0 to 2816.0 meters (260.0-266.0 m) the density readings remain fairly constant. The least porous part of the section at the base shows the highest density readings.

Figure 21 (2820.0-2834.0 m [270.0-284.0 m]) at the top is marked by a return to a more porous lithology, and the crossplot shows a well-stabilized set of values indicating a good degree of homogeneity from 2820.0 to 2827.0 meters (270.0 to 277.0 m). The shift to the left of the plot covering the interval 277.0 to 284.0 meters shows a trend towards increasing gamma-ray values. However, the shift is more a reflection of hole conditions than any marked change in lithology. From a look at the sonic values a tighter grouping in the absence of bad hole is suspected.

Figure 22 (2663.0-2834.0 m [113.0-284.0 m]) is a composite of Figures 19, 20, and 21.

Density vs. Sonic "Z" Plot: Gamma Ray/Relative Intensity Superimposed

This series of plots proved the most discriminatory and diagnostic of all those attempted.

Figure 23 (2664.0-2797.0 m [114.0-247.0 m]) shows the well-marked, compact Unit 2 lithology with a northwest trend towards decreasing Δt from top to bottom of the unit but with increasing scatter due to hole conditions. The top of Sub-unit 3B is displaced to the right of Unit 2 on the plot and from around 203.0 meters shows a gamma-ray intensity in the range of 2 to 3. There is a clear trend of increasing velocity with depth along the line of the northwest arrow, ending at 225.0 meters with the points of lowest gamma-ray intensity marked by values of 1. There is a distinct lithologic unit from 2775.0 to 2796.0 meters (225.0-246.0 m) showing very little scatter.

Bracketing lines have been drawn on the plot to show the areas of meaningful readings. It is of note that there is less scatter on this plot than those previously discussed covering the same depth interval, suggesting the sonic is less affected by hole conditions.

Figure 24 (2797.0-2820.0 m [247.0-270.0 m]) shows this section to have maximum scatter in the zone of cycle skipping from 247.0 to 256.0 meters followed by a more coherent lithology from 256.0 to 266.0 meters (corresponding to Zone 2 of Unit 4) succeeded by a tighter section from 266.0 to 269.0 meters.

Figure 25 (2814.0-2833.0 m [269.0-283.0 m]) shows a distinct and uniform set of density readings at the top of section (270.0-277.0 m) followed by a trend towards higher density readings at the base of the section.

Figure 26 is a composite of all zones showing the good discrimination of this plot.

Conclusions

1. The logging runs have been degraded by the bad hole conditions and the absence of a reliable caliper log has severely hampered the interpretation.
2. Despite the poor hole conditions and caliper log, the *relative* deflections of the logging curves have allowed identification of unit boundaries in agreement with the lithology and suggest further subdivisions, especially within Unit 4.
3. Recording of the logs, wherever possible both up and down in the borehole, proved to be a sound technique to guard against tool failure from bumping and bridging.
4. The recording of the gamma-ray curve inside drill pipe through to sea bed proved a valuable aid in reconciling the initial log/core depths close to sea bed. By depth correlation of the logging runs in open hole all the major unit boundaries recognized by the shipboard party were confirmed (Figure 12).
5. The simultaneous recording of digital data on tape as well as the analog recording enabled the full employment of computer techniques.
6. Crossplotting techniques, especially the density versus sonic, have confirmed their usefulness in determining lithologic boundaries and lithologies.

CORRELATION OF SEISMIC PROFILES WITH DRILLING RESULTS

Site 401, located on the edge of the Meriadzek Terrace, was fixed by several multichannel seismic profiles run by IFP-CNEXO using the same technical parameters as those described for Site 400. The site was situated close to line S21 and near the crossing with line S27 (Figures 2, 3a, 3b). After Leg 48 was completed, new multichannel seismic

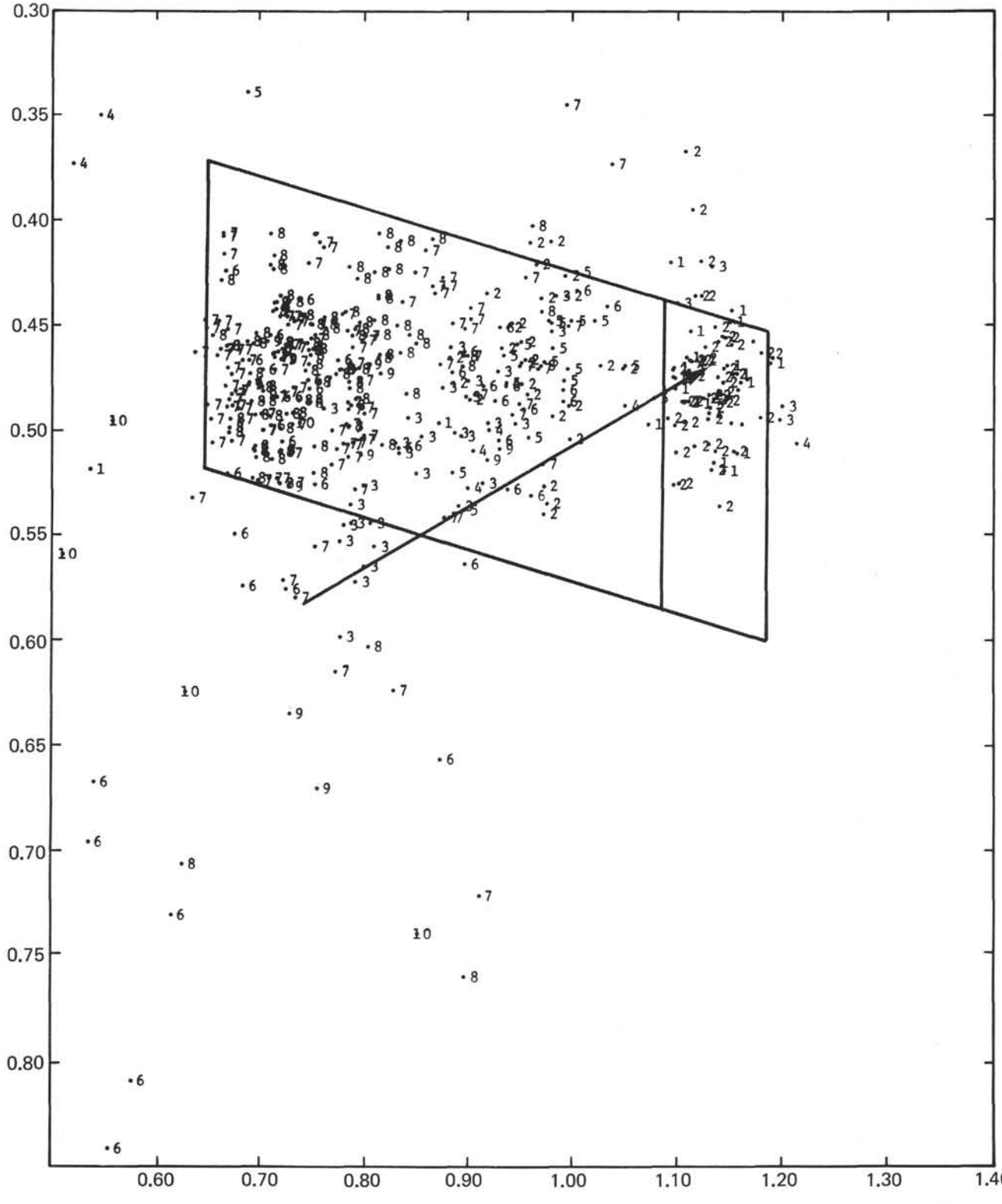

Figure 15. *Lithoporosity "Z" plot – gamma-ray relative intensity superimposed (2663.0 to 2797.0 m, 113.0 to 247.0 m).*

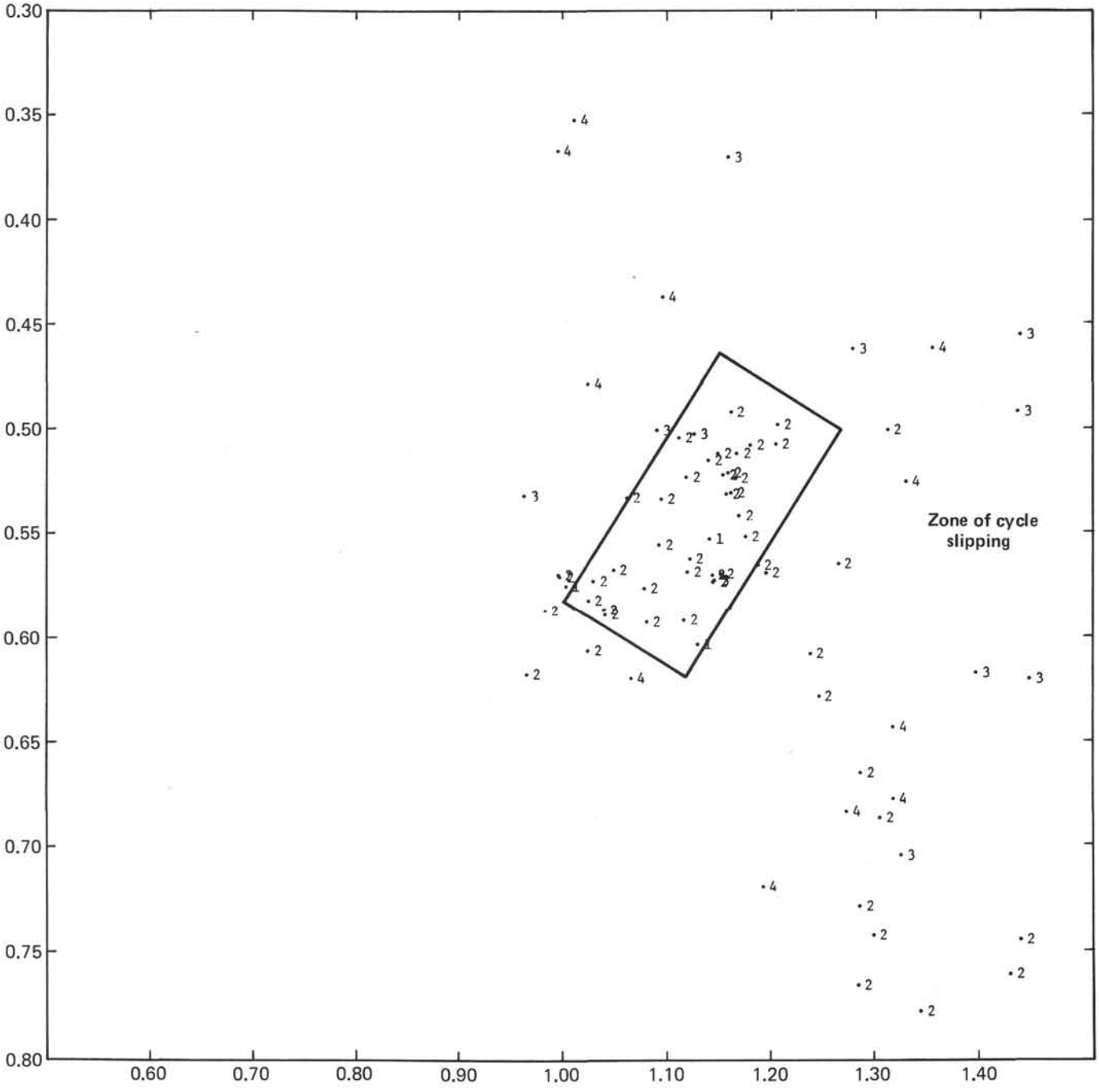

Figure 16. *Lithoporosity "Z" plot – gamma-ray relative intensity superimposed (2797.0 to 2820.0 m, 247.0 to 270.0 m).*

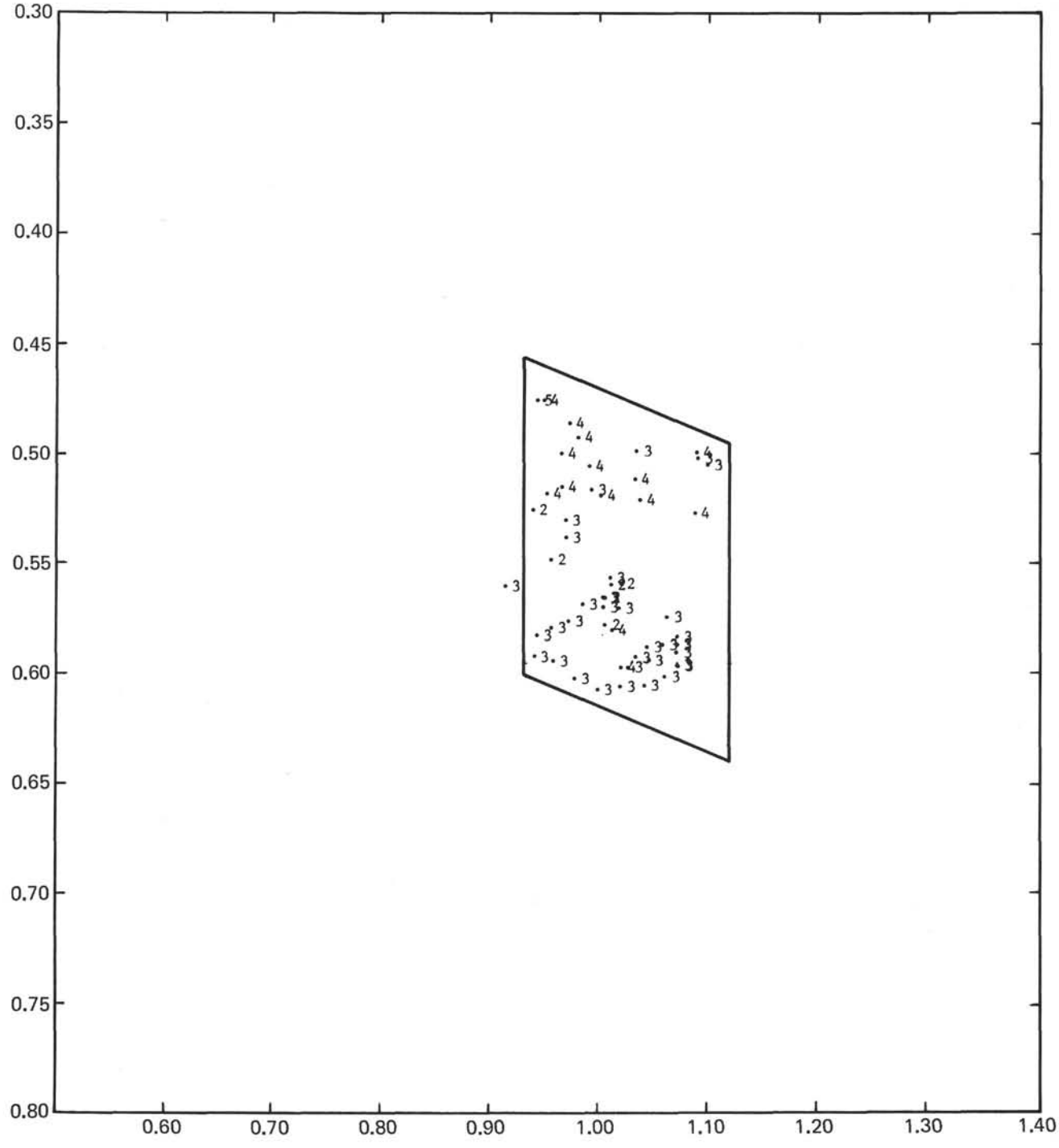

Figure 17. *Lithoporosity "Z" plot – gamma-ray relative intensity superimposed (2820.0 to 2834.0 m, 270.0 to 284.0 m).*

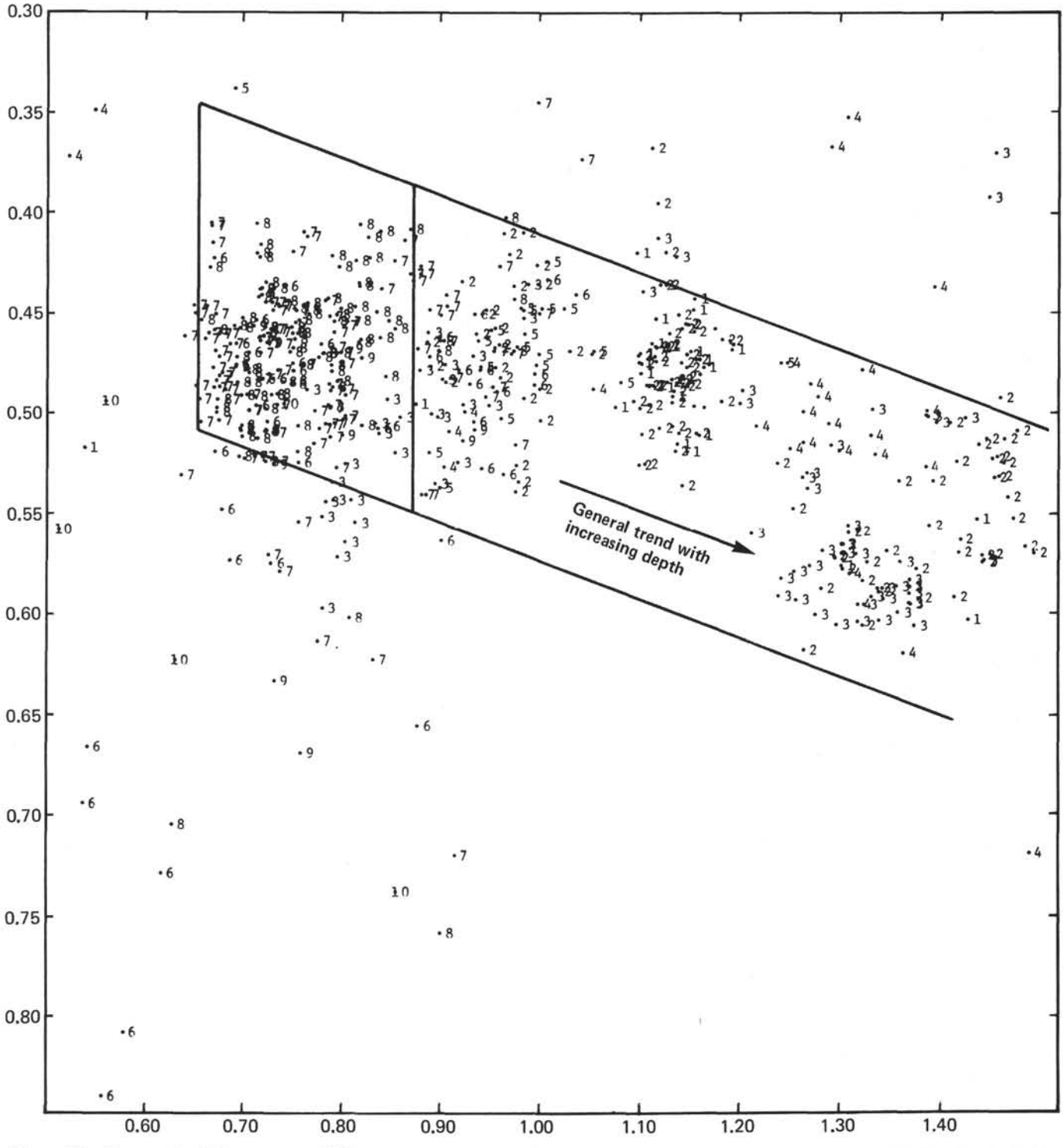

Figure 18. *Composite lithoporosity "Z" plot – gamma-ray relative intensity superimposed for the interval 2663.0 to 2834.0 meters (113.0 to 284.0 m).*

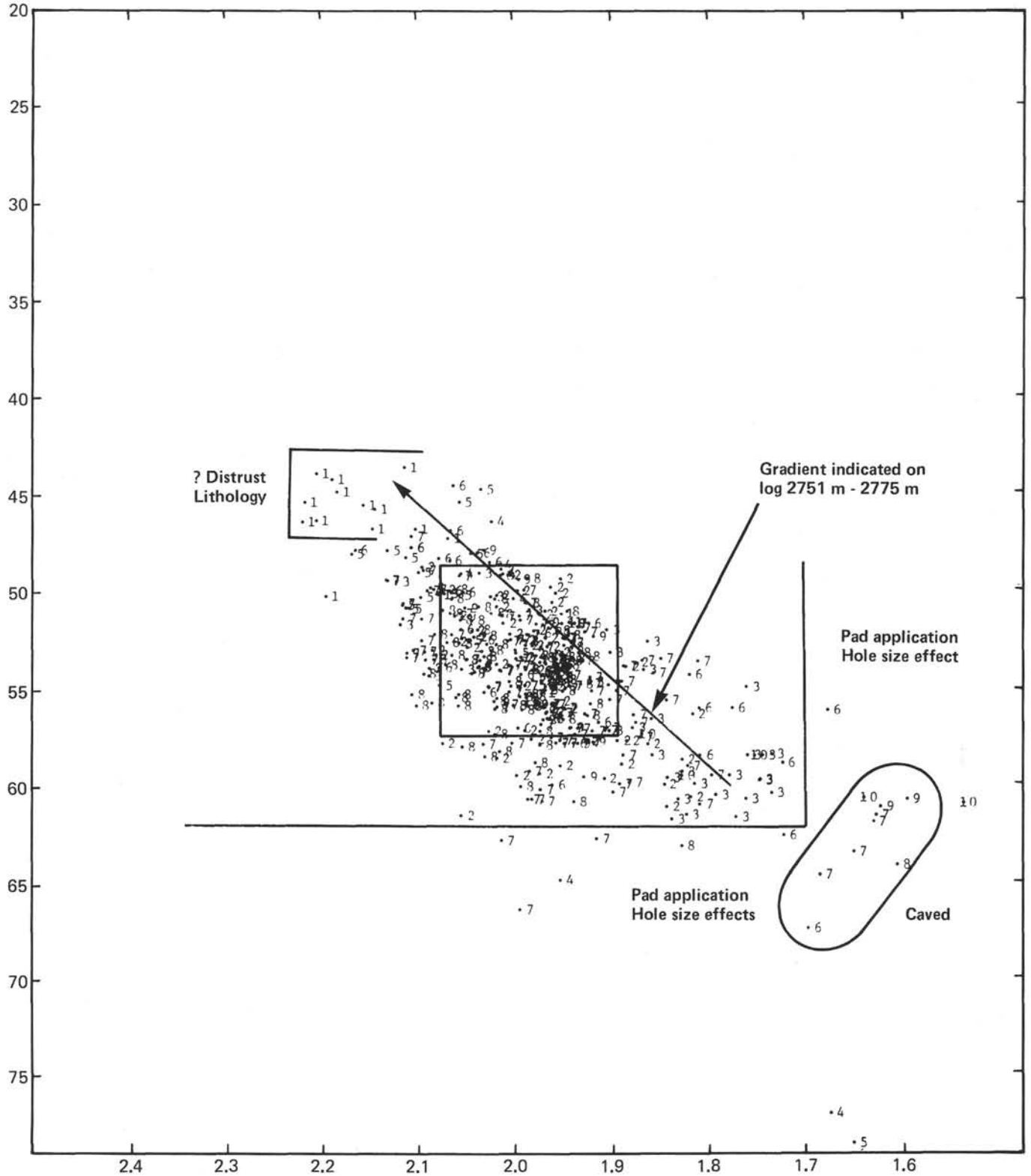

Figure 19. *Neutron versus density "Z" plot – gamma-ray relative intensity superimposed for the interval 2663.0 to 2797.0 meters (113.0 to 247.0 m).*

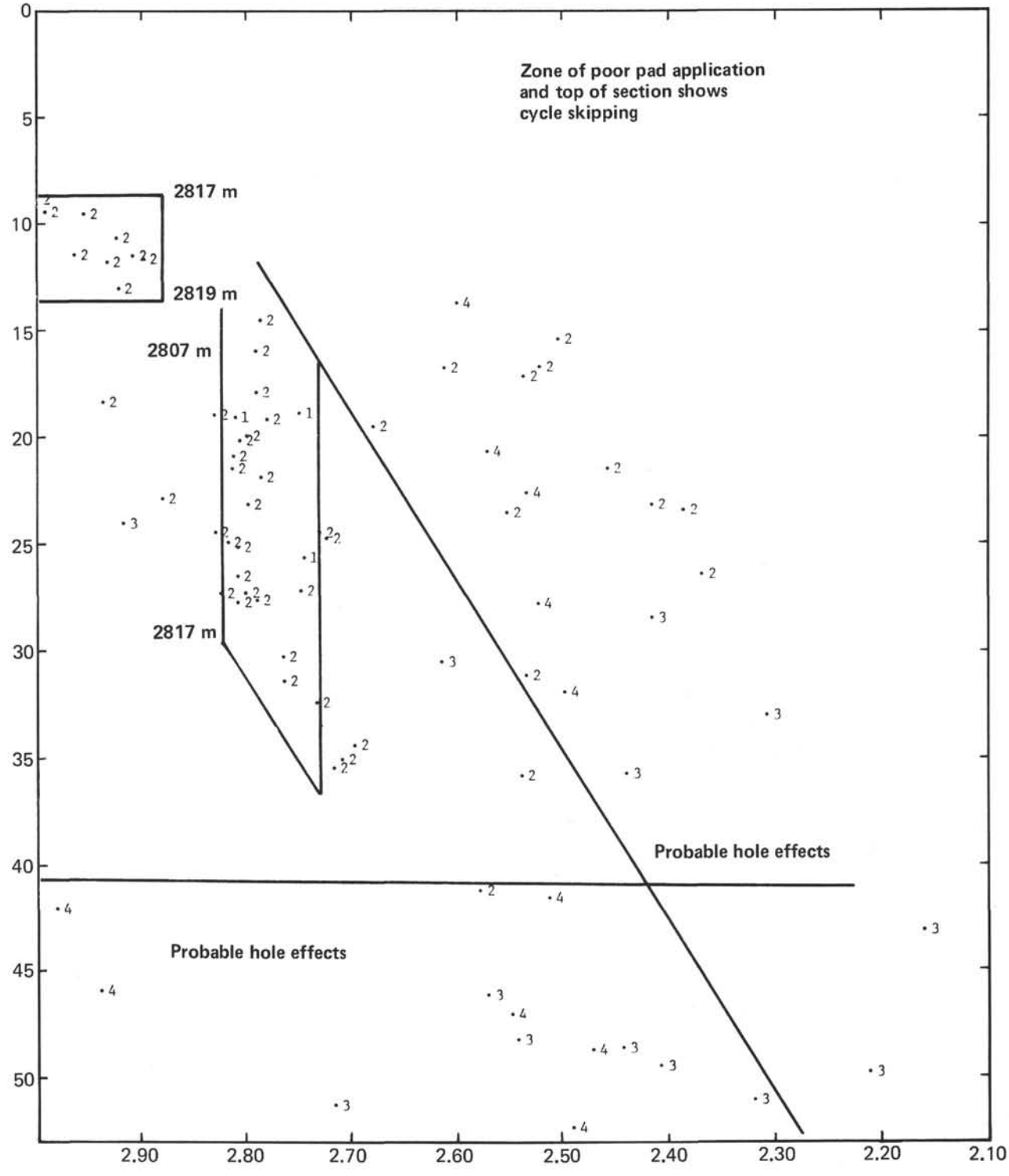

Figure 20. *Neutron versus density "Z" plot – gamma-ray relative intensity superimposed for the interval 2797.0 to 2820.0 meters (247.0 to 270.0 m).*

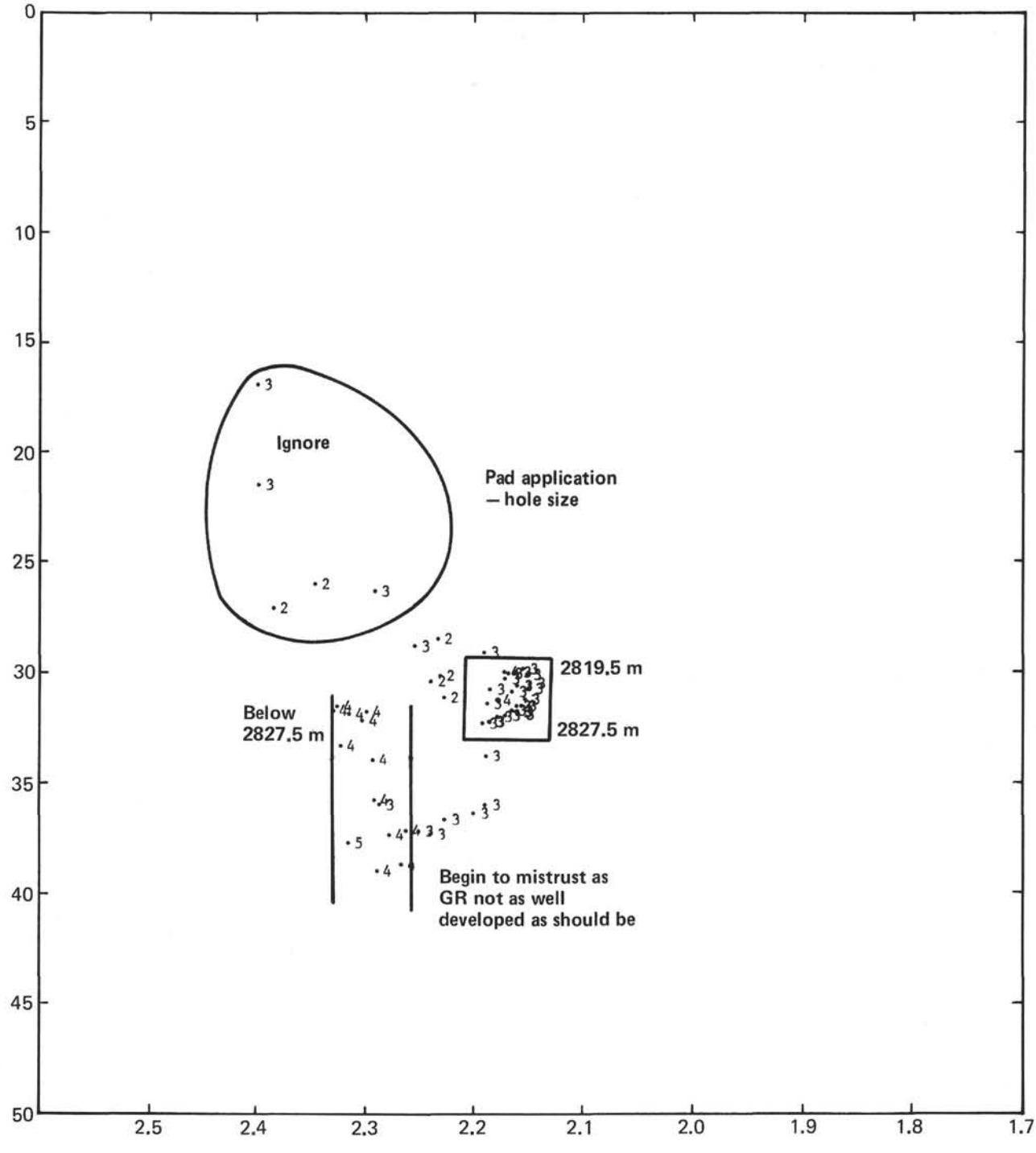

Figure 21. *Neutron versus density "Z" plot – gamma-ray relative intensity superimposed for the interval 2820.0 to 2834.0 meters (270.0 to 284.0 m).*

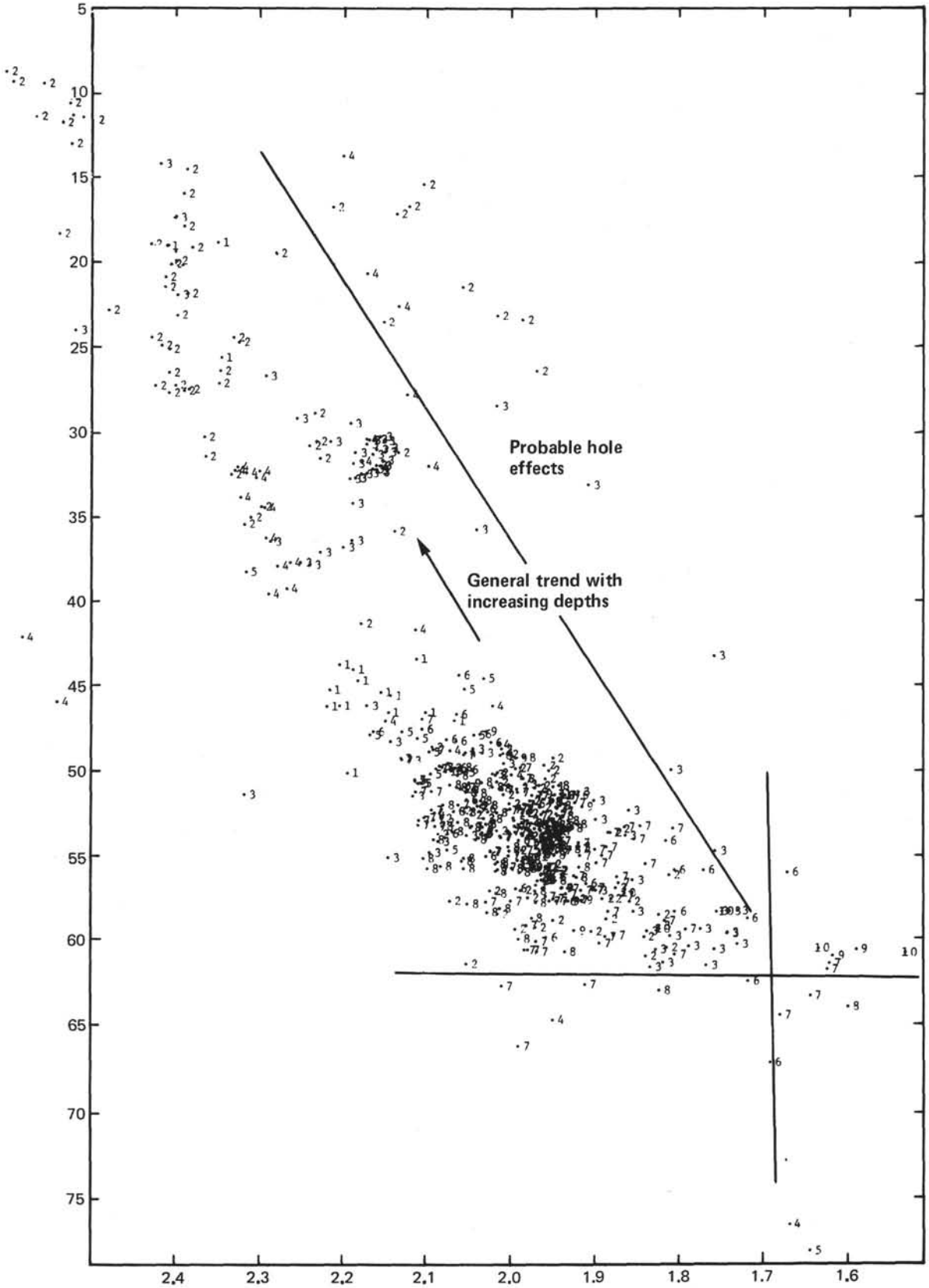

Figure 22. *Composite neutron versus density "Z" plot – gamma-ray relative intensity superimposed for the interval 2663.0 to 2834.0 (113.0 to 284.0 m).*

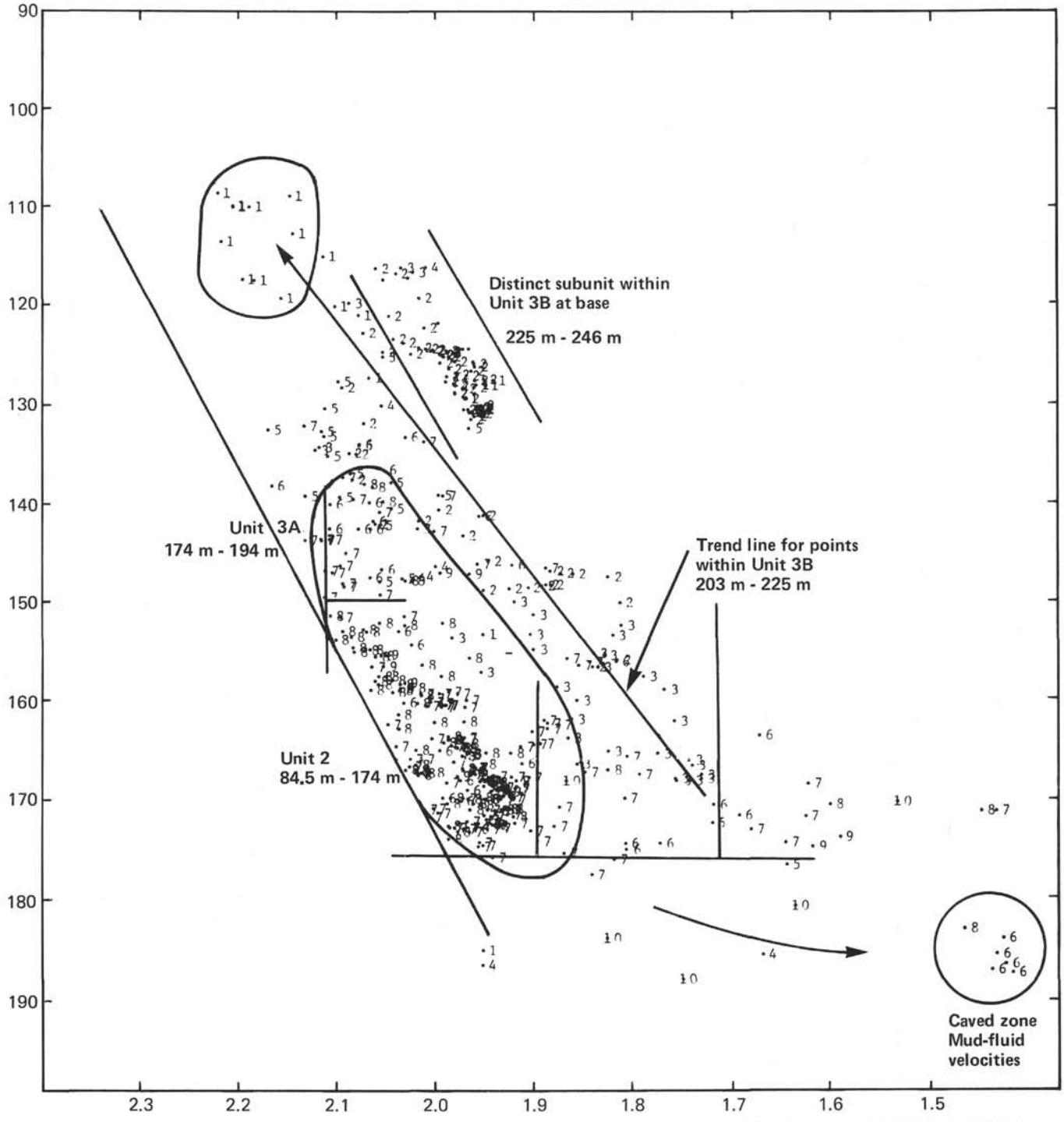

Figure 23. *Density versus sonic "Z" plot – gamma-ray relative intensity superimposed for the interval 2664.0 to 2797.0 meters (114.0 to 247.0 m).*

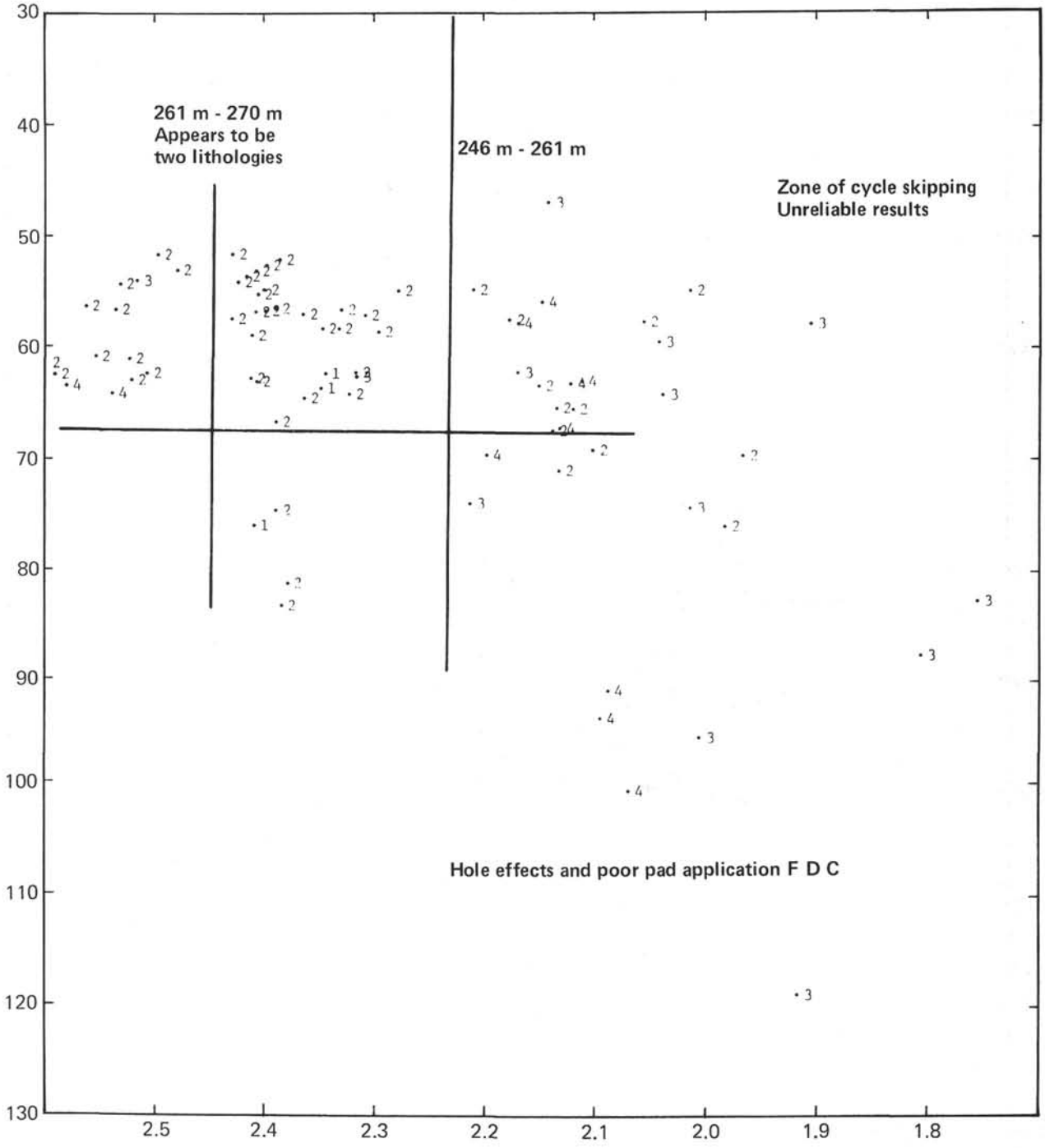

Figure 24. *Density versus sonic "Z" plot – gamma-ray relative intensity superimposed for the interval 2797.0 to 2820.0 meters (247.0 to 270.0 m).*

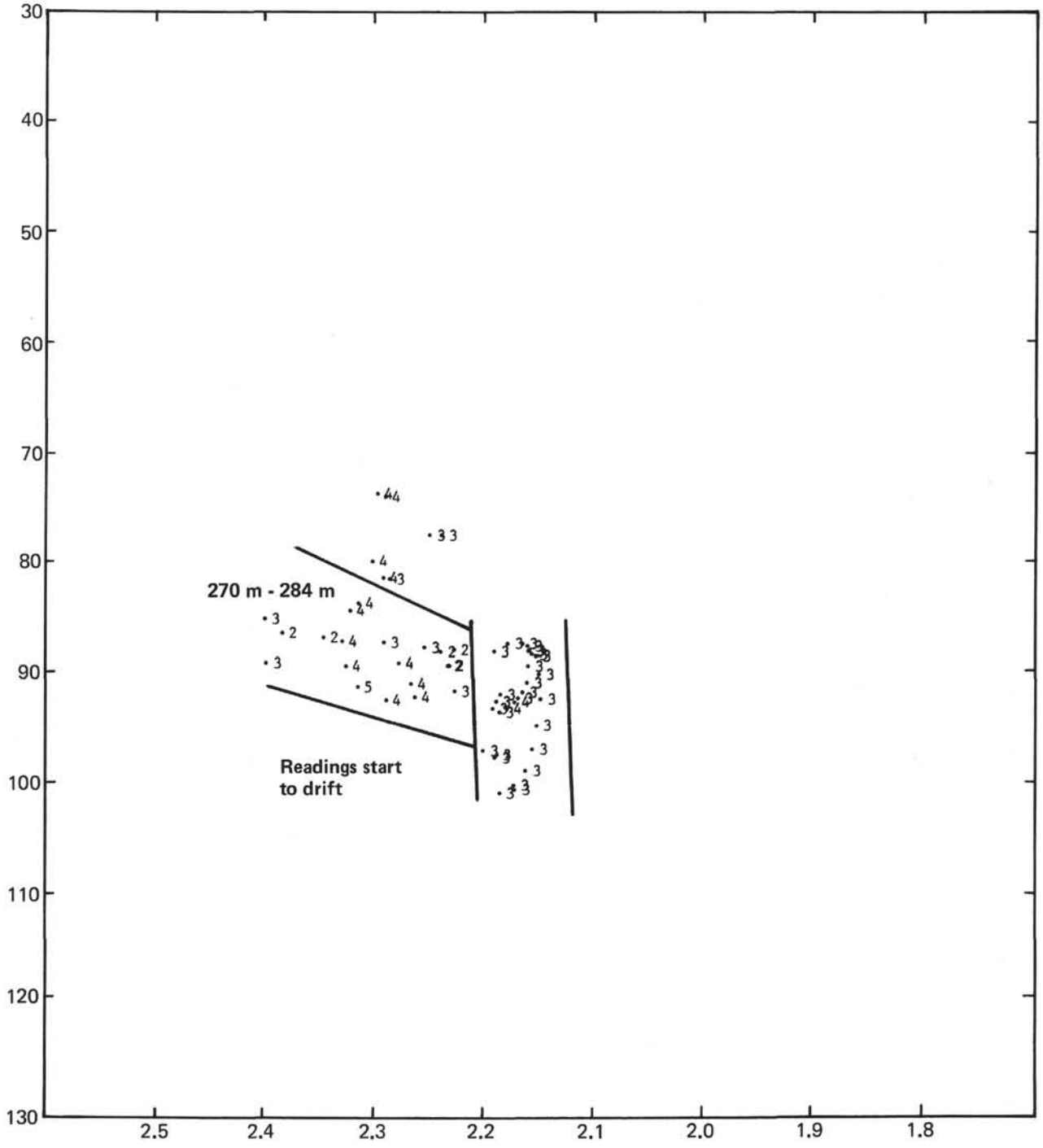

Figure 25. *Density versus sonic "Z" plot – gamma-ray relative intensity superimposed for the interval 2814.0 to 2833.0 meters (269.0 to 283.0 m).*

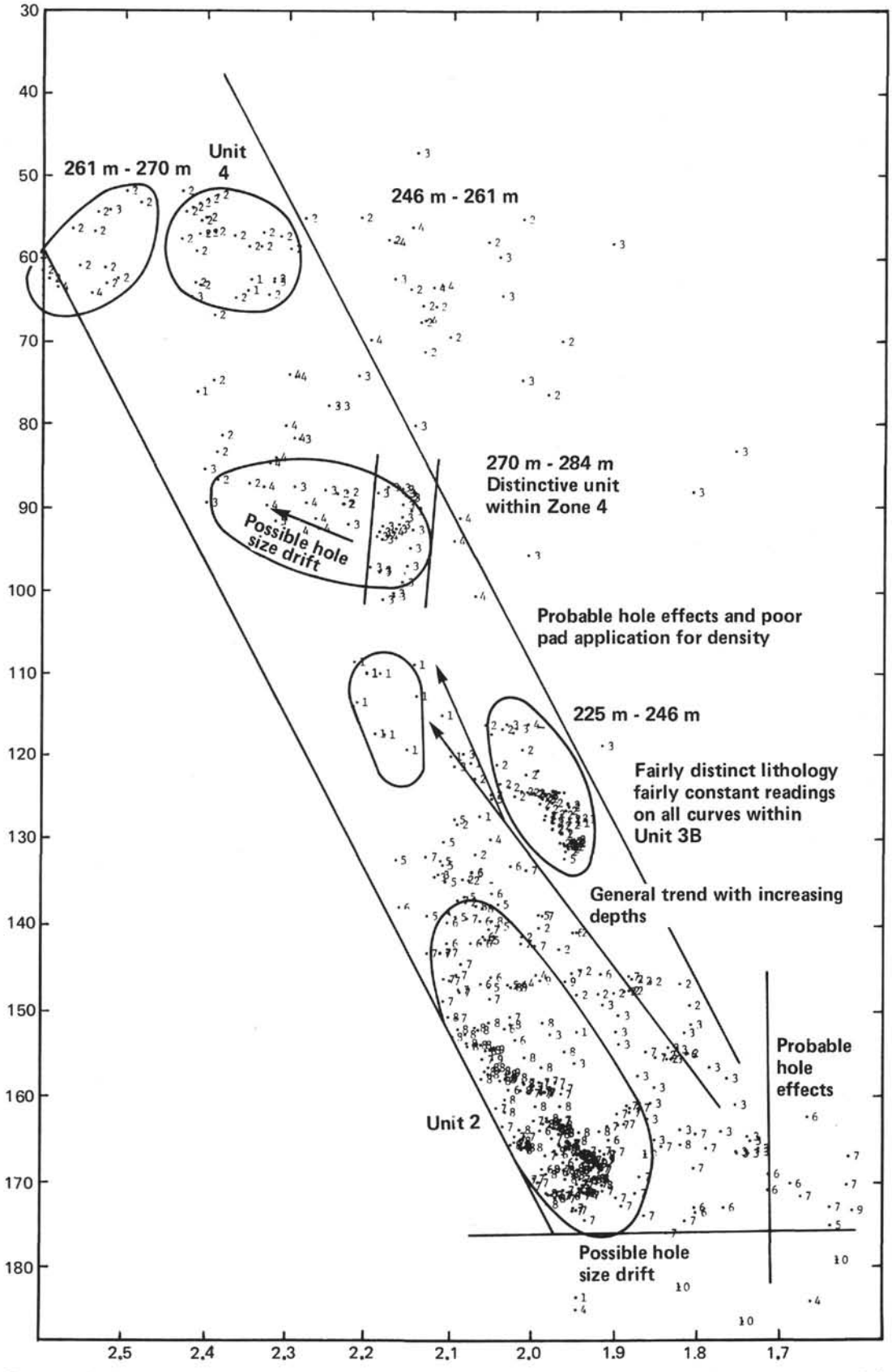

Figure 26. *Composite density versus sonic "Z" plot – gamma-ray relative intensity superimposed for the interval 2664.0 to 2833.0 meters (114.0 to 283.0 m).*

lines were run by IFP-CNEXO-CEPM across the site (profiles GM3, GM5, GM7). In addition, a high-resolution multichannel seismic line was run through the site, parallel to the escarpment (Figure 27).

In this area, the Meriadzek Terrace consists of two tilted blocks with downthrow to the south (Figures 2, 27, 28). Although the northern block is buried, the fault zone bounding the southern block controls the Meriadzek Escarpment. The escarpment is devoid of sedimentary cover so that the "basement" outcrops. Near the site, the crest of the tilted block is flat and corresponds to an erosional surface similar to other surfaces identified on seismic reflection profiles (Montadert et al., this volume). The profiles show, between the two tilted blocks under the terrace, up to 3 seconds (two-way time) of sediments, whereas on the edge of the escarpment, the acoustic basement is covered by only 400 to 450 meters (two-way time) of sediments. Clearly a large part of the sequence infilling the half-graben is not represented at the site location either because of pinch-out on the flank of the crest, or because it is represented by a much reduced section.

In the half-graben several seismic units can be recognized (Figure 28):

Unit A: This youngest unit seems to have been shaped by bottom currents and to correspond to a change in depositional conditions compared to Unit B. Indeed, the base of A is irregular and, locally, erosion has cut into Unit B on the Meriadzek Terrace suggesting the existence of a hiatus at this level. At Site 401, the upper part of this unit was not drilled.

Unit B: This unit is characterized by a number of good reflectors. One of the reflectors (#1), near the top of Unit B, can be followed from the half-graben over the high where it was penetrated at Site 401.

Unit C: This unit is a thin homogeneous unit which can be followed on the Meriadzek Terrace but not over the high.

Unit D: This unit is characterized by a series of very strong reflectors, which, following regional correlation, must comprise the Upper Cretaceous at the base.

Unit E: This unit is almost transparent below and is identified as the black shales sequence of Aptian/Albian age. Below a thick sequence it corresponds to syn-rift and pre-rift sediments of Mesozoic age.

At Site 401, on top of the eroded, tilted block, the following reflectors are present:

1) one reflector internal to Unit A which outcrops on the slope and possibly was not drilled at Site 401.

2) the reflector 1 near the top of seismic Unit B. Following the profiles, around Site 401, it is close to the underlying reflector 2.

3) The strong reflector 2 corresponds to the top of the acoustic basement. Within the acoustic basement on the migrated profile S21 and on adjacent profile OC209 several weak reflectors and discontinuous reflectors clearly dip northward within the acoustic basement. These are cut by the flat surface of the crest which therefore corresponds to a plane of erosion. There reflectors are horizontal on profile GEOM 401 oriented perpendicular to the direction of dip.

To correlate the results of the hole with seismic profiles the following method has been used:

1) Determination of reflection coefficients and synthetic seismograms (Figure 29) using the density and velocity logs and the physical properties measurements, and thus the origin of the seismic reflectors.

2) From the depth of the reflectors converted to sound travel time from the logging, their position has been determined on the seismic profile.

From an examination of the velocity and density logging, and impedance curve, the following observations can be made (Figure 30). There is an obvious, sharp increase of velocity, density, and impedance between 245 and 250 meters. Density increases from 1.95 to 2.10 g/cm^3 to 2.20 to 2.55 g/cm^3 where the velocity increases from 2.3 km/s to 5 km/s. This change, which is corroborated by physical properties data and by an increase in the coring time, marks the change in lithology from Upper Cretaceous chalks (Unit 4) to Lower Cretaceous/Upper Jurassic reefal limestones (Unit 5). This change must generate a strong reflection at around 0.280 s below the sea floor which corresponds to reflector 2 marking the top of acoustic basement.

From the sea floor to 250 meters, velocity seems to increase continuously from 1.5 km/s to 2.5 km/s and the density from 1.7 to 2 g/cm^3 with numerous variations at different levels. However, between 150 and 170 meters a significant break occurs where the velocity increases from 1.8 to 2 km/s and the density from 1.9 to 2.05 g/cm^3. It corresponds also to an increase in the coring time in the lower part of the middle Eocene. Unfortunately, the section recorded by logging is too short and the synthetic seismogram is thus not very useful. Nevertheless, this break can be assumed to generate a reflection at around 0.170 to 0.180 s two-way time below the sea floor. In this case it could therefore correspond to the reflector 1 situated towards the top of the seismic Unit B, defined previously. The unconformity observed on the Meriadzek Terrace may therefore correspond to an important paleoceanographic event which occurred between Eocene and Oligocene.

SEDIMENTATION RATES

Seismic profiles show that at Site 401 the main part of the Quaternary and Miocene to Pliocene is absent. Pleistocene was recovered only in Core 1, thus a sedimentation rate cannot be established. The hole was washed to 84.5 meters, and the core taken below this point indicated that in this interval middle-upper Oligocene nannofossil oozes exist.

The lowermost Oligocene (NP 21 to P.17) and upper Eocene (NP 18 to NP 19/NP 20 to P.16/15) are present in Cores 2 through 4 with a sedimentation rate of about 7 m/m.y. (Figure 31). The upper Eocene and middle Eocene sediments (NP 14 to NP 16 to P.10 to P.11) are probably separated by a small hiatus representing an interval of about 1.8 m.y. that includes the nannoplankton Zone NP 17 and the upper part of NP 16. During the middle Eocene the sedimentation rate was higher (10 m/m.y. according to the nannofossils, 16 m/m.y. according to the foraminifers) due to the high content of siliceous microfossils. The change of the sedimentation rate in the lowermost middle Eocene (NP 14) is related again, as at Site 400, to a lithological change from nannofossil chalk in the lower Eocene to the siliceous nannofossil ooze in the middle Eocene. The sedimentation

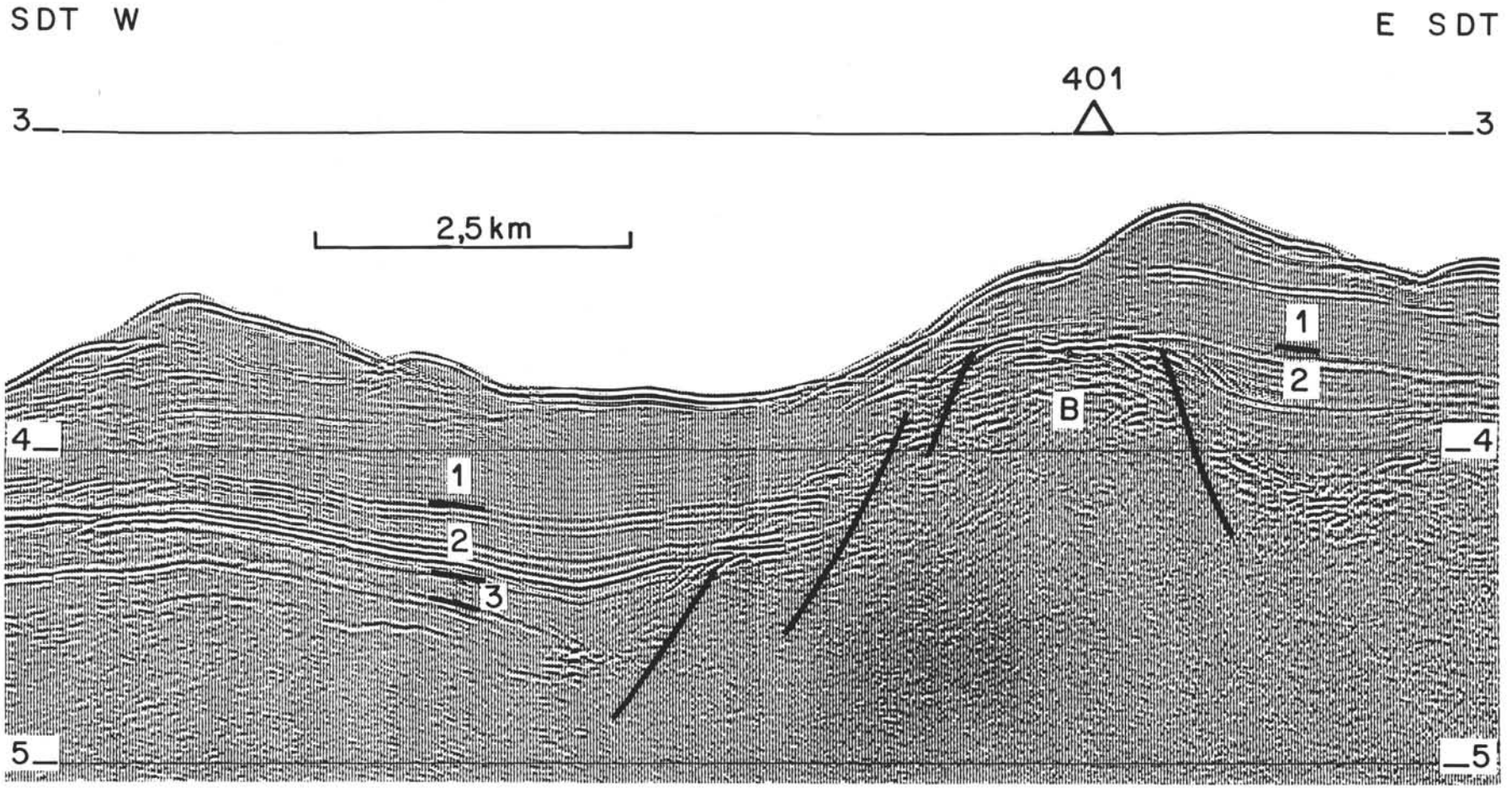

Figure 27. *High-resolution multichannel seismic profile GEOM401 through Site 401.*

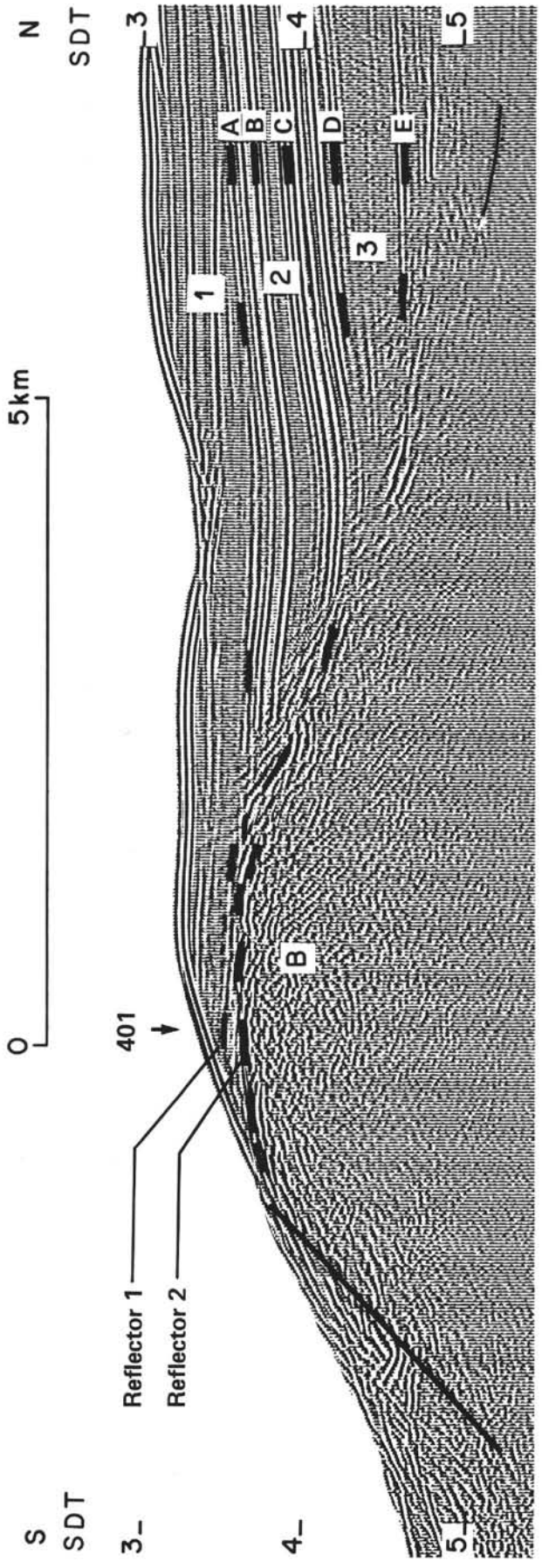

Figure 28. *Detail of multichannel seismic profile S21.*

rate of 5 m/m.y. is also the same for the upper Paleocene and lower Eocene sequence.

A hiatus of at least 2.6 m.y. lies between the lower and upper Paleocene in Core 16, and the Upper Cretaceous is separated from the lower Paleocene by a hiatus of 2 m.y.

The rate of 2 m/m.y. for the Upper Cretaceous sequence is low. The latter sequence is underlain by a few centimeters of upper Aptian sediments and in turn underlain by Upper Jurassic (Kimmeridgian to Portlandian) limestones. The hiatus between the Upper and Lower Cretaceous represents an interval of at least 34 m.y.

SUMMARY AND CONCLUSIONS

Site 401, located on the seaward edge of the Meriadzek Terrace (Figure 3a) in 2495 meters of water, was drilled to 341 meters below sea bottom ending in Kimmeridgian/Portlandian shallow water carbonates.

Multichannel seismic surveys made before and after the leg by IFP-CNEXO and CEPM show that the Meriadzek Terrace in this area is underlain by two major tilted blocks downfaulted to the south. The Meriadzek Escarpment, oriented northwest-southeast, corresponds to the fault zone bounding one of these blocks. A transverse fault, oriented northeast-southwest, exists northwest of the site (Montadert et al., this volume). At Site 401, the crest of the tilted block is flat and is interpreted as a plane of erosion because it truncates several northward-dipping, discontinuous reflectors that are considered to be pre-rift sediments. This acoustic basement was penetrated and is Upper Jurassic shallow water limestones with reef debris. The overlying 250-meter-thick sequence thickens northward to an interval of 3 seconds in the half-graben. In this interval, the lowest seismic interval E is identified as the Albian/Aptian "black shales" and the underlying thick sequence as syn- and pre-rift sediments of Mesozoic age. Overlying interval D, which is considered to be Upper Cretaceous at the base, and interval C cannot be followed from the graben to Site 401. However, the prominent reflector 1 within the seismic interval B was penetrated at Site 401 and may correspond to the middle Eocene. Seismic interval A has been eroded and is partly missing at Site 401.

The sedimentary section penetrated at Site 401 has been divided into four lithological units based on lithology, changes in X-ray mineralogy, and the downhole logs.

Description of Lithological Units

Unit 1

Unit 1 (Core 1 and upper part of the washed zone, 0-20 m) of Quaternary age, is defined by a single 8.5-meter core cut at the mudline and by a sharp decrease in the gamma log. The core consists of olive-gray calcareous mud at the base and yellow-brown marly calcareous ooze at the top; two upward-fining cycles are present in the uppermost 2.5 meters. Carbonate content ranges from 70 per cent at the top to 10 per cent at the base. In the upper part, it consists of 20 to 50 per cent foraminifers, but in the lower part it is mostly nannofossils. Clay content varies from 20 per cent above to 60 per cent below, and quartz averages 2 per cent. Microfaunas show a strong contrast between interglacial (transitional type) and glacial (subarctic type) conditions.

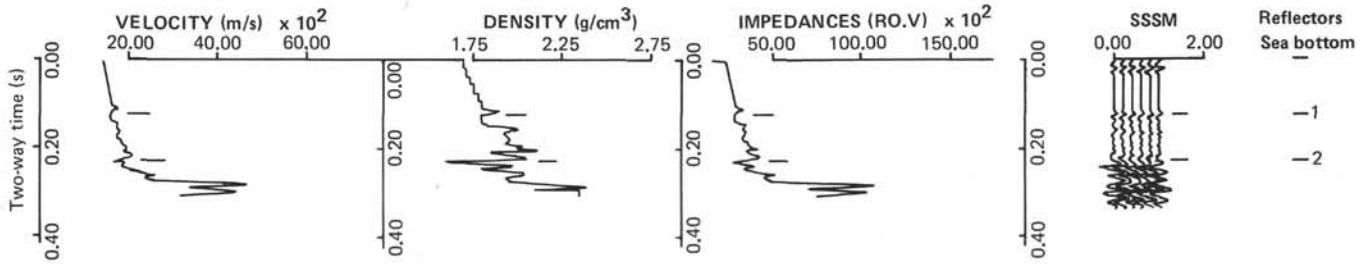

Figure 29. *Synthetic seismogram, Site 401.*

Unit 2

Unit 2 (lower part of the washed zone and Cores 2-11, 20-171.5 m) of middle Oligocene or younger to middle Eocene age was cored only below 84.5 meters. Middle Oligocene nannofossil oozes found in the washed core cut between 20 and 84.5 meters are included in Sub-unit 2A. Division into sub-units is based on a hiatus between the late and middle Eocene in Core 11 and differences in carbonate and quartz above and below this level.

Sub-Unit 2A

This sub-unit (Cores 2-4, 20-113 m) is of middle Oligocene or younger to late Eocene age and is composed of uniform light greenish gray to greenish gray nannofossil chalk. The average carbonate content, composed mostly of nannofossils, is 70 per cent; quartz is 5 per cent. Clay minerals are rare; smectite is the major component with minor amounts of illite, chlorite, and zeolite. Sponge spicules average 5 per cent and sedimentary structures are rare. Lower Oligocene was recognized in Core 2 and upper Eocene in Core 3. Nannofossils are abundant but slightly etched and broken. Deposition rate was around 7 m/m.y. At the base of the sub-unit there is a 1.8-m.y. hiatus between the upper and middle Eocene.

Sub-Unit 2B

This sub-unit (Cores 5-11 [upper part], 113-171.5 m) is of middle Eocene age and consists of pale olive to greenish gray nannofossil chalk, siliceous nannofossil chalk, and marly nannofossil chalk. Carbonate content averages 50 per cent and consists mostly of nannofossils. Quartz averages 10 per cent, and smectite and sepiolite are the dominant clay minerals. Siliceous components average between 12 and 49 per cent. Pyrite is present and probably manganese nodules as well. Laminae are present in Cores 7 and 8 whereas burrows are absent to moderately abundant. The planktonic-benthic foraminifer ratio varies between 20 and 50. The benthic foraminifers indicate deposition in bathyal depths above the CCD. A sedimentation rate of 10 to 16 m/m.y. indicates a large increase in silica productivity also observed at Hole 400A.

Unit 3

Unit 3 (Core 11 lower part to Core 19 upper part, 171.5-247 m) is of early Eocene to Late Cretaceous (Campanian) age. Contact with overlying Unit 2 has been drawn on the basis of a decrease in quartz, illite, and smectite; an increase in carbonate content, and variations in color associated with a sharp rise in the magnetic intensity.

Sub-Unit 3A

This sub-unit (Cores 11-13 upper portion, 171.5-194 m) is of early Eocene age and is composed of nannofossil calcareous and marly chalks of yellowish brown to orange-brown color which contrasts markedly with the unit above. The unit is characterized by low quartz, high kaolinite, and a decrease in smectite. Carbonate content reaches 76 per cent and siliceous components are much reduced. A dark brownish layer of possible collophane is present towards the base of the unit. Burrowing is slight to moderate and slickensided fractures exist in Core 13. The sediments were deposited at the reduced rate of 5 m/m.y. in bathyal conditions.

Sub-Unit 3B

This sub-unit (Core 13 [lower portion] to Core 14, 194-200.5 m) is of lowermost Eocene to uppermost Paleocene age and consists of yellowish brown to grayish orange marly calcareous chalk. It is characterized by a decrease in carbonate to 25 per cent and a concomitant increase in terrigenous components (quartz 12%, smectite 80%). Chlorite and kaolinite are absent towards the base of the sub-unit.

Sub-Unit 3C

This sub-unit (Core 14 [lower portion] to Core 19, upper portion, 200.5-247 m) is of late Paleocene to Late Cretaceous (Campanian) age. Dominant lithology is grayish orange calcareous nannofossil chalk characterized by a sharp increase in carbonate content to between 80 and 90 per cent and by less chlorite and kaolinite. Within the sub-unit a 2.6-m.y. hiatus between the lower and upper Paleocene is present at 219.5 meters and a second 2-m.y. hiatus between the lower Paleocene and Maestrichtian at 236.5 meters. The upper Paleocene nannofossil calcareous chalk (Core 14 to Section 16-3) is composed principally of well-preserved nannofossils and unspecified carbonates. Dark flecks are frequent. Towards the top bioturbation is frequent and a manganese nodule is present. Microfaulting is common. Separated by a hiatus, the lower Paleocene (Section 16-3 to Core 17) consists of nannofossil chalk and foraminiferal calcareous chalk. Attapulgite, sepiolite, and clinoptilolite are locally abundant. Sediments are rich in badly preserved nannofossils.

The Maestrichtian to Campanian (Core 18 to Section 19-1) consists of laminated nannofossil and foraminiferal calcareous chalk. Clay minerals consist of chlorite (5%), illite (35%), mixed-layered clays (5%), smectite (45%), kaolinite (5%), attapulgite (5%), with traces of sepiolite; quartz and feldspars are present. Streaks and laminae of

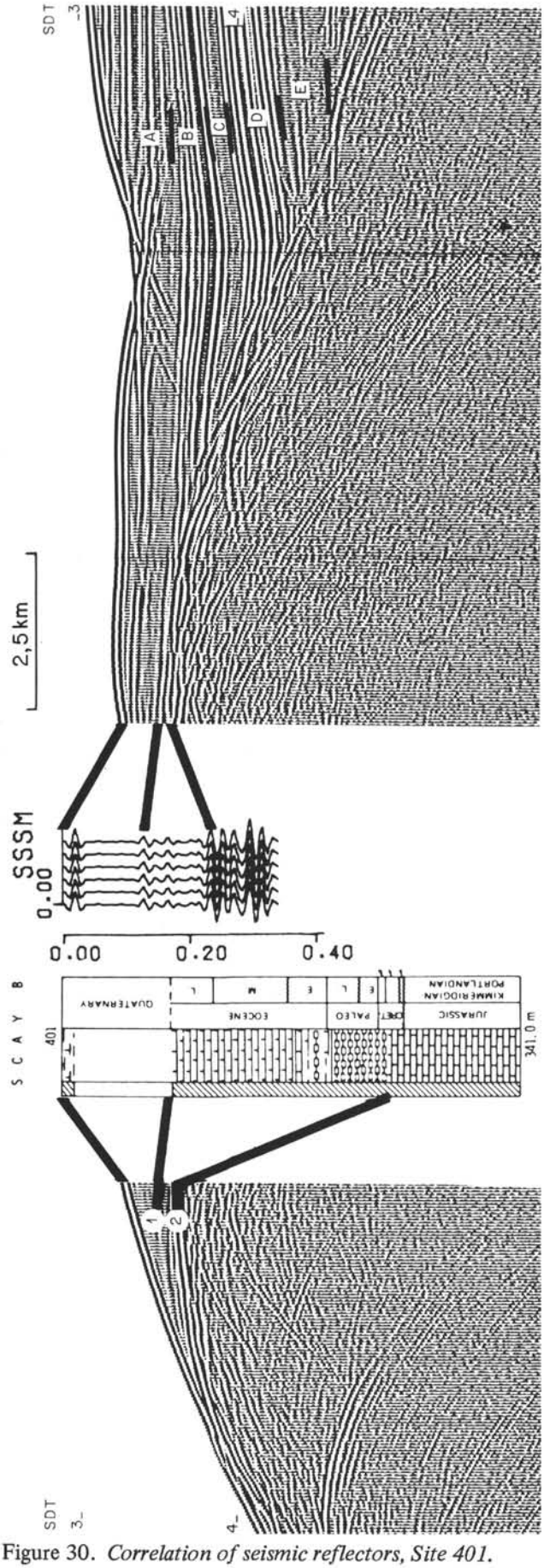

Figure 30. *Correlation of seismic reflectors, Site 401.*

darker brown colors become more common towards the basal contact at Core 19, Section 1, 120 cm, with a manganese nodule at Core 19, Section 1, 118 cm. Benthic foraminifers are rare but indicate a bathyal environment. Nannofossils are highly diversified but often badly preserved.

Unit 4

Unit 4 (Core 19, Section 1, 120 cm to Core 28, 247.3-341 m) is of late Aptian to Kimmeridgian/Portlandian age and is separated by a 34-m.y. hiatus from Unit 3. Recovery in this unit was poor, and identification of the five lithological sub-units has been made mainly from downhole logs.

Sub-Unit 4A

This sub-unit (Core 19, Section 1, 120 cm and Core 20, 247.2-265 m) is of late Aptian to latest Tithonian/Berriasian age and underlies the deep-water chalks of Campanian age. The contact near Core 19, Section 1, 120 cm is sharp and is marked by phosphatic, ferriferous, and manganiferous stromatolitic cauliform concretions generally associated with a hiatus or intense condensation (Bourbon, this chapter). Below, a 5-cm-thick interval of very pale orange calcareous chalk and a 2-cm-thick interval of light brown soft marly calcareous chalk rest at Core 19, Section 1, 128 cm on dense, lithified reddish limestone. In this narrow interval, small broken but non-dissolved planktonic foraminifers indicate a late Aptian age (base of Gargasian MCi 19) and external shelf conditions. A nannoplankton assemblage, which consists mainly of nannoconids, indicates also a late Aptian age and a nearshore environment.

The underlying hard reddish bioclastic limestone in Core 19 is composed of fragments of corals, algae, echinoids, gastropods, lenticulinids with, in some places, sponge spicules, and *Neotrocholina*. The facies has similarities to the Neocomian of southwest France and Portugal. The underlying white limestones of Core 20 have a porosity not exceeding 20 per cent. They consist of intraclast grainstones, micrites, and packstones that contain fragments of corals, algae, pelecypods, foraminifers, crinoids, and ostracodes. Rare calpionelids indicate a late Tithonian to Berriasian age.

Sub-Unit 4B

This sub-unit (Core 21, 265-274.5 m) is also of late Tithonian-Berriasian age and consists of pellet grainstones of low porosity (5-10%).

Sub-Unit 4C

This sub-unit (Core 22, 274.5-284 m) comprises pellet grainstones rich in large coral fragments, echinoids, pelecypods, and algae fragments; some foraminifers suggest a Late Jurassic age.

Sub-Unit 4D

This sub-unit (Cores 23 and 24, 284-303 m) is composed of intraclast grainstones with porosity values, determined from the logs, ranging from 5 to 30 per cent. The fauna is comparable to that found in Core 22. The assemblage of foraminifers and algae suggests a Kimmeridgian to Portlandian age.

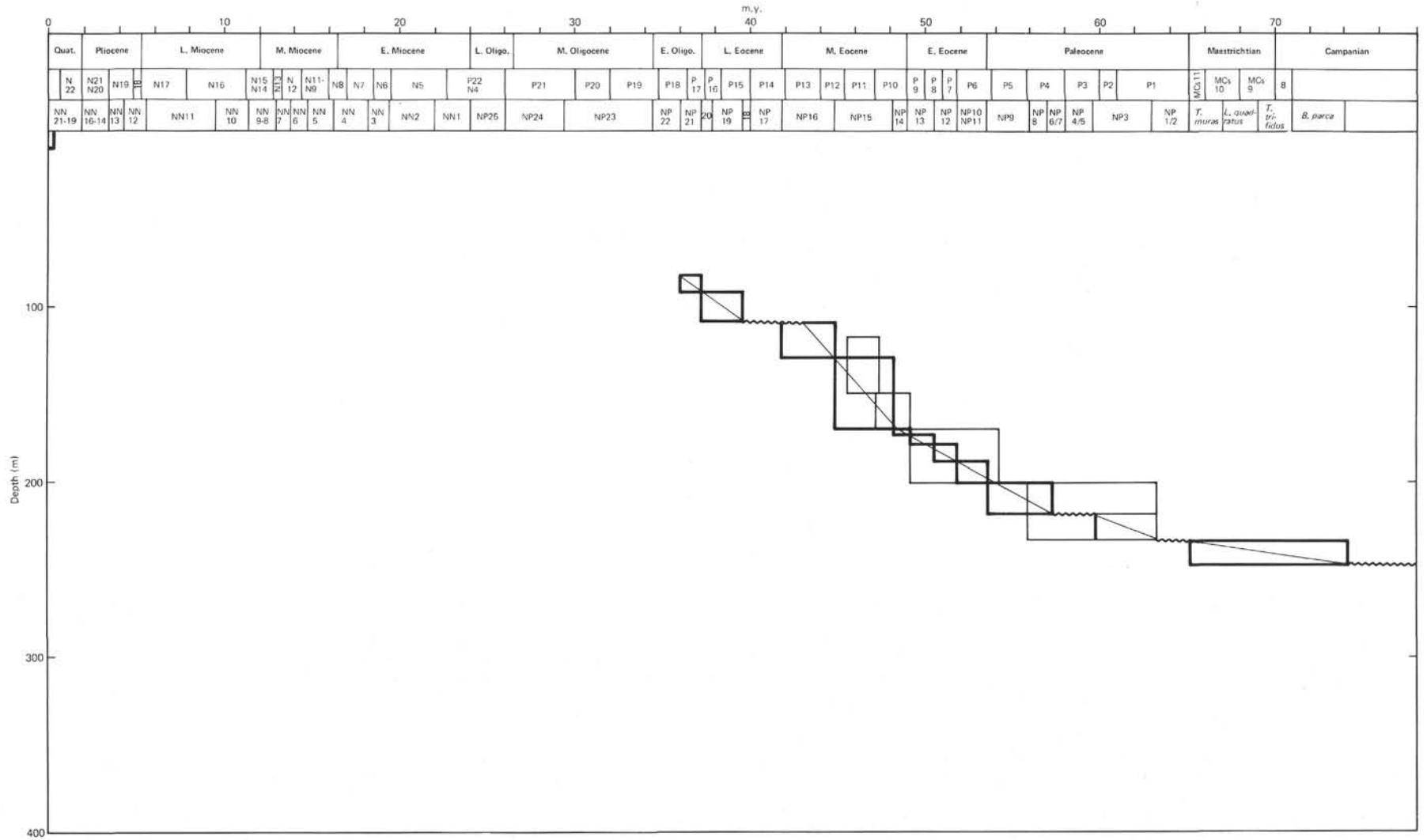

Figure 31. *Sedimentation rates, Site 401.*

Depositional History

The Portlandian/Kimmeridgian calcarenites at the base of the hole were deposited in a shallow environment favorable to reef development. The limestone is dominantly coarse sand peloidal grainstone and very coarse sand to pebble coral-algal boundstone (Lumsden, this chapter) with micritized fossils and algal lumps as dominant grain components. Algae, corals, crinoids, pelecypods, gastropods, and foraminifers are abundant. Two phases of cementation may have occurred, the last being a postdepositional meteoric phase. Nearly 50 meters of such beds were penetrated, the upper part being perhaps late Tithonian to Berriasian in age as indicated by some rare calpionellids. The top is a hard reddish bioclastic limestone also deposited in shallow water. Its facies has some similarities with the Neocomian of southwest France and Portugal. On the seismic profiles the top of these hard limestones correspond to the acoustic basement and to the flat plane cutting the crest of the tilted block.

The few centimeters of upper Aptian calcareous chalk at the top of Unit 4 show an important change in environment to less shallow water depth, characterized by deposition of oozes. Another major hiatus exists between this unit and the overlying deep water Campanian chalks of Unit 3.

Seismic reflection profiles and the stratigraphy of Unit 4 suggest that rifting of a shallow water carbonate Mesozoic platform took place during Early Cretaceous time, creating tilted blocks and half-grabens. At the edge of the Meriadzek Terrace, the crest of one of these blocks was at sea level and was eroded during rotation of the block in the interval between the Jurassic and the Aptian. Lower Cretaceous shallow water carbonates were deposited on this abrasion platform as shown by lower Aptian calcarenites with rudists, algae, orbitolinae dredged near the site (Auffret et al., this volume). During Aptian time, a change to a somewhat deeper environment occurred, permitting deposition of late Aptian chalks. This could be related to the beginning of the thermal subsidence of the margin after the onset of spreading in Biscay. At the same time, black shales and carbonate turbidites were deposited in deep waters at the foot of the Meriadzek Escarpment (Hole 400A). Sediments of the same age and seismic facies were also deposited at shallower depth in the half-graben north of Site 401 as shown by seismic reflection profiling (see correlation of seismic reflection profile and drilling results). However, the exact age of the beginning of the rifting phase has not been established on this margin. An alternative hypothesis would therefore be to interpret the Late Jurassic shallow water limestones drilled at Site 401 as deposits restricted to the top of already existing tilted blocks (Kimmeridgian) as has been suggested for the Parentis basin in Aquitaine.

A 34-m.y. hiatus (Figure 31) separates the late Aptian chalks from the Campanian/Maestrichtian lower bathyal chalks of which planktonics represent 98 to 99 per cent of the foraminiferal assemblages; within them, signs of dissolution suggest proximity of the foraminifer lysocline. Phosphatic, ferruginous, and manganiferous stromatolitic cauliform concretions (Bourbon, this chapter) are associated with the hiatus. From these facts, it can be interpreted that, from the Aptian to Late Cretaceous the margin subsided rapidly to lower bathyal depths which accords with a thermal subsidence history starting at the onset of spreading in Biscay during the Aptian. The hiatus between the Lower and the Upper Cretaceous is present in every hole on the Biscay margin and it separates shallow water Lower Cretaceous from deep water Upper Cretaceous sediments. It is contemporaneous with the worldwide Cenomanian/Turonian transgression. Its possible significance has been discussed in the previous chapter (Holes 400/400A).

In Hole 400A a single 8-m.y. hiatus separates Maestrichtian and lower Paleocene beds, but at Site 401 a part of the lower Paleocene was deposited as nannofossil chalk separated from the Maestrichtian by a 2-m.y. hiatus and from the upper Paleocene above by a 2.6-m.y. hiatus. Benthic foraminifers (Schnitker, this volume) and ostracodes (Ducasse et al., this volume) show that during the Paleocene, Site 401 was close to its present depth and significantly shallower than Site 400. Exact significance of the Paleocene hiatus is not clear from these holes because it affects sites which were at very different depths at that time. It is noteworthy that late Paleocene time was characterized by a general warming that culminated in the early Eocene (Grazzini et al., this volume).

As observed at Site 400, a marked change occurred close to the early-middle Miocene boundary. In the middle Eocene deposits the carbonate content decreases to 50 per cent and siliceous components become more abundant. The change is associated with a gradual decrease in surface and bottom temperatures in the last 50 m.y. (Grazzini et al., this volume). During this time, silica productivity increased greatly, as witnessed by the change in ostracode assemblages which become richer and more diversified (Ducasse et al., this volume).

Microfauna and carbonate content demonstrate that during middle Eocene time, Sites 400 and 401 were at significantly different water depths. A 1.8-m.y. hiatus separates the middle Eocene from the uppermost Eocene/lower Oligocene; this Eocene paleoceanographic event is well defined on the seismic profiles particularly on the Meriadzek Terrace where it is marked by an erosional unconformity (see Correlations of Seismic Profiles With Drilling Results, this chapter; and Montadert et al., this volume). This event was widespread in the Atlantic and is generally linked to the opening of circulation between the Atlantic and the Arctic-Norwegian Sea (Berggren and Hollister, 1977) and also to the flow of the Antarctic Bottom Water into the Atlantic. At Sites 400 and 401, the abrupt change (within nannofossil Zone NP 14) from early Eocene yellow-brown marly chalks to middle Eocene green-gray chalks and siliceous chalks correlates precisely with a sharp reduction in NRM intensity and magnetic susceptibility (Hailwood, this volume), testifying to reduction in the supply of detrital magnetite which was cut off by the change in circulation patterns.

Upper Eocene and lowermost Oligocene greenish gray nannofossil chalks at Site 401 have a carbonate content reaching 70 per cent, but still contain some biogenic silica.

The Neogene history of the site cannot be interpreted due to spot coring and the location of the hole on a slope where the section is incomplete.

Site 401 thus demonstrates the existence of Late Jurassic shallow water carbonates that probably predate the rifting of the margin. During rifting in the Early Cretaceous, Site 401

was at sea level. The erosional planes cutting the tilted blocks on the margin can thus be dated. Thermal subsidence started during Aptian time and the site was already in bathyal depths during the Late Cretaceous. Data from this site confirm that the Meriadzek Escarpment separating Hole 400A and Site 401 was already in existence at the end of the rifting phase.

REFERENCES

Bathurst, R. G. C., 1966. Boring algae, micrite envelopes and lithification of molluscan biosparites, *J. Geol.*, v. 5, p. 15-32.

_____ , 1975. *Carbonate sediments and their diagenesis,* 2nd ed.: New York (Elsevier).

Bé, A. W. H. and Tolderlund, D. S., 1971. Distribution and ecology of living planktonic foraminifera in surface waters of the Atlantic and Indian Oceans. *In* Funnell, B. M. and Riedel, W. R. (Eds.), *Micropaleontology of oceans:* Cambridge (Cambridge Univ. Press), p. 105-149.

Berggren, W. A. and Aubert, J., 1975. Paleocene benthonic foraminiferal biostratigraphy, paleobiogeography and paleoecology of Atlantic-Tethyan regions: midway-type fauna, *Palaeogeogr., Paleoclimatol., Paleoecol.*, v. 18, p. 73-192.

Blow, W. H., 1969. Late middle Eocene to Recent planktonic foraminiferal biostratigraphy. *In* Brönnimann, P. and Renz, H. H. (Eds.), *Int'l Conf., Plankt. Microfossils, Proc. 1st:* Leiden (E. J. Brill), v. 1, p. 199-422.

Bourbon, M., 1971. Structure et signification de quelques nodules ferrugineux, manganésifères et phosphatés liés aux lacunes de la série crétacée et paléocène briançonnaise, *C. R. Acad. Sci. Paris,* v. 273, p. 2060-2062.

_____ , in press. Nature et répartition des minéralisations liées aux lacunes dans le Mésozoïque et le Paléocène pélagiques briançonnais (région de Briançon). Essai de comparaison avec certaines minéralisations des océans actuels, Colloque ATP "Géodynamique de la Méditerranee et de ses abords."

Cayeux, L., 1935. *Les Roches Sédimentaires de France: Roches Carbonatées:* Paris (Masson).

Cook, H. E., Johnson, P. O., Matti, J. C., and Zemmels, I., 1972. Methods of sample preparation and X-ray diffraction data analysis, X-ray mineralogy laboratory, Deep Sea Drilling Project, University of California, Riverside. *In* Hayes, D., Frakes, L. A., et al., *Initial Reports of the Deep Sea Drilling Project,* v. 28: Washington (U. S. Government Printing Office), p. 999-1007.

Dunham, R. J., 1962. Classification of carbonate rocks according to depositional texture. *In Classification of carbonate rocks: Am. Assoc. Petrol. Geol. Mem. 1,* p. 108-121.

_____ , 1971. Meniscus cement. *In* Bricker, O. P. (Ed.), *Carbonate cements:* Baltimore (Johns Hopkins Univ. Press), p. 297-300.

Evamy, B. D., 1969. The precipitational environment and correlation of some calcite cements deduced from artificial staining, *J. Sediment Petrol.*, v. 39, p. 787-793.

Folk, R. L., 1962. Spectral subdivision of limestone types. *In Classification of carbonate rocks: Am. Assoc. Petrol. Geol. Mem. 1,* p. 62-84.

_____ , 1965. Some aspects of recrystallization in ancient limestones. *In* Pray, L. C. and Murray, R. C. (Eds.), *Dolomitization and limestone diagenesis,* p. 14-48.

Friedman, G. M., 1959.. Identification of carbonate minerals by staining methods, *J. Sediment. Petrol.*, v. 29, p. 87-97.

Ginsburg, R. N., Schroeder, J. H., Shinn, E. A., 1971. Recent synsedimentary cementation in subtidal Bermuda reefs. *In* Pricker, O. P. (Ed.), *Carbonate cements:* Baltimore (Johns Hopkins Univ. Press), p. 54-58.

Herker, S.D. and Sarjeant, W.A.S., 1975. The stratigraphic distribution of organic-walled dinoflagellate cysts in the Cretaceous and Tertiary, *Rev.* Paleobot. Palynol., v. 20, p. 217-315.

Hesse, R., 1973. Diagenesis of a seamount oolite from the west Pacific, Leg 20, DSDP. *In* Heezen, B. C., MacGregor, I. D., et al., *Initial Reports of the Deep Sea Drilling Project,* v. 20: Washington (U. S. Government Printing Office), p. 363-387.

James, N. P. and Hopkins, J. C., 1972. Lithology and correlation of Cretaceous limestones from Orphan Knoll. *In* Laughton, A.S., Berggren, W. A., et al., *Initial Reports of the Deep Sea Drilling Project,* v. 12: Washington (U. S. Government Printing Office), p. 51-56.

Johnson, J. H., 1969. A review of the Lower Cretaceous algae. *Professional Contrib. 6,* Colorado Sch. Mines.

Lemoine, M., 1953. Le probléme de la transgression des marbres en plaquettes dans la zone briançonnaise, *C. R. Acad. Sci. Paris,* 236, p. 1056-1058.

Logan, B. W., Rezak, R., and Ginsburg, R. N., 1964. Classification and environmental significance of algal stromatolites, *J. Geol.*, v. 72, p. 68-83.

Matter, A. and Gardner, J. U., 1975. Carbonate Diagenesis at Site 308 Koko Guyot. *In* Larson, R., Moberly, R., et al., *Initial Reports of the Deep Sea Drilling Project,* v. 32: Washington (U. S. Government Printing Office), p. 521-535.

Monty, C., 1973. Les nodules de manganèse sont des stromatolites océaniques, *C. R. Acad. Sci. Paris,* v. 276, p. 3285-3288.

Schroeder, J. H., 1973. Submarine and vadose cements. *In* Pleistocene Bermuda reef rock, *Sediment. Geol.*, v. 10, p. 179-204.

Swinchatt, J. P., 1969. Algal boring: a possible depth indicator in carbonate rocks and sediments, *Geol. Soc. Am. Bull.*, v. 80, p. 1391-1396.

van Andel, T. H., Thiede, J., Sclater, J. G., and Hay, W. W., in press. Depositional history of the south Atlantic Ocean during the last 125 million years, *J. Geol.*

PLATE 1
Thin Sections of Stromatolitic Cauliform Concretions

Figures 1, 2 — Top: pelagic ooze; medium: phosphatic (white on the figure), ferriferous and manganiferous (black on the figure) stromatolitic cauliform concretions; bottom: mixture of transparent (P) and opaque (Fe-Mn oxides or hydroxides) minerals. Sample 19-1, 121-125 cm. Hiatus in the Lower Cretaceous, before the upper Aptian.

Figures 3-5 — P (apatite, Figure 4) or P-Mn-Fe (apatite, psilomelane, hematite, Figures 3 and 5) cauliform concretions.

3. Briançonnais, hiatus between Norian beds and Oxfordian nodular limestones.
4. Briançonnais, hiatus between white Tithonian-Berriasian limestones and Turonian clayey limestones.
5. Briançonnais, hiatus at the Cretaceous/Paleocene boundary, concretions around a dolomitic nucleus, coming from eroded Triassic beds.

PLATE 1

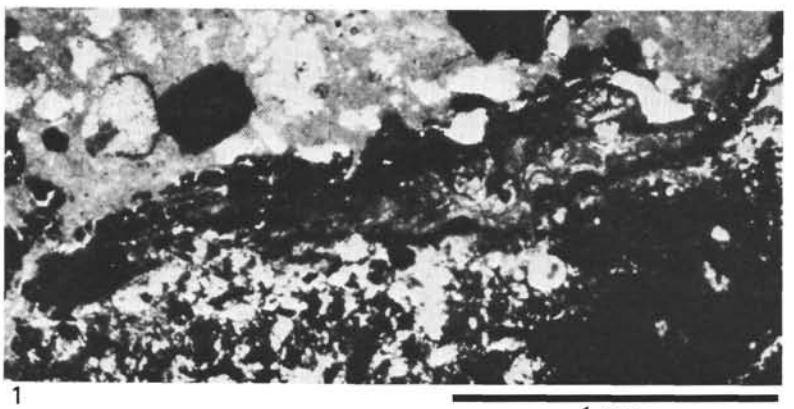

1

1 mm

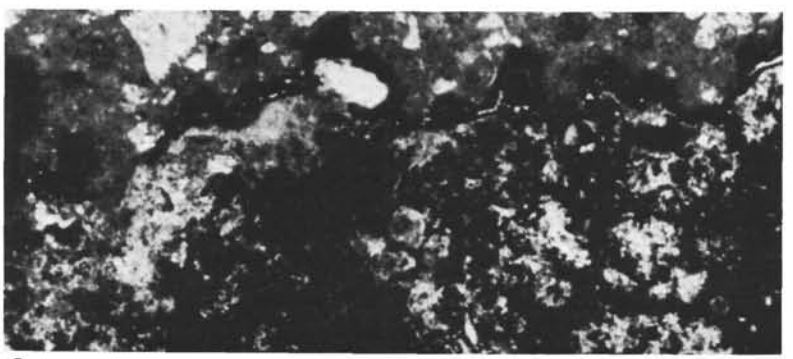

2

1 mm

3

2 mm

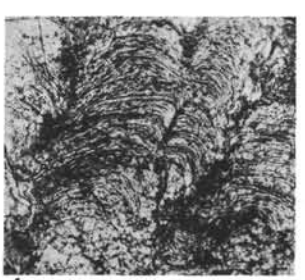

4

4 mm

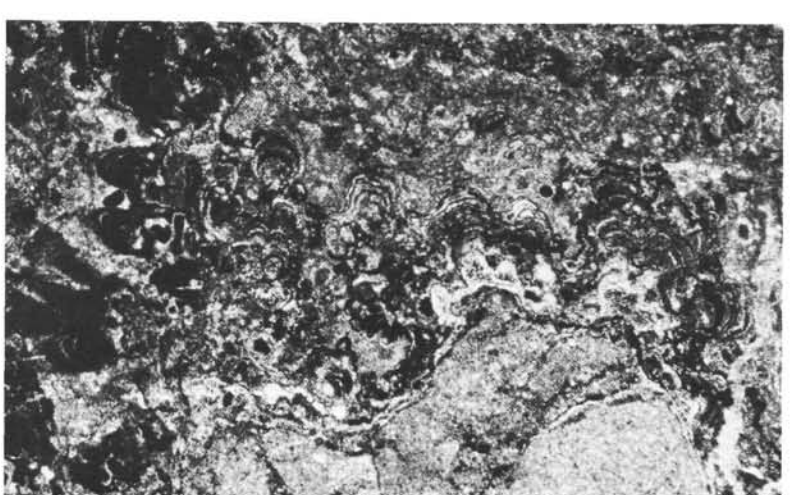

5

1 mm

PLATE 2

Figure 1 Peloids-micritized grains. On the right a crinoid columnal has been deeply bored by endolithic algae. On the left is a grain of uncertain origin. It probably is a micritized and rounded foraminifer or bryozoan (note the intraparticle voids), but may be a composite grain. Note the planar grain contact and the absence of cement spar. Sample 401-23-1, 106 cm, uncrossed nicols, bar is 0.5 mm.

Figure 2 Clumps-algal lumps. The large rounded grain in the center and the larger grain cut off by the right margin have complex cores involving micrite and unidentified fossil debris. In addition the clump has a micrite rim. Isopachous cement is clearly visible (A). Sample 401-23-1, 85 cm, crossed nicols, bar is 0.5 mm.

Figure 3 Algae. This form resembles the genus *Lithocodium* (Johnson, 1969). Many of the grains counted as peloids may in fact be algae. Note the many small surrounding peloids. In the top right center is one of the uncommon fractured grains. Sample 401-23-2, 32 cm, uncrossed nicols, bar is 0.5 mm.

Figure 4 Algae. The red coralline algal crust at the lower right created a shelter void now completely filled with medium to coarse crystalline spar. Above the crust is grumeleuse fine spar containing the circular sections of green algal tubes. Sample 401-19-1, 141 cm, crossed nicols, bar is 0.5 mm.

Figure 5 Two generations of spar cement. Optically continuous crystals are transected by a dog-tooth line of inclusions that may represent a hiatus in cementation (A). Potassium ferricyanide stain did not react with any portion of the cement. Sample 401-19-1, 144 cm, uncrossed nicols, bar is 0.2 mm.

Figure 6 A rim of finely crystalline spar laths (A) that resembles the palisade cement common in modern beachrock and reef environments. This grain was selected because it shows well in photos; most grains in this sample have this rim but also have blocky spar in the adjacent void and are difficult to photograph. Sample 403-23-1, 134 cm, uncrossed nicols, bar is 0.1 mm.

PLATE 2

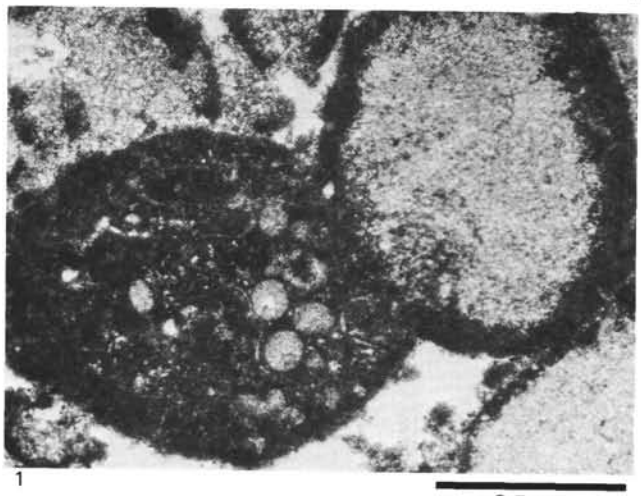

1

0.5 mm

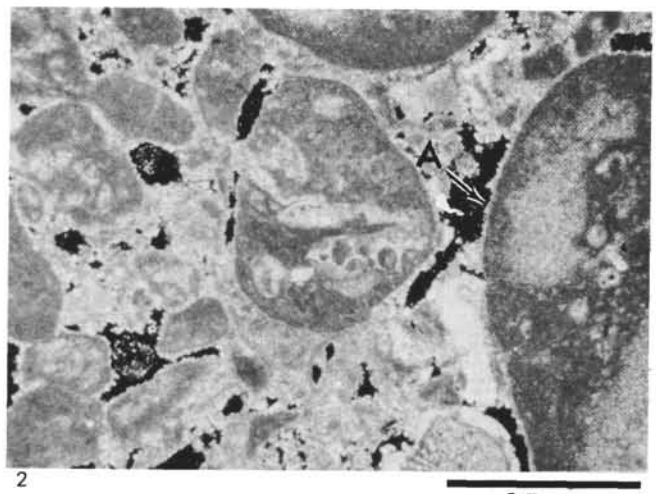

2

0.5 mm

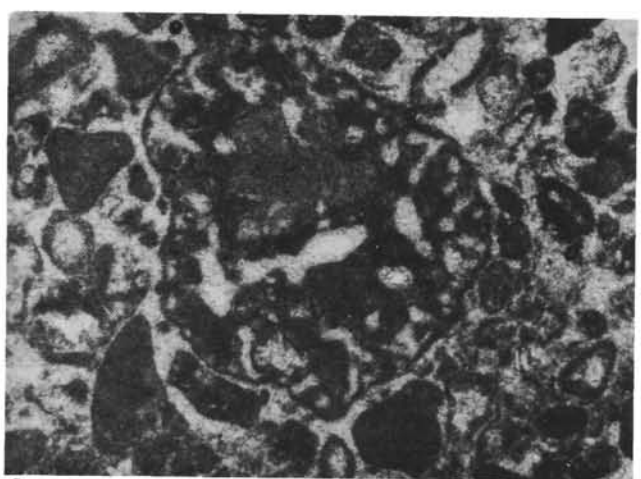

3

0.5 mm

4

0.5 mm

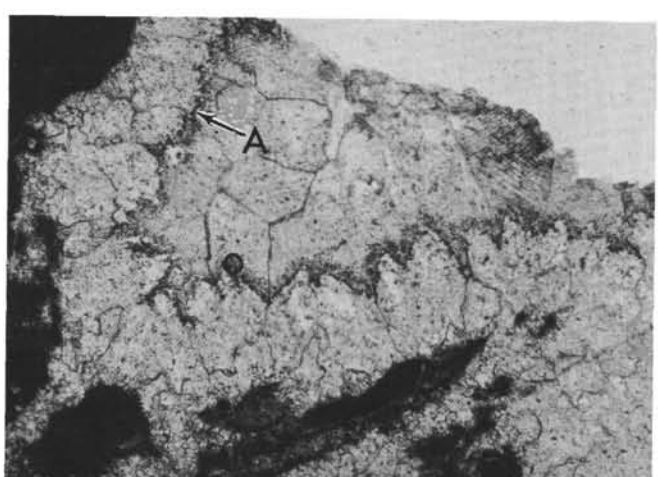

5

0.2 mm

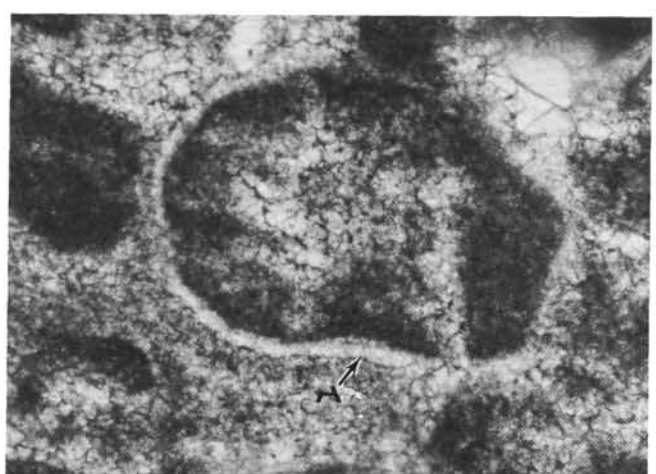

6

0.1 mm

PLATE 3

Figure 1 Two generations of cement are indicated by the: (1) cloudy spar adjacent to the grain margin and (2) optically continuous, clear centripetal spar. Sample 19-1, CC, uncrossed nicols, bar is 0.2 mm.

Figure 2 Same as Figure 1, crossed nicols.

Figure 3 Meniscus cement (?). Peloids cemented with a small amount of fine crystalline spar. Points lettered A indicate texture interpreted as meniscus cement. Note that elsewhere on the grains cement is spotty to absent. Sample 23-2, 17 cm, uncrossed nicols, bar is 0.1 mm.

Figure 4 Displacive rim cement. The clear rim on the left has grown from the uncoated end of a crinoid columnal. The rim on the right, though apparently nucleated on a peloid, probably originated on a crinoid fragment out of the plane of the thin section. Both have very sharp borders with the surrounding micrite-microspar but do not replace peloids. Note the cracked peloids. Sample 23-1, 119 cm, uncrossed nicols, bar is 0.5 mm.

PLATE 3

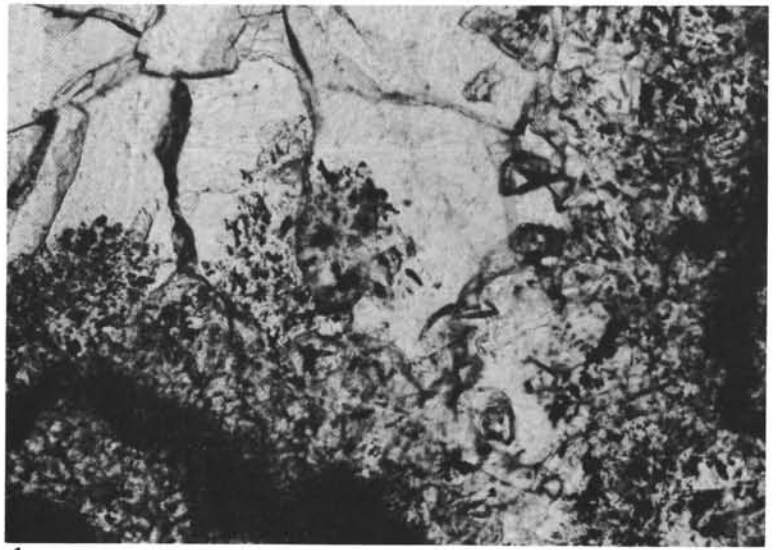

1

0.2 mm

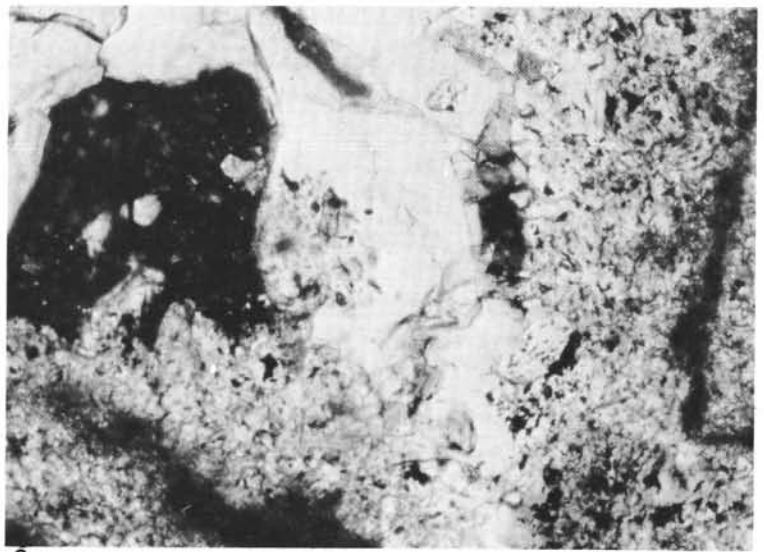

2

2 mm

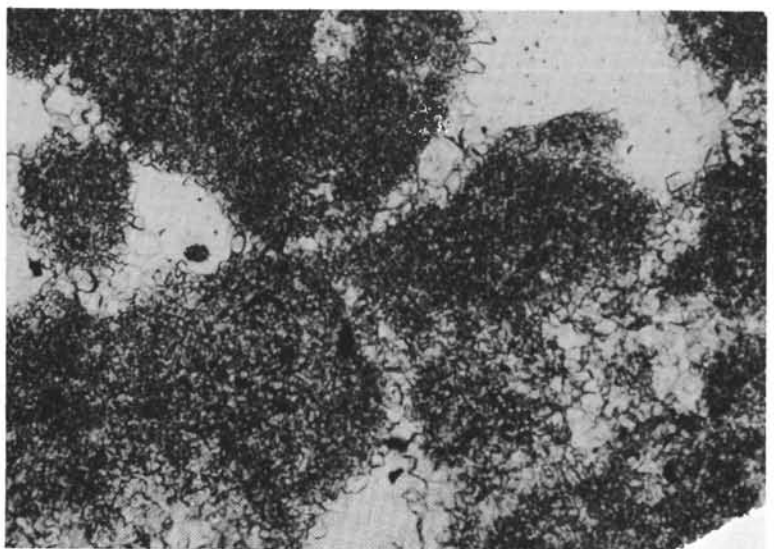

3

1 mm

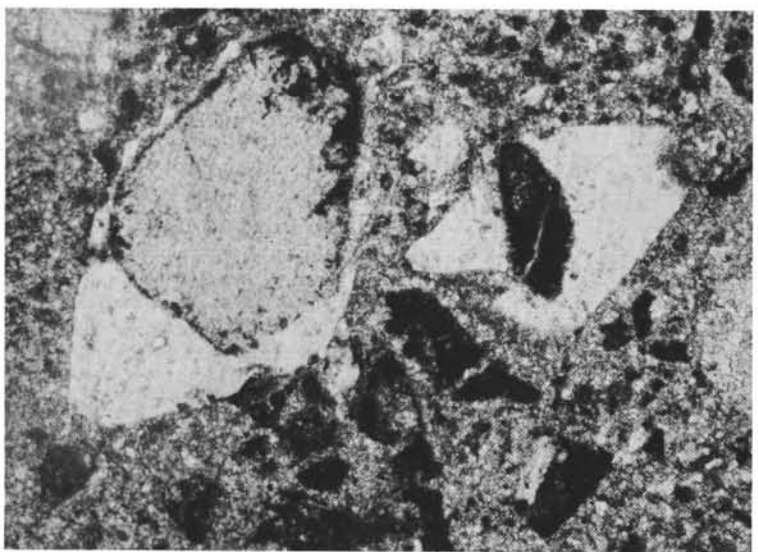

4

0.5 mm